

# IDŐJÁRÁS

## QUARTERLY JOURNAL OF THE HUNGARIAN METEOROLOGICAL SERVICE

### CONTENTS

- Ágnes Kenéz and Attila László Joó*: Parameter estimation and threshold selection uncertainty in extreme wind speed distribution - A frequentist approach with generalized Pareto distribution using automatic threshold selection..... 311
- Ivana Tošić, Stanimir Živanović, and Milica Tošić*: Influence of extreme climate conditions on the forest fire risk in the Timočka Krajina region (northeastern Serbia)..... 331
- Csilla Hajas and András Zempléni*: Dependent weighted bootstrap for European temperature data: is global warming speeding up? ..... 349
- Mila Pavlović, Filip Krstić, Vedran Živanović, and Aleksandar Kovjanić*: Valorisation of climate conditions in tourist centres of South Serbia ..... 363
- Dragan Papić, Nikola R. Bačević, Aleksandar Valjarević, Nikola Milentijević, Milivoj B. Gavrilov, Milenko Živković, and Slobodan B. Marković*: Assessment of air temperature trend in South and Southeast Bosnia and Herzegovina from 1961 to 2017 ..... 381
- Simona Tascu, Mirela Pietrisi, Christoph Wittmann, Florian Weidle, and Yong Wang*: Forecast skill of regional ensemble system compared to the higher resolution deterministic model..... 401
- Thomas Foken*: From Geiger to the modern micrometeorology – the textbook of Dénes Berényi (Short Contribution)..... 419

# IDŐJÁRÁS

*Quarterly Journal of the Hungarian Meteorological Service*

*Editor-in-Chief*

**LÁSZLÓ BOZÓ**

*Executive Editor*

**MÁRTA T. PUSKÁS**

## EDITORIAL BOARD

- |                                       |  |
|---------------------------------------|--|
| ANTAL, E. (Budapest, Hungary)         | MIKA, J. (Eger, Hungary)                   |
| BARTHOLY, J. (Budapest, Hungary)      | MERSICH, I. (Budapest, Hungary)            |
| BATCHVAROVA, E. (Sofia, Bulgaria)     | MÖLLER, D. (Berlin, Germany)               |
| BRIMBLECOMBE, P. (Hong Kong, SAR)     | PINTO, J. (Res. Triangle Park, NC, U.S.A.) |
| CZELNAI, R. (Dörcicse, Hungary)       | PRÁGER, T. (Budapest, Hungary)             |
| DUNKEL, Z. (Budapest, Hungary)        | PROBÁLD, F. (Budapest, Hungary)            |
| FERENCZI, Z. (Budapest, Hungary)      | RADNÓTI, G. (Reading, U.K.)                |
| GERESDI, I. (Pécs, Hungary)           | S. BURÁNSZKI, M. (Budapest, Hungary)       |
| HASZPRA, L. (Budapest, Hungary)       | SZALAI, S. (Budapest, Hungary)             |
| HORVÁTH, Á. (Siófok, Hungary)         | SZEIDL, L. (Budapest, Hungary)             |
| HORVÁTH, L. (Budapest, Hungary)       | SZUNYOGH, I. (College Station, TX, U.S.A.) |
| HUNKÁR, M. (Keszthely, Hungary)       | TAR, K. (Debrecen, Hungary)                |
| LASZLO, I. (Camp Springs, MD, U.S.A.) | TÁNCZER, T. (Budapest, Hungary)            |
| MAJOR, G. (Budapest, Hungary)         | TOTH, Z. (Camp Springs, MD, U.S.A.)        |
| MÉSZÁROS, E. (Veszprém, Hungary)      | VALI, G. (Laramie, WY, U.S.A.)             |
| MÉSZÁROS, R. (Budapest, Hungary)      | WEIDINGER, T. (Budapest, Hungary)          |

*Editorial Office: Kitaibel P.u. 1, H-1024 Budapest, Hungary*

*P.O. Box 38, H-1525 Budapest, Hungary*

*E-mail: [journal.idojaras@met.hu](mailto:journal.idojaras@met.hu)*

*Fax: (36-1) 346-4669*

---

**Indexed and abstracted in Science Citation Index Expanded™ and**

**Journal Citation Reports/Science Edition**

**Covered in the abstract and citation database SCOPUS®**

**Included in EBSCO's databases**

---

*Subscription by mail:*

*IDŐJÁRÁS, P.O. Box 38, H-1525 Budapest, Hungary*

*E-mail: [journal.idojaras@met.hu](mailto:journal.idojaras@met.hu)*

# IDŐJÁRÁS

*Quarterly Journal of the Hungarian Meteorological Service*  
Vol. 124, No. 3, July – September, 2020, pp. 311–330

## **Parameter estimation and threshold selection uncertainty in extreme wind speed distribution – A frequentist approach with generalized Pareto distribution using automatic threshold selection**

**Ágnes Kenéz \*** and **Attila László Joó**

*Department of Structural Engineering  
Budapest University of Technology and Economics  
Műegyetem rkp. 3-9, H-1111 Budapest, Hungary*

\* *Corresponding author E-mail: kenez.agnes@epito.bme.hu*

*(Manuscript received in final form August 13, 2019)*

**Abstract**— Nowadays, the use of probabilistic modeling for the design of engineering structures is becoming more and more widespread due to the advances in computer technology. In order to have a comprehensive picture about a meteorological phenomenon, e.g., wind actions on structures, uncertainties must be taken into account. From structural engineering and practical points of view, the effect of the length of short time series available for the analysis on the final results can be interesting to define a minimum observation-length. In this way, the real condition at the site can be utilized to assess wind loading effects on the structure.

This paper deals with the effect of uncertainties associated with the parameter estimation and threshold selection. A four-year record of wind speed data of Sződliget is analyzed, and these results are compared with the results of neighboring sites, Penc, and Budapest. The peak over threshold (POT) method with maximum likelihood estimation are selected to obtain the basic wind velocity. The suitable threshold is chosen using an automatic threshold selection approach.

According to our results, the applied automated threshold selection method provide reliable results, and it is simple and computationally inexpensive. This method may reduce associate errors of threshold selection in the future. It was found that at least approximately 100 realizations should exceed the specified threshold to earn reliable results. It means that 1–1.5-year and 4-year records of wind speeds are necessary for statistical inference in case of weakly dependent observations and for statistically independent events, respectively.

*Key-words:* extreme wind speed, basic wind velocity, generalized Pareto distribution, automated threshold selection, parameter estimation uncertainty

## 1. Introduction

Most design codes are based on the semi-probabilistic partial factor method, where design values should be conservative estimates. However, the advances in computer technology suggests the introduction of alternative design procedures based on fully probabilistic approaches and simulation techniques. This has led to the development of a promising design methodology, the Performance-based Wind Engineering (PBWE). The PBWE was first published in 2004 (*Paulotto et al.*, 2004), that paper provides a general framework for these investigations. After that, the major parameters and uncertainties were summarized in *Ciampoli et al.* (2011), *Petrini and Ciampoli* (2012), and *Tessari et al.* (2017). These publications help to understand of many aspects of structural behavior and its modeling. A cell tower equipped with wind speed (and strain) sensors in Sződliget (Central Hungary) is selected as the subject of this research, which is used as a radio tower. According to the experience of expert engineers and our observations, the utilization of the structure can be even smaller with precise modeling of wind load, thus, more antenna can be placed on the structure. The aim of the present study is to determine the point estimate and the parameter estimation uncertainty in the environmental field in case of Hungarian climate.

A lattice tower can be used as an electricity transmission tower (especially for voltages above 100 kilovolts), as a radio tower (a self-radiating tower or as a carrier for aerials), or as an observation tower. As reported in *Ducloux and Figueroa* (2016), the structural behavior and response of a tangent suspension tower and a radio tower are quite different. Furthermore, major international wind codes and standards were compared in previous studies to identify the differences and similarities between them *Kwon and Kareem* (2013), *Lungu et al.* (1996), and *Gatey and Miller* (2007). One of the main conclusions is that alongwind responses are fairly consistent in the codes/standards, but there are discrepancies in acrosswind responses. Moreover, most of these codes use the global method, i.e., the solidity ratio and global shielding factors. Although this approach is very effective for conventional structures, it is difficult to apply for atypical configurations. As recommended by *Prud'homme et al.* (2018), an empirical local method could be used to determine the wind loads in such a case. Their approach is based on the reduction of wind velocity in a turbulent wake accounting the shielding effect on each member.

Future extreme wind speeds should be considered in a reliable design. The available techniques to determine the 50-year return period wind speed was reviewed and summarized in *Palutikof et al.* (1999) and *Cooley* (2016). In this paper, the measured data of a 50-meter-high steel structure antenna tower equipped with wind speed sensors is analyzed and compared to the data provided by the Hungarian Meteorological Service (OMSZ). The fundamental value of the basic wind velocity defined at 10m above ground of terrain category II (*EN 1991-1-4* (2010) and *EN 1990* (2002)) is determined.

## 2. Measured data

The data from the abovementioned antenna tower was provided by Hungarian Telekom Telecommunications Plc.. The wind speed was measured for the period between August 2011 and March 2015, with a sampling interval of 0.9 s at 25 m, and 50 m height above ground. The lattice tower is located in Sződliget, and the nearest meteorological station is in Penc. To identify terrain categories, the map is shown in *Fig. 1*. Terrain category III are chosen for both sites. The following data from Penc and Budapest were provided by the OMSZ:

- 1999–2017 annual maxima of 10 minutes mean wind velocity,
- 2012–2017 daily maxima of 10 minutes mean wind velocity,
- 1998–2017 annual maxima of wind gusts.



*Fig. 1.* Map and terrain category of Sződliget and Penc.

The time series records of maxima for 3 and 7 days are shown in *Figs. 2* and *3*.

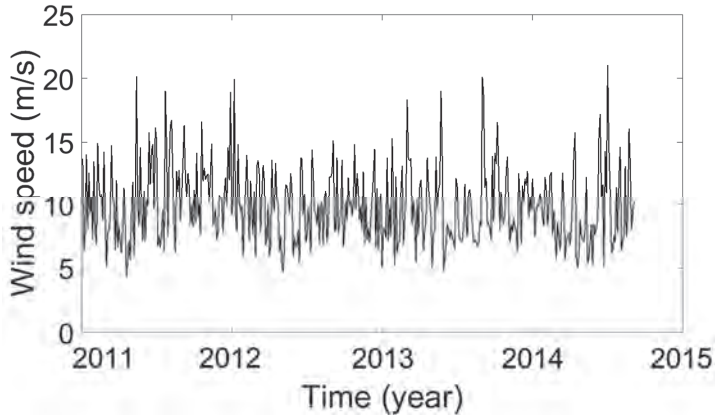


Fig. 2. Time series plot of 3-day maxima of wind speed measured at Szödliget.

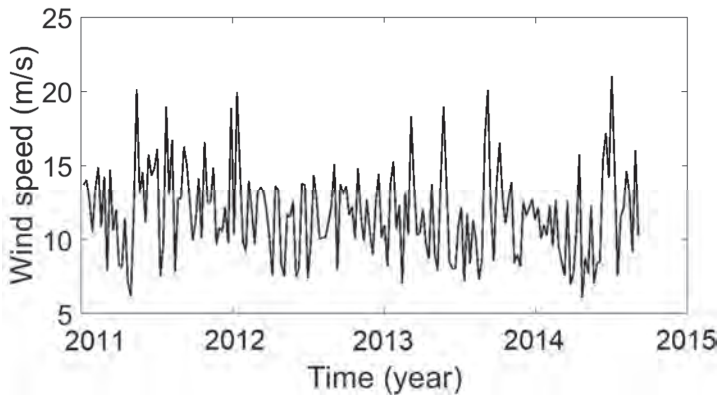


Fig. 3. Time series plot of 7-day maxima of wind speed measured at Szödliget.

### 3. Applied methods

#### 3.1. Independent events

First, an autocorrelation analysis is adopted to obtain the dependencies among the data and determine statistically independent events. A previous paper (Liu *et al.*, 2016) deals with repeating patterns and wind characteristics. Since an obvious daily periodicity of the change rate was recognized, the maxima for 3 and 7 days are analyzed in this study. This selection results in 441 and 189 data, respectively.

In case of the 3-day maxima, the presence of a slight periodicity was identified in the autocorrelation function of the stochastic time series (Fig. 4). However, the autocorrelation function of maxima for 7 days verifies the statistical independences of events clearly (Fig. 5). The detailed results for the 7-day maxima are presented in Section 4.

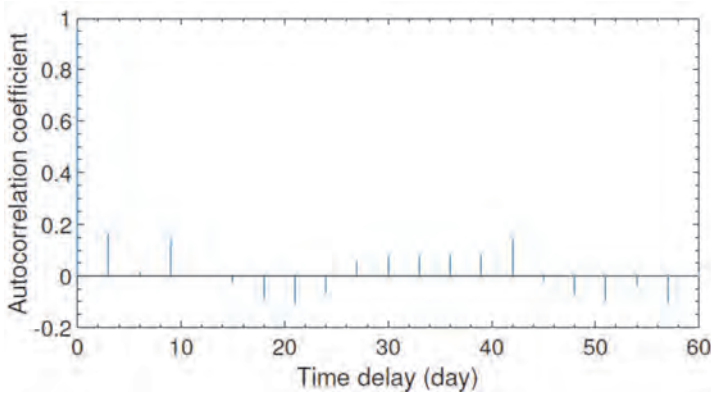


Fig. 4. Autocorrelation function of maxima for 3 days.

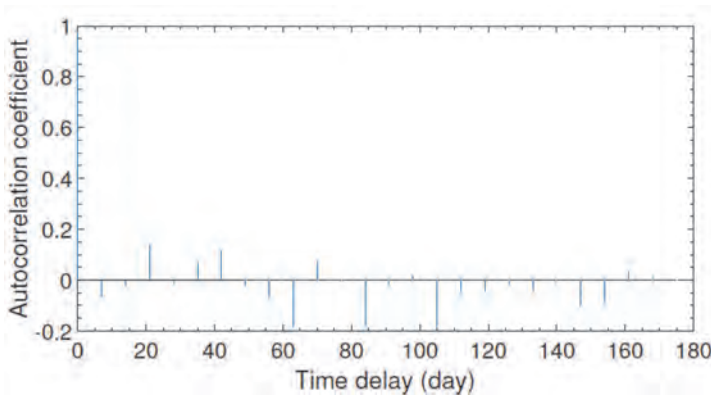


Fig. 5. Autocorrelation function of maxima for 7 days.

### 3.2. Extreme value theory

According to the classical extreme value theory (Fisher and Tippett, 1928; Gnedenko, 1943), the distribution of extreme wind speeds has an asymptotic limit. Moreover, the only possible limit  $F$  is the generalized extreme value distribution (GEV), which has the following cumulative distribution function (CDF):

$$F_{\xi,\sigma,\eta}(x) = \begin{cases} \exp\left(-\left(1 + \frac{\xi(x-\eta)}{\sigma}\right)^{-\frac{1}{\xi}}\right) & \text{for } \xi \neq 0 \\ \exp\left(-\exp\left(-\frac{(x-\eta)}{\sigma}\right)\right) & \text{for } \xi = 0, \end{cases} \quad (1)$$

where  $\xi$ ,  $\sigma$ , and  $\eta$  are the shape, scale, and location parameters, respectively. The shape parameter determines the type of the distribution. The three distributions are Gumbel ( $\xi = 0$ ), Fréchet ( $\xi > 0$ ), and Weibull ( $\xi < 0$ ), also known as type I, II, and III extreme value distributions. The Fréchet distribution has a lower limit and the Gumbel distribution is unlimited which results unlimited values as the return period increases. Thus, the Weibull distribution can be more appropriate to model extreme wind speeds for geophysical reasons (*Holmes and Moriarty, 1999, 2001; Cook and Harris, 2001*). The fundamental value of the basic wind velocity of Hungary has been determined using Gumbel distribution. However, the Joint Committee on Structural Safety recommends Weibull distribution in the Probabilistic Model Code.

A traditional approach of applying classical extreme value theory is the method of annual maxima. A major drawback of this approach is the data reduction, therefore, the wind measurement must be long. *Cook (1985)* advises that at least 20 extremes should be used to determine reliable results. To improve the efficiency, three main techniques have been developed: block method, peaks-over threshold (POT) method, and method of independent storms (MIS). In this study, we focus on the POT method, which is based on a conditional distribution, i.e., the exceedances over a specified threshold. The generalized Pareto distribution (GPD) is the asymptotic distribution to model the tails of the generalized extreme value (GEV) distribution under certain condition (*Pickands III, 1975*). Several papers deal with the application of GPD to extreme value analysis (*Holmes and Moriarty, 1999, 2001; Cook and Harris, 2001*). The CDF of the GPD is

$$F_{\xi,\sigma,\eta}(x) = \begin{cases} 1 - \left(1 + \frac{\xi(x-\eta)}{\sigma}\right)^{-\frac{1}{\xi}} & \text{for } \xi \neq 0 \\ 1 - e^{-z} & \text{for } \xi = 0, \end{cases} \quad (2)$$

where  $\xi$ ,  $\sigma$ , and  $\eta$  are the shape, scale, and location parameters, respectively. The shape parameter  $\xi$  of the GPD is the same as for the GEV (*Pickands III, 1975*). The threshold selection has a great influence on the result, and it is a compromise between bias and variance. While the variance decreases and the bias increases with lower threshold, higher threshold results that the bias decreases and the variance increases. The performance of threshold selection on visual basis is widely used, e.g., mean excess plot (or mean residual life plot; by plotting the mean of the excesses over the selected threshold against the wind velocity) which may cause associate errors.

### 3.3. Automatic threshold selection method for GPD

An automatic threshold selection method was proposed in (Thompson et al., 2009), which was implemented in this study. This automated technique is simple and computationally inexpensive. They recommend that the suitable values of thresholds ( $u_j, j = 1 \dots, n$ ) should be chosen between the median and the 98% quantile of the data (unless fewer than 100 values exceed it). Let us define

$$\tau_{u_j} = \hat{\sigma}_{u_j} - \hat{\xi}_{u_j} u_j, \quad j = 1, \dots, n, \quad (3)$$

where the differences

$$\tau_{u_j} - \tau_{u_{j-1}}, \quad j = 2, \dots, n, \quad (4)$$

should approximately follows normal distribution with zero mean.

### 3.4. Wind velocity profile

Finally, since available wind time series are measured at different heights, a conversion is required. The logarithmic law is utilized for wind velocity profile to calculate the basic wind velocity at 10 m height:

$$V(z) = \frac{u^*}{0.4} \ln \left( \frac{z}{z_0} \right) V_0, \quad (5)$$

where  $u^*$  is the friction velocity,  $z$  is the height of interest, and  $z_0$  is the roughness length.

## 4. Results and discussion

### 4.1. Traditional graphical diagnostics

The decreasing behavior of the mean excess plot (Fig. 6) indicates lighter tail (shape parameter  $\zeta < 0$ ). The conditional distribution is in the domain of attraction of GPD if the mean excess plot follows a straight line. Hence, one should select the proper threshold beyond the graph appears to be linear. In this case, linearity occurs between 7 and 12. The dotted lines indicate the upper and lower 95% confidence intervals.

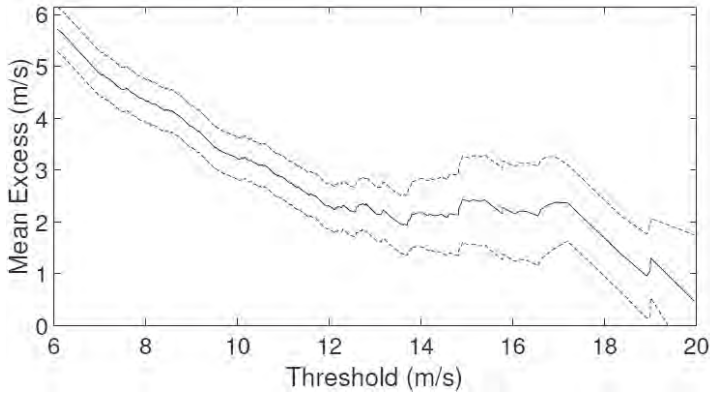


Fig. 6. Mean excess plot of the maxima for 7 days and the associated 95% confidence envelope.

Six estimation methods were considered and compared in *Kang and Song (2017)*. Two methods are based on the maximum likelihood estimation (MLE), three methods are based on the nonlinear least squares (NLS), and the last one is the Hill estimator. They found that the MLE performs well and better than the others in most cases. However, the MLE only hold when  $\xi > -0.5$  (*Cooley, 2016*). Therefore, the estimated parameters were calculated using MLE.

Furthermore, the suitable threshold can be selected with the help of shape and scale parameter plots presented in *Figs. 7 and 8*. One should find the point where the shape parameter is constant (approx. 11–13) and the scale parameter is linear (about 7–13).

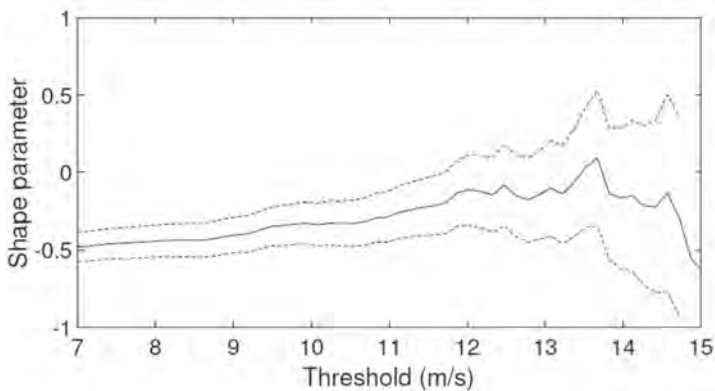


Fig. 7: Shape parameter for 7-day maxima.

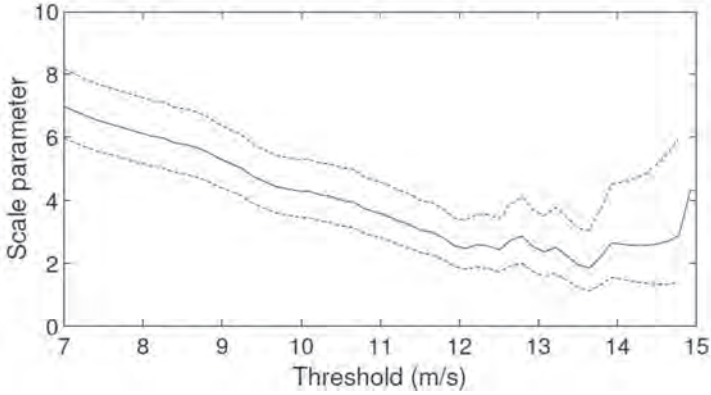


Fig. 8: Scale parameter for 7-day maxima.

#### 4.2. Automatic threshold selection for GPD

The differences  $\tau_{uj} - \tau_{uj-1}$  are calculated (Fig. 9) and the Pearson's chi-square test is used to establish whether or not the observed differences follow a normal distribution with zero mean. The red vertical line indicates the automated threshold selection choice of 11.73 m/s.

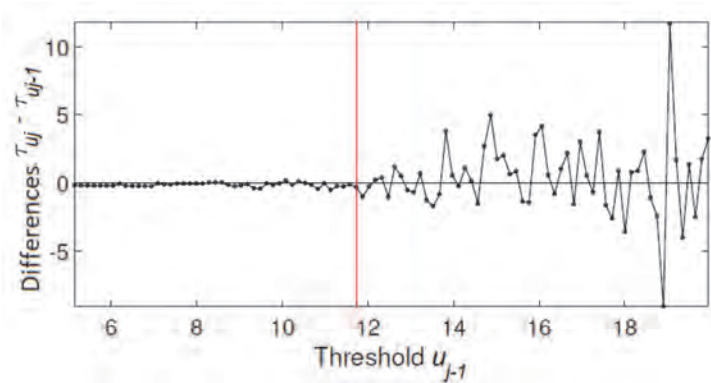


Fig. 9. Graph of the differences  $\tau_{uj} - \tau_{uj-1}$  for 7-day maxima.

Fig. 10 shows the empirical and fitted cumulative distribution functions. Although the case of  $\zeta < 0$  (belongs to Weibull distribution) would be more

appropriate, the case of  $\xi = 0$  (Gumbel distribution) can be considered to be on the safe side (results greater basic wind velocity).

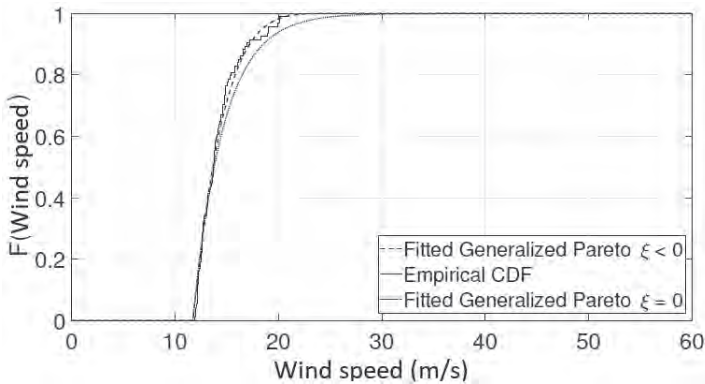


Fig. 10. Empirical and fitted cumulative distribution functions.

The quantile plot (Fig. 11) shows the quantiles of resampled estimates versus theoretical quantiles from a normal distribution. Hence, one can check that the estimated parameter follows the normal distribution, and the delta method (Coles, 2011) can be applied. This quantile plot indicates that the fitted GPD model is satisfactory.

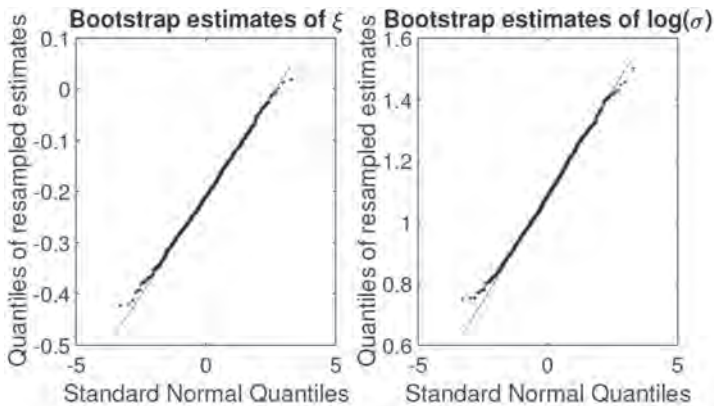


Fig. 11. Quantile plot.

### 4.3. Wind return level plot

After the parameter estimates were determined, the wind speed for a return period is calculated from the GPD as

$$V_R = \begin{cases} \mu + \frac{\sigma}{\xi} \left[ \left( \frac{1}{R} \right)^{-\xi} \right] & \text{for } \xi \neq 0 \\ \mu - \sigma \ln \left( \frac{1}{R} \right) & \text{for } \xi = 0, \end{cases} \quad (6)$$

where  $R$  is the return period. In this research, 95% confidence intervals were calculated using the delta method. The wind return period is obtained with the estimated shape parameter (Fig. 12) and zero shape parameter Fig. 13 as well, and it is plotted with a logarithmic scale for the horizontal axis. In these plots, the bounded and unbounded behavior of the two distributions can be clearly seen.

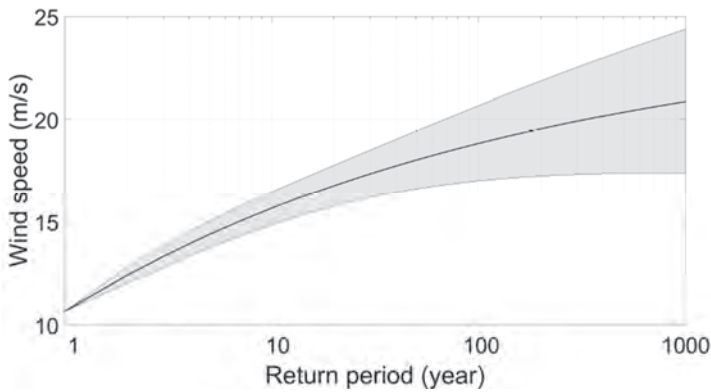


Fig. 12: Wind return plot,  $\xi < 0$ .

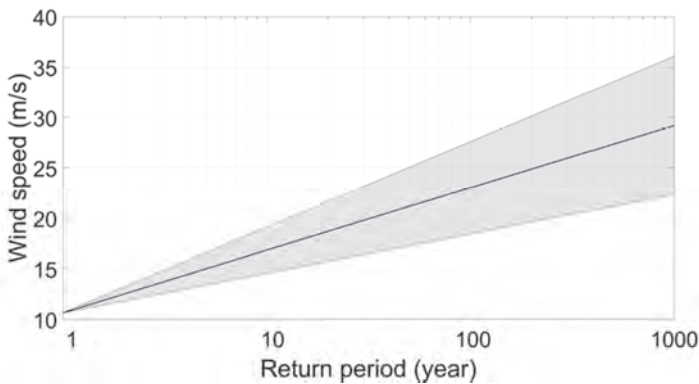


Fig. 13: Wind return plot,  $\xi = 0$ .

The  $\zeta = 0$  shape parameter yields 17% greater basic wind velocity than the estimation of  $\zeta < 0$ . The range of 95% confidence intervals of the 50-year return period wind velocities are about 7% and 13% of the associated point estimate for 3- and 7-day maxima, respectively. Certainly, this value is increasing with increasing return periods.

#### 4.4. 4.4 Basic wind velocity and parameter estimation uncertainties

The maximum likelihood estimations and the 95% confidence intervals of the 50-year return period for 3- and 7-day maxima of 10 min mean wind speed measured at 10 m height are shown in Fig. 14. The detailed results (e.g., number of observations) can be found in Appendix A, Tables A.1 to A.5. The automated threshold selection choices are 11.93 m/s and 11.73 m/s for 3- and 7-day maxima, respectively.

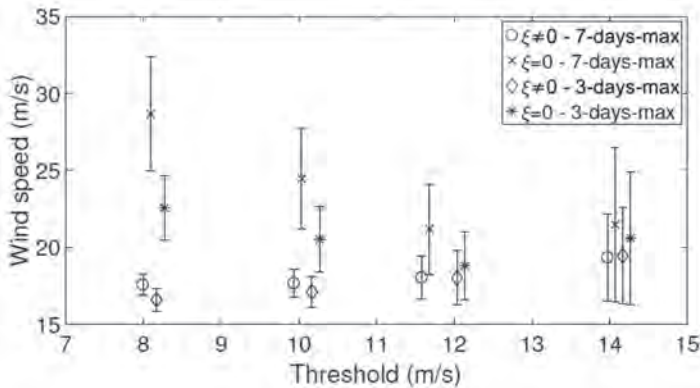


Fig. 14: Point estimates and confidence intervals of wind extremes for Szödliget.

While the point estimate calculated by shape parameter  $\zeta = 0$  decreases with increasing threshold, maximum likelihood estimations calculated by shape parameter  $\zeta < 0$  increases with increasing threshold due to the decreasing shape parameter. Moreover, the increasing confidence interval can be clearly seen.

Nevertheless, in case of threshold of 8 m/s for 7-day maxima, bias was observed in the quantile plot. Reliable results are obtained in the range of 8.5 m/s and 12.5 m/s for 3-day maxima, 10.5 m/s and 13 m/s for 7-day maxima. Although there are only small differences (max 5%) between estimations with shape parameter  $\zeta < 0$  of the 3- and 7-day maxima, the differences of these estimates with shape parameter  $\zeta = 0$  are statistically significant (4–25%). The range of 95% confidence intervals are about 7–10% of the associated point estimates.

Furthermore, instantaneous wind speeds are analyzed to make simple comparison between the two cases (Fig. 15). It is transformed to the basic wind velocity (10 min mean) by the exposure factor provided by Eurocode 1991-1-4 (EN 1991, 2010). Similar consequences can be stated for these results, and the two calculations are in good agreement. The estimated basic wind velocity calculated from 10 min mean wind data and instantaneous wind speeds are 18.0–21.1 m/s and 17.2–21.7 m/s, respectively. The automated threshold selection choices are 15.37 m/s and 17.75 m/s for 3- and 7-day maxima.

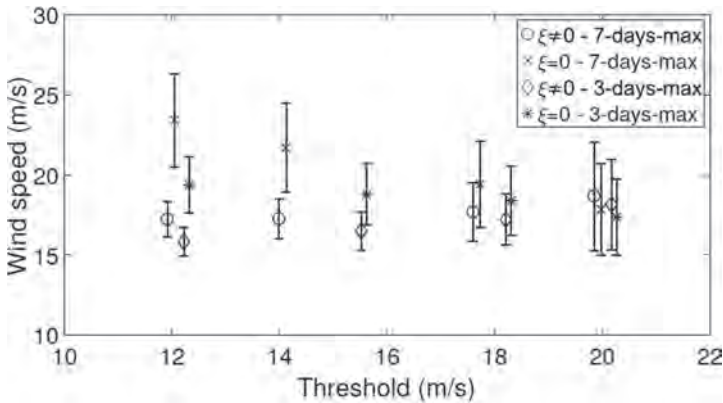


Fig. 15: Point estimates and confidence intervals of wind extremes for Sződliget (1s measured values are converted to 10 min mean).

In case of Penc, wind speeds with estimated 50-year return period are much lower than the estimates for Sződliget (about 30%). Moreover, these values (12-16 m/s) are also substantially lower than the basic wind velocity of Hungary (23.6 m/s). The automated threshold selections are 5.42 m/s 7.16 m/s for 3- and 7-day maxima, respectively. For Penc, the range of 95% confidence intervals are about 4-5% of the associated point estimates due to the higher number of observations and lower estimated values (Fig. 16).

The assessed basic wind speed of Budapest is in good agreement with results of Sződliget. The automated choices are 11.22 m/s and 10.93 m/s for 3- and 7-day maxima, respectively. The range of 95% confidence intervals of these 50-year return period wind velocities are about 5% and 14% of the associated point estimate for 3- and 7-day maxima, respectively. The  $\xi = 0$  shape parameter yields approximately 20% greater basic wind velocity than the estimation of  $\xi < 0$ . The result of the 3- and 7-day maxima data are quite equivalent for  $\xi < 0$ . A previous study (Rózsás and Sýkora, 2016) investigated the probabilistic modeling of basic wind speeds for Budapest based on Carpatclim data covering a 50-year observation period. Although, the point estimates of 20.9–21.4 m/s are obtained

using the POT method, the uncertainty interval is narrower due to the greater sample size (3–4 times more observations).

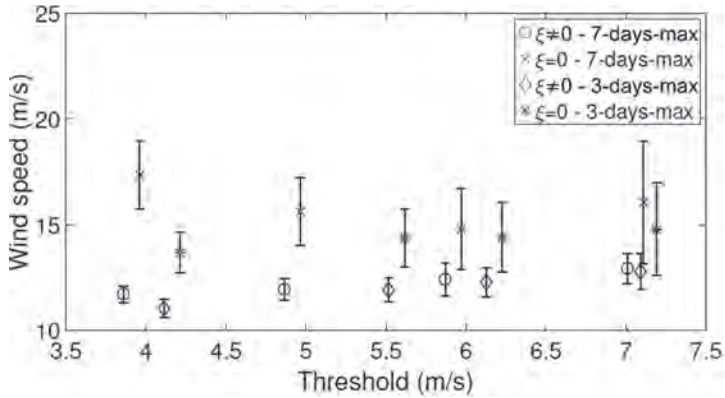


Fig. 16. Point estimates and confidence intervals of wind extremes for Penc.

Moreover, 20 years of annual maxima are analyzed using the classical GEV method for Penc and Budapest as it was suggested in *Cook (1985)*. However, discrepancies were found in these results. Basic wind velocities calculated from 10 min mean annual maxima (see *Table A.3*) are slightly greater (differences are 12–15%, about 2 m/s) than results calculated using the POT method, but still lower than the basic wind velocity of Hungary. Nevertheless, wind extremes calculated from instantaneous wind speeds are much greater (differences are 30-94%) and these values are also greater than the fundamental basic wind velocity of Hungary.

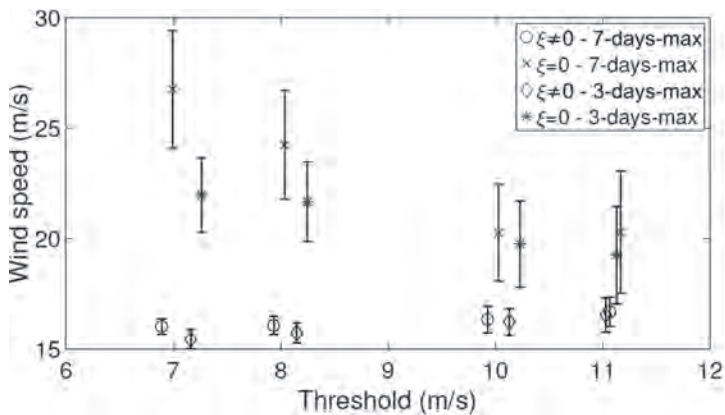


Fig. 17: Point estimates and confidence intervals of wind extremes for Budapest

## 5. Concluding remarks

Eurocodes are based on the limit state concept used in conjunction with a partial factor method, where the basic variables (i.e., actions, resistances and geometrical properties) are given through the use of partial factors and design values (1990, 2002). If one would like to apply alternative design procedures based on fully probabilistic approaches, uncertainties must be taken into account. From structural engineering point of view, the effect of the length of short time series available for the analysis can be interesting to define a minimum observation-length, i.e., minimum number of realizations or exceedances.

In this study, uncertainties associated with the parameter estimation of the 50-year return period wind velocity was assessed using frequentist statistical approach. This uncertainty is quantified by 95% confidence intervals. The peak over threshold (POT) method with maximum likelihood estimation are applied to analyze a four-year record of wind speed data. The threshold selection may have a great influence on the result, and it is a compromise between bias and variance. In this paper, the suitable threshold for the POT method is chosen using an automatic threshold selection approach. The following statements are valid for the dataset under consideration, since different climatic conditions can cause different behavior.

The applied automated threshold selection method provides reliable results in our case. All automated threshold choices are in the linear range in the mean excess plot, i.e., in the domain of attraction of the GPD. This automated method is simple and computationally inexpensive, and it may be able to reduce associate errors of threshold selection in the future. It was found that at least 100 realizations should exceed the specified threshold to earn reliable results. It means that 1–1.5-year and 4-year records of wind speeds are necessary in case of weakly dependent observations and for statistically independent events, respectively. The range of 95% confidence intervals are about 7–10% of the associated point estimates in case of about 100 exceedances. This confidence intervals reduce to 3–5% when the number of exceedances increases by 2–3-times.

The GPD with shape parameter  $\zeta = 0$  yields about 10–20% greater 50-return period wind speeds than with  $\zeta < 0$ . The former one is unbounded and conservative. The difference between point estimates calculated using the shape parameter  $\zeta < 0$  with various thresholds is approximately 0.1–5% and the difference is 3–12% for  $\zeta = 0$ . Thus, the effect of number of realizations and the determination of independent events have greater influence on the results of shape parameter  $\zeta = 0$ . According to present results, more than 20 extremes should be used for the classical GEV method to obtain reliable results. While basic wind velocities of GPD with  $\zeta = 0$  approximate the standard basic wind velocity of Hungary (23.6 m/s), wind velocities of GPD with  $\zeta < 0$  are also substantially lower than the standard value.

However, the effect of parameter estimation uncertainty in extreme wind speeds on the assessed reliability index should be investigated later to see its influence on the final result. If this impact is considerable, then this uncertainty should be taken into account in the model.

**Acknowledgments:** The authors would like to thank the Hungarian Meteorological Service (OMSZ) and the Hungarian Telekom Telecommunications Plc. for providing their meteorological data. The research reported in this paper was supported by the Higher Education Excellence Program of the Ministry of Human Capacities (BME FIKP).

## References

- Ciampoli, M., Petrini, F. and Augusti G., 2011: Performance-based wind engineering: Towards a general procedure. *Structural Safety*, 33, 367–378. <https://doi.org/10.1016/j.strusafe.2011.07.001>
- Coles S., 2011: An Introduction to Statistical Modeling of Extreme Values. Springer Series in Statistics. Springer, London, ISBN 9781849968744.
- Cook, N.J. and Harris, R.I., 2001: Discussion of application of the generalized pareto distribution to extreme value analysis in wind engineering by J. D. Holmes, W. W. Moriarty. *J. Wind Engineer. Industrial Aerodynam.* 89, 215–224. [https://doi.org/10.1016/S0167-6105\(00\)00063-5](https://doi.org/10.1016/S0167-6105(00)00063-5)
- Cook, N.J., 1985: The Designer's Guide to Wind Loading of Building Structures: N.J. Cook of Building Structures. Building Research Establishment Dept. of the Environment,; London; Boston: Butterworths, - Building Research Establishment report.
- Cooley, D., 2016: Dipak K. Dey, Jun Yan., Extreme value modeling and risk analysis: Methods and applications. Crc press, Boca Raton.<https://doi.org/10.1201/b19721>
- Ducloux, H. and Figueroa, L., 2016: Background information about the wind action model of cenelec en 50341-1 (2012) and associated expected reliability of electrical overhead lines. *J. Wind Engineer. Industrial Aerodynam.* 157, 104–117. <https://doi.org/10.1016/j.jweia.2016.08.006>
- EN 1990, 2002: Eurocode - Basis of Structural Design
- EN 1991-1-4, Eurocode 1, 2010: Actions on structures: part 1-4: general actions - wind actions. Brussels, CEN.
- Fisher, R.A. and Tippett, L.H.C., 1928: Limiting forms of the frequency distribution of the largest or smallest member of a sample, *Math. Proc. Cambridge Philosoph. Soc.* 24, 180–190 <https://doi.org/10.1017/S0305004100015681>
- Gatey, D.A., and Miller, C.A., 2007: An investigation into 50-year return period wind speed differences for Europe. *J. Wind Engineer. Industrial Aerodynam.* 95., 1040–1052. <https://doi.org/10.1016/j.jweia.2007.01.016>
- Gnedenko, B., 1943: Sur la distribution limite du terme maximum d'une serie aleatoire. *Ann. Mathematics*, 44, 423–453. (In France) <https://doi.org/10.2307/1968974>
- Holmes, J. and Moriarty, W.W., 2001: Response to discussion by N.J. Cook and R.I. Harris. *J. Wind Engineer. Industrial Aerodynam.* 89, 225–227. [https://doi.org/10.1016/S0167-6105\(00\)00064-7](https://doi.org/10.1016/S0167-6105(00)00064-7)
- Holmes, J.D. and Moriarty, W.W., 1999: Application of the generalized pareto distribution to extreme value analysis in wind engineering. *J. Wind Engineer. Industrial Aerodynam.* 83, 1–10. [https://doi.org/10.1016/S0167-6105\(99\)00056-2](https://doi.org/10.1016/S0167-6105(99)00056-2)
- Kang, S. and Song J., 2017: Parameter and quantile estimation for the generalized pareto distribution in peaks over threshold framework. *J. Korean Statistic. Soc.* 46, 487–501. <https://doi.org/10.1016/j.jkss.2017.02.003>
- Kwon, D. K., and Kareem, A., 2013: Comparative study of major international wind codes and standards for wind effects on tall buildings. *Engineering Structures.* 51, 23–35 <https://doi.org/10.1016/j.engstruct.2013.01.008>
- Liu, J., Ren, G., Wan, J., Guo, Y., Yu, D. 2016: Variogram time-series analysis of wind speed, *Renew. Energy* 99, 483–491. <https://doi.org/10.1016/j.renene.2016.07.013>

- Lungu D., P.H.A.J.M. Gelder, and Trandafir R., 1996: Comparative study of Eurocode 1, ISO and ASCE procedures for calculating wind loads. *International Association for Bridge and Structural Engineering (IABSE) Report. Vol. 74*, pp. 345–354, Delft, 05
- Palutikof, J. P., Brabson, B., Lister, D., Adcock, S. T., 1999: A review of methods to calculate extreme wind speeds., *Meteorol.Appl.* 6, 119–132. <https://doi.org/10.1017/S1350482799001103>
- Paulotto, C., Ciampoli, M., Augusti, G., 2004: Some proposals for a first step towards a performance-based wind engineering. *Proceedings of the IFED international forum in engineering decision making; First Forum, December, 5–9, Stoos, Switzerland*, <http://www.ifed.ethz.ch> 01.
- Petrini, F., and Ciampoli, M., 2012: Performance-based wind design of tall buildings. *Struct.Infrastruct. Engineer.* 8, 954–966. <https://doi.org/10.1080/15732479.2011.574815>
- Pickands III, J., 1975: Statistical inference using extreme order statistics. *Ann. Statistics* 3, 119–131. <https://doi.org/10.1214/aos/1176343003>
- Prud'homme, S., Legeron, F., and Langlois, S., 2018: Calculation of wind forces on lattice structures made of round bars by a local approach, *Engineering Structures*, 156, 548–555. <https://doi.org/10.1016/j.engstruct.2017.11.065>
- Rózsás, Á., and Sýkora, M., 2016: Effect of statistical uncertainties on predicted extreme wind speeds. *7th International Workshop on Reliable Engineering Computing (REC), June 15-17, Ruhr University Bochum, Germany*
- Tessari, R. K., Kroetz, H. M., Beck, A. T., 2017: Performance-based design of steel towers subject to wind action. *Engineering Structures*, 143, 549-557, ISSN 0141-0296. <https://doi.org/10.1016/j.engstruct.2017.03.053>
- Thompson, P., Cai, Y., Reeve, D., Stander, J., 2009: Automated threshold selection methods for extreme wave analysis. *Coastal Engineering*, 56(10), 1013–1021. <https://doi.org/10.1016/j.coastaleng.2009.06.003>

Table 1. Point estimates and confidence intervals of wind extremes for Szödliget, calculated from 10 min mean wind speeds

	N <sup>a</sup>	N <sup>b</sup>	Threshold	$\xi$	$\sigma$	GPD - $\xi < 0$			GPD - $\xi = 0$			
						lower 95	MLE	upper 95	lower 95	MLE	upper 95	
h = 50m	7-day maximum	189	165	8	-0.44	5.98	16.88	17.56	18.24	24.98	28.66	32.33
		128	10	10	-0.34	4.30	16.75	17.66	18.58	21.18	24.44	27.70
		94	11.73	14	-0.19	2.96	16.61	18.03	19.44	18.24	21.18	24.12
	3-day maximum	441	296	8	-0.28	4.28	15.87	16.59	17.32	20.47	22.56	24.65
		192	10	10	-0.20	3.20	16.09	17.10	18.10	18.41	20.52	22.62
		113	11.93	14	-0.05	2.23	16.24	18.00	19.77	16.60	18.79	20.98
h = 25m	7-day maximum	42	14	14	-0.08	2.19	16.33	19.45	22.57	16.28	20.59	24.89
		189	135	5.65	-0.39	4.26	14.14	14.89	15.64	20.10	23.48	26.85
		77	8	8	-0.23	2.50	14.01	15.32	16.63	15.73	18.82	21.92
	3-day maximum	441	197	6	-0.24	2.98	13.36	14.21	15.05	16.44	18.56	20.68
		143	6.97	8	-0.21	2.57	13.55	14.59	15.63	15.64	17.91	20.18
		91	8	8	-0.22	2.41	13.93	15.11	16.29	15.68	18.36	21.05
25	10.64	10.64	-0.22	1.85	14.32	16.35	18.39	14.30	18.82	23.35		

<sup>a</sup> Number of data<sup>b</sup> Number of data above threshold

## Appendix A.

Table 2. Point estimates and confidence intervals of wind extremes for Szódliget, calculated from instantaneous wind speeds transformed to 10 min mean

	N <sup>a</sup>	N <sup>b</sup>	Threshold	$\xi$	$\sigma$	GPD - $\xi < 0$			GPD - $\xi = 0$		
						lower 95	MLE	upper 95	lower 95	MLE	upper 95
h = 50m	189	159	12	-0.25	8.08	16.14	17.23	18.33	20.51	23.41	26.32
		132	14.14	-0.21	6.73	16.01	17.26	18.50	18.95	21.7	24.45
		83	17.75	-0.10	4.71	15.86	17.69	19.52	16.70	19.4	22.10
		55	20	0.06	3.39	15.28	18.67	22.07	14.99	17.85	20.71
3-day maximum	441	280	12	-0.17	6.15	14.95	15.84	16.74	17.64	19.38	21.12
		168	15.37	-0.13	5.03	15.34	16.51	17.67	16.86	18.78	20.70
		100	18	-0.08	4.16	15.63	17.22	18.82	16.26	18.40	20.55
		65	20	0.06	3.16	15.32	18.16	20.99	15.00	17.37	19.74

<sup>a</sup> Number of data

<sup>b</sup> Number of data above threshold

Table 3. Point estimates and confidence intervals of wind extremes for Penc and Budapest, calculated from annual maximum wind speeds

	N <sup>a</sup>	$\xi$	$\sigma$	$\mu$	GPD - $\xi < 0$			GPD - $\xi = 0$		
					lower 95	MLE	upper 95	lower 95	MLE	upper 95
Penc	19	-0.70	1.14	9.51	14.09	14.6	15.11	14.10	18.46	22.83
		-0.17	2.56	20.98	22.12	25.17	28.21	24.03	27.55	31.07
Budapest	19	-0.10	0.96	13.45	16.95	18.76	20.57	17.79	19.51	21.22
		0.08	2.33	26.53	21.66	28.35	35.04	23.83	27.15	30.46

<sup>a</sup> Number of data

Table 4. Point estimates and confidence intervals of wind extremes for Penc, calculated from 10 min mean wind speeds

h = 10m	N <sup>a</sup>	N <sup>b</sup>	Threshold	$\xi$	$\sigma$	GPD - $\xi < 0$			GPD - $\xi = 0$		
						lower 95	MLE	upper 95	lower 95	MLE	upper 95
7-day maximum	313	270	4.01	-0.36	2.32	11.33	11.72	12.11	15.74	17.33	18.92
		175	5.02	-0.30	1.73	11.42	11.93	12.45	14.02	15.62	17.22
		91	6.02	-0.24	1.32	11.62	12.41	13.19	12.88	14.79	16.71
		33	7.16	-0.37	1.27	12.23	12.93	13.63	13.17	16.04	18.91
3-day maximum	730	474	4.01	-0.21	1.61	10.6	11.04	11.48	12.71	13.67	14.64
		175	5.42	-0.23	1.39	11.34	11.91	12.48	13.01	14.38	15.75
		108	6.03	-0.22	1.24	11.57	12.27	12.98	12.77	14.40	16.02
		46	6.99	-0.25	1.07	11.92	12.78	13.64	12.6	14.78	16.96

<sup>a</sup> Number of data<sup>b</sup> Number of data above threshold

Table 5. Point estimates and confidence intervals of wind extremes for Budapest, calculate from 10 min mean wind speeds

h = 43m	N <sup>a</sup>	N <sup>b</sup>	Threshold	$\xi$	$\sigma$	GPD - $\xi < 0$			GPD - $\xi = 0$		
						lower 95	MLE	upper 95	lower 95	MLE	upper 95
7-day maximum	313	227	7.04	-0.52	4.23	15.65	16.01	16.36	24.06	26.74	29.43
		185	8.09	-0.47	3.39	15.65	16.06	16.46	21.77	24.23	26.69
		101	10.08	-0.34	1.99	15.71	16.32	16.93	18.06	20.26	22.46
		50	11.22	-0.38	1.7	16.01	16.68	17.35	17.53	20.29	23.04
3-day maximum	730	357	7.06	-0.36	3.14	15.01	15.44	15.86	20.26	21.96	23.66
		253	8.05	-0.37	2.82	15.29	15.72	16.16	19.84	21.65	23.46
		114	10.03	-0.31	1.89	15.62	16.22	16.83	17.8	19.75	21.71
		69	10.93	-0.28	1.54	15.78	16.54	17.31	17.04	19.25	21.45

<sup>a</sup> Number of data<sup>b</sup> Number of data above threshold

# IDŐJÁRÁS

*Quarterly Journal of the Hungarian Meteorological Service*  
Vol. 124, No. 3, July – September, 2020, pp. 331–347

## **Influence of extreme climate conditions on the forest fire risk in the Timočka Krajina region (northeastern Serbia)**

**Ivana Tošić<sup>1\*</sup>, Stanimir Živanović<sup>2</sup>, and Milica Tošić<sup>1</sup>**

<sup>1</sup>*University of Belgrade-Faculty of Physics  
Institute for Meteorology  
Dobračina 16, 11000 Belgrade, Serbia*

<sup>2</sup>*Emergency Management Sector of Serbia  
Omladinskih brigada 31, 11000 Belgrade, Serbia*

*\*Corresponding author E-mail: itosic@ff.bg.ac.rs*

*(Manuscript received in final form September 3, 2019)*

**Abstract**—The dependence of the influence of extreme climate conditions on the variability of forest fires in the Timočka Krajina region of northeastern Serbia was studied. The impact of extreme conditions was investigated with extreme climate indices using air temperature, relative humidity, and precipitation measured at three meteorological stations in northeastern Serbia. The De Martonne index was used to analyze climate conditions as a measure for aridity. The study analyzes trends in extreme climate indices with an emphasis on the two contrasting years, 2012 and 2014, and compares them to the baseline period 1961–1990. The year 2012 was very warm and dry, while 2014 was one of the wettest recorded in Serbia. There was an increase (decrease) in warm (cold) temperature indices. Non-significant increases in extreme precipitation indices were observed, while the number of precipitation events greater than 1 mm decreased, as did relative humidity.

Ångström index values were used as an index for assessing the risk of forest fires. These indices were analyzed and a correlation between them and forest fires in northeastern Serbia was established. The aridity index was low during the years 2012, 2011, and 2017, correlating with the large number of forest fires. High values of the Ångström index in 2013 and 2014 were associated with a minimum number of registered forest fires. As an improved indicator for the number of forest fires, the modified Ångström index using daily maximum temperature is proposed.

**pKey-words:** extreme climate indices, air temperature, precipitation, forest fires,  
**Key-words:** extreme climate indices, air temperature, precipitation, forest fires, Timočka Krajina region, Serbia

## 1. Introduction

There is a general agreement that changes in the frequency or intensity of extreme weather and climate events will have profound impacts on both human society and natural environment (Easterling *et al.*, 2000). Every region of the world is already experiencing extreme events (e.g., Yan *et al.*, 2002; Bartholy and Pongrácz, 2007; Santos *et al.*, 2011; Finkel and Katz, 2018).

Forest resources are becoming increasingly sensitive to extremes and climatic conditions. The interest of the competent services for the protection of forests from fires usually focuses on extreme indicators of fire danger. The territory of Serbia is exposed to extreme climate conditions, which are more pronounced in the 21st century (Vuković *et al.*, 2018). The Fourth Assessment Report (AR4) from the Intergovernmental Panel on Climate Change (IPCC, 2007) defines an extreme event as rare at a particular place and time during the year. The implications of extreme climatic events depend on their intensity, duration, and frequency of occurrence. Heat waves, droughts, and storms can have a devastating and a wide range of impacts on forest resources. Fire danger is greater if the dry season is longer, especially during periods when the air temperature is extremely high. Many studies (e.g., Moritz, 2003; McKenzie *et al.*, 2004; Keeley, 2004) indicate that prolonged drought combined with extreme weather conditions, such as high air temperature, wind speed, and low relative humidity, often lead to fires. Drought is relatively common in the northeastern region of Serbia (Aleksić *et al.*, 2004) and it increases the risk of fires of combustible materials. Applying the De Martonne aridity index for 26 meteorological stations in central Serbia, Radaković *et al.* (2018) showed that humidity decreases towards the east. Vegetation drying that reduces the moisture content in fuel material creates conditions favorable for the occurrence and spread of fire (Živanović, 2017). Studies from domestic and foreign authors (Popović *et al.*, 2005, 2008; Kadović and Medarević, 2007; Seidling, 2007; Carnicer *et al.*, 2011; De la Cruz *et al.*, 2014) suggest that the impacts of climate change extremes, such as heat waves and droughts, significantly contribute to the exposure and vulnerability of certain ecosystems. The predicted changes in temperature and precipitation regime in Serbia (Djurdjević *et al.*, 2015; Vuković *et al.*, 2018) suggest that climate changes in the near or distant future may have even stronger impacts on forest ecosystems and the whole environment.

The appearance of fire in Serbia changes from period to period and largely depends on weather conditions and the humidity of combustible materials (Tabaković-Tošić *et al.*, 2009; Živanović *et al.*, 2018). Variability in climate elements indicates when and to what extent there is a risk of the emergence and spread of fire in the forest (Živanović, 2012; 2015).

Air temperatures over 25 °C present an elevated risk for the occurrence and spread of forest fires. Some areas in the northeastern territory of Serbia can

experience more than 26 days a month when air temperature is over 25 °C, creating favorable conditions for the occurrence of forest fires (Vasić, 1992). Particularly dangerous forest fire risk is present during days without atmospheric precipitation and air temperature greater than 30 °C (Živanović *et al.*, 2015). Some areas in the summer months can experience more than 15 consecutive days with air temperatures greater than 30 °C, greatly exacerbating the danger for forest fires.

The aim of this study is to determine the vulnerability of forest resources to fire on the basis of extreme climate conditions in the Timočka Krajina region. The results are useful as planning criteria to manage adaptation to extreme climate conditions and reduce the future risk of forest fires.

## 2. The study area

Timočka Krajina is located in the northeastern (NE) region of the Republic of Serbia, between 21° 40' to 22° 46' E, and 43° 20' to 44° 42' N (*Fig. 1*). Timočka Krajina is the geographic area from which the water is flowing into all five Timok (Svrljiški, Trgoviški, Beli, Crni Timok, and Veliki Timok) originates. The Timok region is separated by several natural boundaries, including on the Danube River on the north, the Stara Planina (Old Mountain) and Veliki Timok River to the east (with Bulgaria), the mountain range from Gramade and Svrljiške mountains to Midžor to the south, and the Severnokučajske Mountains to the west (*Manojlović*, 1986). In the area of Timok region (7,130 km<sup>2</sup>), there are two administrative-territorial units, the Bor and Zaječar districts. Specific places and their locations and altitudes are listed in *Table 1*. There are 249,959 residents in this area.

The Timok forested area in 2008 was 3014.79 km<sup>2</sup> covering 42.28% of the territory. Forest cover ranges from a minimum of 25.28% in Negotin to 86.47% in the municipality of Majdanpek. The northeast part of the Republic of Serbia is the Djerdap National Park with nearly untouched flora and fauna. The forest cover stock is large (over 64%) and has an extremely rich and diverse flora (more than 1,100 plant species) and fauna, which carries all the marks of relictness.

The forests are primarily hardwood (76.13%) consisting of 38% beech wood, which is the dominant forest type. Coniferous forests are underrepresented and occupy less than 5% of the forest fund (*RZS*, 2008). In accordance with general European floras, floral elements of the area belong to a pontic South-Siberian group within the Pannonian-Vlach subregion, though some other groups (e.g., sub-Mediterranean, Central European) are represented as a result from migration processes (*Stevanović*, 1999).

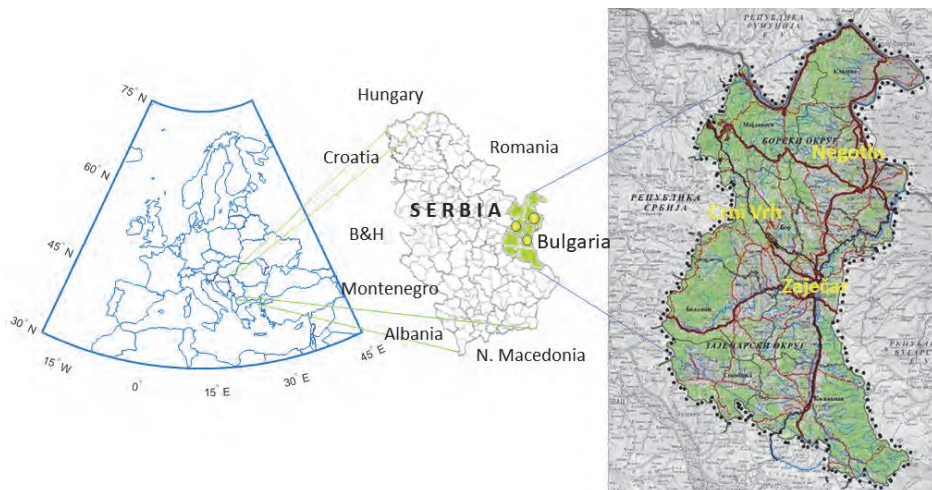


Fig. 1. Timočka Krajina region in northeastern Serbia with location of meteorological stations: Zaječar, Negotin, and Crni Vrh.

Table 1. Geographical location of places in Timočka Krajina with altitude

Place	Latitude ( $\varphi$ )	Longitude ( $\lambda$ )	Altitude [m]
Crni Vrh	44° 07' N	21° 57' E	1037
Negotin	44° 13' N	22° 31' E	42
Zaječar	43° 53' N	22° 18' E	144
Bor	44° 05' N	22° 06' E	378
Knjaževac	43° 30' N	22° 06' E	276
Sokobanja	43° 39' N	21° 52' E	400
Kladovo	44° 37' N	22° 37' E	45
Boljevac	43° 50' N	21° 58' E	349
Majdanpek	44° 25' N	21° 56' E	340
Timočka Krajina region	43°20' – 44°42'N	21°40' – 22°46'E	35 – 1978

Orographic characteristics of this area in northeastern Serbia are shown in Table 2. The largest surface area is found at altitudes from 200 to 500 m. At higher altitudes above 500 m, mountain slopes are very steep. Quality beech wood is preserved in this region (Manojlović, 1986).

Table 2. Surface elevation zones of Timočka Krajina (%)

Place	0–200 (m)	200–500 (m)	500–1000 (m)	1000–1500 (m)	1500–2000 (m)
Bor	1.38	57.22	38.96	2.44	0.00
Kladovo	51.54	46.79	1.67	0.00	0.00
Majdanpek	9.63	58.33	32.04	0.00	0.00
Negotin	43.51	52.68	3.80	0.01	0.00
Zaječar	21.10	71.37	7.39	0.19	0.00
Boljevac	1.16	49.40	48.35	1.10	0.00
Knjaževac	1.26	33.17	57.32	7.03	1.23
Sokobanja	0.00	32.81	61.28	5.90	0.00

### 3. Data and methods used

#### 3.1. Data

Daily air temperature [maximum (*TX*), mean (*TG*), and minimum (*TN*)], precipitation, and relative humidity obtained from three meteorological stations in northeastern Serbia (*Fig. 1*) were analyzed and compared in order to assess changes in climatic conditions. Data were available from 1961 to 2017 for the meteorological stations in Zaječar and Negotin, and from 1982 to 2017 for the Crni Vrh meteorological station situated at the altitude of 1,037 m (*Table 1*). Measurements were performed every day without a break using the same type of instruments. The Serbian Meteorological Service made technical and quality control of these measurements.

#### 3.2. Methods

As a numerical indicator of the degree of dryness of the climate at a given location, annual values of the De Martonne aridity index (*Is*) were determined as (*De Martonne, 1925*):

$$Is = RR / (T + 10), \quad (1)$$

where *RR* is the annual sum of precipitation (mm) and *T* is the mean annual air temperature (°C). Humidity reduces with the decrease in value of *Is*, and vice versa. Climatic classification according to the De Martonne aridity index is shown in *Table 3*. The De Martonne aridity index was shown to give good results for northern Serbia (*Hrnjak et al., 2014*) and central Serbia (*Radaković et al., 2018*), as well as for Greece (*Baltas, 2007*), Romania (*Croitoru et al., 2013*), and Spain (*Moral et al., 2017*).

Table 3. De Martonne index climatic classification

Values of $I_s$	Climate
$I_s < 10$	Arid
$10 \leq I_s < 20$	Semi-arid
$20 \leq I_s < 24$	Mediterranean
$24 \leq I_s < 28$	Subhumid
$28 \leq I_s < 35$	Humid
$35 \leq I_s \leq 55$	Very humid
$I_s > 55$	Extremely humid

The Ångström index ( $I$ ) was used to assess the risk of forest fires and was calculated as (Chandler *et al.*, 1983):

$$I = RH / 20 + (27 - T) / 10, \quad (2)$$

where  $RH$  is the relative humidity (%) and  $T$  is the annual mean air temperature (°C). A reduced index indicates a higher risk of fire (Lukić *et al.*, 2017). The values for  $I$  were translated into fire risk as follows:

- when  $I > 4.0$ , fire occurrence was unlikely;
- when  $2.5 < I \leq 4.0$ , fire conditions were unfavorable;
- when  $2.0 < I \leq 2.5$ , fire conditions were favorable; and
- when  $I \leq 2.0$ , fire occurrence was very likely.

Although the Ångström index is a simple day-to-day fire danger indicator, it was successfully applied for different regions in the central part of Europe: Slovakia (Skvarenina *et al.*, 2003), southern Germany (Schunk *et al.*, 2013), Austria (Arpaci *et al.*, 2013), Serbia (Lukić *et al.*, 2017), etc. The Ångström index might be a good indicator if there are rapid changes in weather situations, which increase the fire danger situation so quickly, that fuel or soil moisture models are not able to capture that moment (Arpaci *et al.*, 2013).

For this study, we used statistical data about forest fires from the Department for Emergency Situations, Ministry of the Republic of Serbia for the period from 2009 to 2017.

To assess extreme fire danger conditions, we used extreme climate indices selected from the list recommended by the World Meteorological Organization (WMO) – Commission for Climatology and the Research Programme on Climate Variability and Predictability (CLIVAR). This paper concentrates on indices that refer to climate change estimates (conditions suitable for the

development of fire): the number of summer days (*SU25*), number of tropical days (*SU30*), number of tropical nights (*TR20*), annual maximum of daily maximum temperatures ( $TX_x$ ), annual minimum of daily minimum temperatures ( $TN_n$ ), precipitation sum (mm), relative humidity (*RH*), wet days (*RR1*), heavy precipitation days (*RR10*), maximum number of consecutive dry days (*CDD*), maximum number of consecutive wet days (*CWD*), and growing season length (*GSL*). Definitions of extreme climate indices are given in *Alexander et al.* (2006) and defined here as follows:

*SU25* - number of summer days: annual count of days with  $TX > 25$  °C;

*SU30* - number of tropical days: annual count of days when  $TX > 30$  °C;

*TR20* - number of tropical nights: annual count of days when  $TN > 20$  °C;

$TX_x$  - annual maximum value of daily maximum temperature;

$TN_n$  - annual minimum value of daily minimum temperature;

*RR1* - wet days: annual count of days with  $RR \geq 1$  mm;

*RR10* - heavy precipitation days: annual count of days when  $RR \geq 10$  mm;

*RRsum* - annual precipitation sum;

*RH* - annual mean relative humidity;

*CDD* - maximum number of consecutive dry days;

*CWD* - maximum number of consecutive wet days, and

*GSL* - growing season length, annual count between first span of at least 6 days with  $TG > 5$  °C and the first span after July 1 of 6 days with  $TG < 5$  °C.

## 4. Results

### 4.1. Climate analysis

The climate of northeastern Serbia is determined by geographic location, distance from the sea, relief, and forest cover. The climate can be described as moderate-continental with major or minor variations. In the lowest parts of the Negotin region and along the Danube and Timok rivers, there is steppe-continental climate. The characteristics of continental climate are determined by the increase in altitude (*Rakićević, 1976*). Continentality of the area is reflected in extreme temperatures. During the winter months, air temperature below  $-10$  °C can last longer than 10 days.

The average annual temperature is 10.8 °C in Zaječar, 11.5 °C in Negotin, and 6.6 °C in Crni Vrh. The warmest month is July and the coldest month is January (*Table 4*). Mean annual precipitation is 606.9 mm in Zaječar, 639.5 mm

in Negotin, and 768.2 mm in Crni Vrh. Maximum precipitation occurs in June or May, while the minimum occurs in January or February (*Table 4*). Mean annual relative humidity is about 75 %, with maximum *RH* in December and minimum in July or August.

*Table 4.* Monthly values of mean temperature (*T*), precipitation sum (*RR*), and relative humidity (*RH*) in: Zaječar (ZA), Negotin (NE), and Crni Vrh (CV)

Month	Station			Station			Station		
	ZA	NE	CV	ZA	NE	CV	ZA	NE	CV
	<i>T</i> (°C)			<i>RR</i> (mm)			<i>RH</i> (%)		
1	-0.9	-0.4	-3.3	41.6	44.4	47.7	80.1	80.4	85.2
2	1.2	1.6	-2.6	41.1	48.8	47.2	77.5	77.6	83.7
3	5.7	6.3	1.0	45.0	51.4	51.2	72.5	71.1	79.0
4	11.4	12.0	6.4	54.3	54.4	70.6	70.0	66.7	73.8
5	16.4	17.2	11.2	65.1	60.6	83.6	71.3	66.7	74.4
6	20.0	20.8	14.5	63.8	63.9	85.0	70.4	64.5	75.3
7	21.8	22.7	16.8	56.8	52.0	69.2	66.7	61.3	70.9
8	21.2	21.9	16.8	41.2	40.8	61.6	67.6	63.0	69.5
9	16.5	17.3	12.2	43.1	50.3	66.9	72.3	68.8	75.4
10	10.6	11.2	7.0	48.6	53.5	70.0	78.2	76.1	82.3
11	5.3	5.8	1.9	53.0	59.5	59.0	81.2	80.7	85.1
12	0.7	1.3	-2.0	53.2	59.8	56.1	82.1	81.7	85.7
Average	10.8	11.5	6.6	606.9	639.5	768.2	74.1	71.6	78.4

The number of days with an average temperature above 10 °C, namely with temperature conditions suitable for the occurrence of forest fires, is about 200 days in Zaječar and Negotin and about 150 days at Crni Vrh. Mean temperatures above 20 °C occur in the summer months for about 94 days in Negotin, 65 days in Zaječar, and 21 days in Crni Vrh.

Annual values of the De Martonne index are presented in *Table 5*. Values of the De Martonne aridity index (*Is*) point to particularly pronounced low annual values in 2011, when for Zaječar and Negotin, *Is* values were less than 20, which characterizes these areas as semi-dry. The year 2014 was very humid with *Is* values greater than 49 (*Table 5*). 2011 and 2017 were dry years. Very few fires were recorded when conditions were extremely wet, as in 2014. From 2011 to 2013, *Is* were extremely low, particularly during the active growing season when the occurrence of forest fires is observed.

Climate indices for Negotin, Zaječar, and Crni Vrh for the base period 1961–1990 and the two years 2012 and 2014 are presented in *Table 6*.

Table 5. Annual aridity index (*I<sub>s</sub>*) according to the De Martonne index

Station	Year								
	2009	2010	2011	2012	2013	2014	2015	2016	2017
Zaječar	36.7	38.0	18.0	28.0	24.6	49.0	23.7	36.1	26.5
Negotin	34.2	33.2	15.8	22.9	30.6	54.7	30.8	32.1	24.4
CrniVrh	56.5	61.3	34.6	42.3	39.3	65.4	42.0	51.3	35.4

Table 6. Climate indices for Negotin, Zaječar, and Crni Vrh for the base period (1961–1990), 2012 and 2014

Parameter	Negotin			Zaječar			Crni Vrh		
	1961-1990	2012	2014	1961-1990	2012	2014	1961-1990	2012	2014
Mean temperature	11.1	13.2	12.7	10.4	11.7	11.4	6.4	7.9	7.4
Absolute maximum temperature $TX_v$	41.2	40.4	34.3	41.9	40.8	33.7	33.8	32.9	27.0
Absolute minimum temperature $TN_n$	-28.5	-27.5	-13.1	-29.0	-25.6	-16.6	-22.2	-22.1	-20.2
Precipitation sum	646.0	532.5	1244.8	610.5	608.7	1046.1	810.1	758.2	1137.4
Tropical nights $TN > 20^\circ\text{C}$	1.7	13	6	0.13	1	0	1.6*	12	2
Tropical days $TX > 30^\circ\text{C}$	29.1	80	32	28.0	80	22	0.8	11	0
Summer days $TX > 25^\circ\text{C}$	95.9	146	99	93.8	144	89	13.7*	49	5
Relative humidity	73.1	64.3	76.5	75.6	68.5	77.9	81.8	74.1	84.9
Daily maximum of precipitation	116.3	42.8	161.3	83.1	40.5	46.5	107.0	64.7	85.8
Number of days $RR > 1.0$ mm	82.0	66	97	82.2	78	111	96.7*	96	125
Number of days $RR > 10.0$ mm	19.4	14	39	19.1	17	37	23.8	22	33
Sunshine length	2035.9	2582.8	1897.8	2050.2	2144.2	1527.4	2016.1	2400.2	1785.3
Number of clear days	77	133	68	66.1	90	32	55.7	107	51
Number of cloudy days	110	87	135	113.1	101	161	141.5	113	152
Consecutive dry days $CDD$	29.5	50	21	29.5	46	18	27.8*	25	21
Consecutive wet days $CWD$	6.4	6	10	5.7	7	5	5.3*	7	7
Growing season length $GSL$	247.6	265	280	245.7	263	281	200.9*	236	219

Numbers with asterics for Crni Vrh are calculated during the period 1982–1990.

During 2012, a high number of tropical days (about 80) and summer days (about 145) were recorded in Negotin and Zaječar. The number of consecutive dry days (*CDD*) in 2012 was almost double that of the 1961–1990 baseline period. In contrast to the dry 2012, precipitation sums in 2014 were greater than 1000 mm, which was high even compared to the 600 mm 1961–1990 annual baseline. The observed maximum daily precipitation was 161.3 mm in Negotin 2014 (*Tošić et al.*, 2017). The number of days when daily precipitation was greater than 10.0 mm in 2014 was double that of the 1961–1990 baseline (*Table 6*).

Climate parameters (*Table 6*) were most impactful to forest ecosystems in 2012 when mean temperature, the number of tropical nights, the number of tropical days (*SU30*), and the number of summer days (*SU25*) were highest, and simultaneously the precipitation sum (*RRsum*), minimum number of wet (*RR1*) and heavy precipitation (*RR10*) days were lowest. The number of consecutive dry days (*CDD*), as well as sunshine length and the number of clear days were highest in 2012. The greatest precipitation, maximum daily precipitation (*RRdmax*), relative humidity (*RH*), and number of cloudy days were observed in 2014 at all three stations (*Table 6*).

Trends for 12 climate indices for Zaječar, Negotin, and Crni Vrh are presented in *Table 7*. Several indices increased at the 5% significance level, including *SU25*, *SU30*, *TX*, *GSL*. Negative trends in *RR1* and *RH* were observed in Zaječar and Negotin. Significant positive trends in *SU25*, *RR10*, *RRsum*, and *RRdmax* were found at Crni Vrh, which is located at an altitude of 1,037 m.

*Table 7.* Trend coefficients of climate indices for Zaječar, Negotin, and Crni Vrh

<b>Index</b>	<b>Zaječar (1961-2017)</b>	<b>Negotin (1961-2017)</b>	<b>Crni Vrh (1982-2017)</b>
<i>SU25</i>	<b>0.5566</b>	<b>0.4821</b>	<b>0.5033</b>
<i>SU30</i>	<b>0.6781</b>	<b>0.6266</b>	0.0400
<i>TX<sub>x</sub></i>	<b>0.0588</b>	<b>0.0520</b>	0.0147
<i>TN<sub>n</sub></i>	0.0178	0.0537	-0.0393
<i>RR1</i>	-0.0731	<b>-0.2568</b>	0.3921
<i>RR10</i>	0.0152	0.0573	<b>0.2956</b>
<i>RRsum</i>	0.3722	0.5831	<b>6.6343</b>
<i>RRdmax</i>	0.0914	0.4934	<b>0.7724</b>
<i>RH</i>	<b>-0.0930</b>	<b>-0.0978</b>	-0.0137
<i>CDD</i>	-0.0006	0.1121	-0.2045
<i>CWD</i>	0.0091	<b>-0.0031</b>	0.0556
<i>GSL</i>	<b>0.4934</b>	<b>0.8131</b>	0.4082

Coefficients being significant at the 5% level are indicated by bold.

#### 4.2. Analysis of forest fires in Timočka Krajina

The occurrence of forest fires in the Timočka Krajina region changes from period to period. The number of forest fires in the territory of Timočka Krajina and Zaječar during the period 2009-2017 is shown in Fig. 2. There was a marked difference in the number of fires in 2012 compared to 2014. Namely, during 2014 only one/zero fire was registered in the Timočka Krajina region/Zaječar, while in 2012, 69/17 fires were recorded.

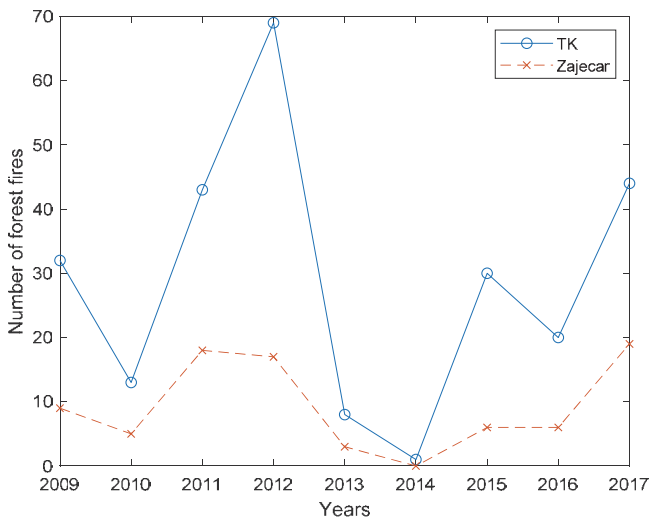


Fig. 2. Number of total forest fires at the territory of Timočka Krajina (TK) and Zaječar during the period 2009-2017.

Daily fluctuations of the Ångström index for Negotin, Zaječar, and Crni Vrh in 2012 and 2014 are presented in Fig. 3. The Ångström index was lower during 2012 indicating that the risk of fire was elevated. For a long period during the growing season of 2012, the Ångström indices were lower than 2.5. The lowest value of the Ångström index (1.02) was observed on September 2, 2012 at Crni Vrh. The longest period with an Ångström index less than 2.5 was in the period from June 21 to July 22, 2012 in Negotin. The Ångström index in 2014 was above 3, which means that the risk of fire was significantly lower in 2014 (Fig. 3).

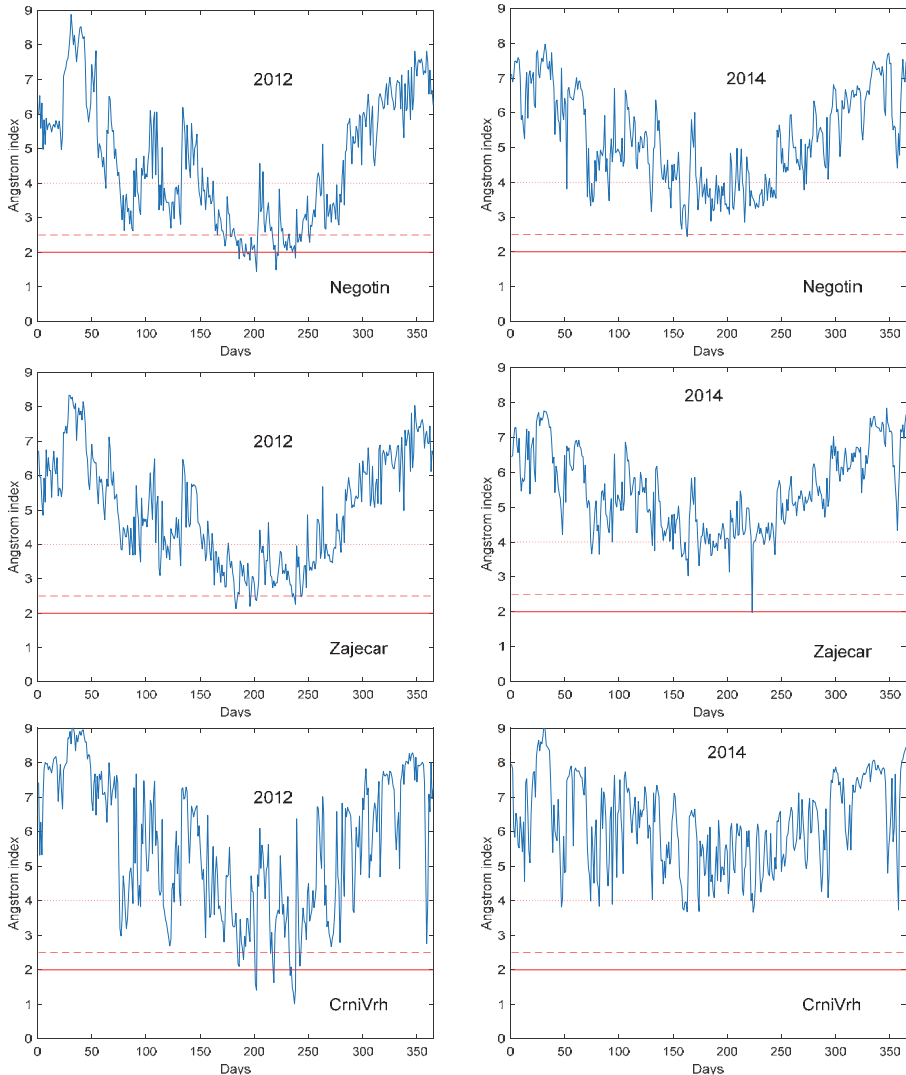


Fig. 3. Time series of the Ångström index for Negotin, Zajecar, and Crni Vrh in 2012 (left) and 2014 (right) with fire danger classes  $I=2.0$  (noted by horizontal solid line),  $I=2.5$  (dashed line), and  $I=4.0$  (dotted line).

## 5. Discussion

This study was motivated by an interest in examining the influence of extreme climate conditions on forest fire risk in northeastern Serbia. A significant increase in summer and tropical days, absolute maximum temperature, and growing season length, and a significant decrease in relative humidity was found

in Zaječar and Negotin. A significant increase in summer days and precipitation indices was found for Crni Vrh. According to the meteorological station in Crni Vrh, this location was considered very humid, which is explained by the high altitude of the station in the Carpathian Mountains (*Radaković et al.*, 2018).

Previous studies of changes in air temperature in Serbia, both average annual and seasonal air temperatures, have clearly indicated an increase (e.g., *Gavrilov et al.*, 2016). The observed warming was also confirmed by the increased frequency of warm extremes (*Unkašević and Tošić*, 2013). The changes taking place were also documented for the whole of Europe (*Klein Tank and Können*, 2003; *Della-Marta et al.*, 2007; *Shevchenko et al.*, 2014; *Tomczyk et al.*, 2019) and globally (e.g., *Alexander et al.*, 2006).

The highest number of tropical nights, number of tropical days, number of summer days, number of consecutive dry days, and the lowest precipitation sums, minimum number of wet and heavy precipitation days were registered in 2012. All these conditions were favorable for the development of fires. The Balkans and the central part of Europe were affected by unprecedented drought in the summer of 2012 (*Unkašević and Tošić*, 2015). The longest heat waves, caused by the flow of warm and dry air from North Africa towards southeastern Europe, were observed during the summer of 2012 in Serbia at ten out of 15 stations (*Unkašević and Tošić*, 2015). More than 1,000 forest fires occurred in Serbia in 2012 (*Lukić et al.*, 2017). The highest number of fires was recorded in 2012, creating the greatest damage with 7,460 ha and 63,118 m<sup>3</sup> wood mass burned (*Šorak and Rvović*, 2016).

The year 2014 was one of the wettest recorded in Serbia (*Tošić et al.*, 2017). The highest values of precipitation sums, daily maximum of precipitation, relative humidity, and number of cloudy days were observed in 2014 at all three stations considered. Precipitation was high during the vegetation period in 2014, and the number of forest fires was smallest.

As a measure of fire risk, the Ångström index provides good results even when using only meteorological variables. Ångström index values in 2012 were below 2.5, indicating favorable fire conditions, while in 2014 they were above 3, indicating that the risk of fire was significantly lower. Replacing *TX* instead of *TG* in definition of the Ångström index provides better results. Values of the Ångström index were below 2 for Zaječar (*Fig. 4*), indicating very favorable fire conditions during the summer of 2012 when 17 forest fires were recorded (*Fig. 3*). In addition, the minimum Ångström index value was not below 2 (*Fig. 4*) compared to 2014 (*Fig. 3*) when no forest fires were registered in Zaječar (*Fig. 2*).

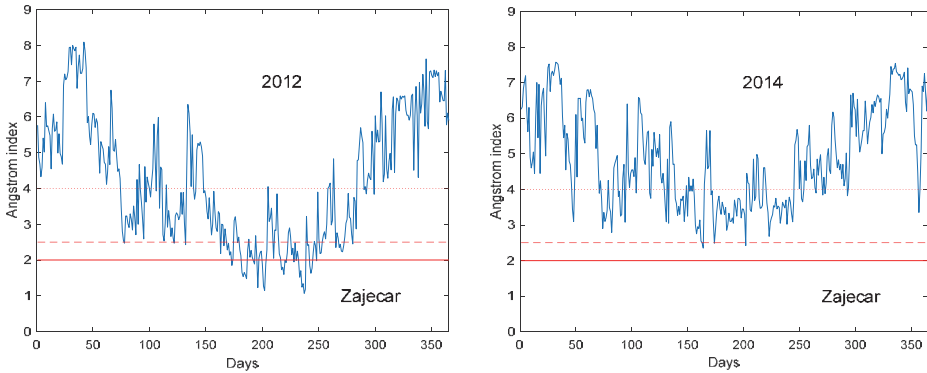


Fig. 4. Time series of the Ångström index (with  $T_X$  instead of  $T_G$ ) for Zajecar in 2012 (left) and 2014 (right) with fire danger classes  $I=2.0$  (noted by horizontal solid line),  $I=2.5$  (dashed line), and  $I=4.0$  (dotted line).

Živanović *et al.* (2020) suggested that increased air temperature and reduced precipitation in the period 1981–2010 compared to the period 1961–1990 had substantial influence on the probability of fire occurrence in Serbia. They have also concluded that particular attention has to be paid to the eastern and southern parts of Serbia, where the decrease in precipitation was greatest.

## 6. Conclusions

Extreme climate conditions are crucial for forecasting and managing forest potential in Serbia, and posing a challenge for policy makers. If extreme climate effects are implemented in risk assessments of forest fires, adverse effects can be minimized. Many climate scenarios predict further increases in the frequency of climate extremes in the future, and it is necessary to take adequate measures to adapt.

Our research reveals that understanding extreme climate conditions and their impact on the occurrence of forest fires are important variables to consider when selecting adaptation strategies. Determining priorities for adaptation measures and their implementation are of great importance. Forest protection should be based on good organization and a hierarchy of responsibility for planning and implementing preventive and repressive measures to protect forests from fire. Evaluation of impacts of extreme climate conditions that are conducive to the emergence and spread of forest fires has particular importance. Synoptic situation unfavorable to the occurrence of forest fires are those that

occur because of long dry periods with high air temperatures and low relative humidity. Our study showed that the Ångström index calculated with meteorological variables only provided a good indicator for forecasting forest fires. Better results were obtained when the daily maximum temperature instead of daily mean temperature were included in the definition of the Ångström index. The competent authorities for the protection of forests against fire in Serbia should define indices to assess climate extremes that can be used to estimate conditions indicative of extreme fire danger (with the levels of risk of danger). Successful implementation of the strategies for adaptation to extreme climate conditions should lead to the active promotion and education of the population by the competent institutions.

**Acknowledgements:** This study was supported by the Serbian Ministry of Science, Education and Technological Development, under Grant No. 176013. The authors appreciate the efforts of anonymous reviewer in improving this manuscript.

## *References*

- Aleksić, V., Milutinović, S., Marić, M. and Dorđević, N., 2004: Drought in the Timok region and its impact on crop production. Proceedings of the Conference with international participation 'Ecological truth', Borsko jezero, 224–228.
- Alexander, L., Zhang, X., Peterson, T.C., Caesar, J., Gleason, B., Klein Tank, A.M.G., Haylock, M., Collins, D., Trewin, B., Rahimzadeh, F., Tagipour, A., Rupa Kumar, K., Revadekar, J., Griffiths, G., Vincent, L., Stephenson, D.B., Burn, J., Aguilar, E., Brunet, M., Taylor, M., New, M., Zhai, P., Rusticucci, M. and Vazquez-Aguirre, J.L., 2006: Global Observed Changes in Daily Climate Extremes of Temperature and Precipitation. *J. Geophys. Res.* 111, D05109. <https://doi.org/10.1029/2005JD006290>
- Arpaci, A., Eastaugh, C.S., and Vacik, H., 2013: Selecting the best performing fire weather indices for Austrian ecoregions. *Theor. Appl. Climatol.* 114, 393–406. <https://doi.org/10.1007/s00704-013-0839-7>
- Baltas, E., 2007: Spatial distribution of climatic indices in northern Greece. *Meteorol. Appl.* 14, 69–78. <https://doi.org/10.1002/met.7>
- Bartholy, J. and Pongrácz, R., 2007: Regional analysis of extreme temperature and precipitation indices for the Carpathian Basin from 1946 to 2001. *Glob. Planet. Change* 57, 83–95. <https://doi.org/10.1016/j.gloplacha.2006.11.002>
- Chandler, C., Cheney, P., Thomas, P., Trabaud, L., and Williams, D., 1983: Fire in forestry. Vol. I, John Wiley & Sons. Inc., Canada.
- Carnicer, J., Coll, M., Ninyerola, M., Pons, X., Sanchez, G., and Penuelas, J., 2011: Widespread crown condition decline, food web disruption, and amplified tree mortality with increased climate change-type drought. Proceedings of the National Academy of Science of USA (PNAS) 108, 1474–1478. <https://doi.org/10.1073/pnas.1010070108>
- Croitoru, A.E., Pițicar, A., Imbroane, A.M. and Burada, D.C., 2013: Spatiotemporal distribution of aridity indices based on temperature and precipitation in the extra-Carpathian regions of Romania. *Theor. Appl. Climatol.* 112, 597–607. <https://doi.org/10.1007/s00704-012-0755-2>
- De la Cruz, A., Gil, P.M., Fernandez-Cancio, A., Minaya, M., Navaro-Cerrillo, R.M., Sanchez-Salguero, R., and Grau, J.M., 2014: Defoliation triggered by climate induced effects in Spanish ICP Forests monitoring plots. *Forests Ecol. Manag.* 331, 245–255. <https://doi.org/10.1016/j.foreco.2014.08.010>
- De Martonne, E., 1925: Traité de géographie physique, Vol. I: Notions generales, climat, hydrographie. *Geogr. Rev.* 15, 336–337.

- Della-Marta, P. M., Haylock, M. R., Luterbacher, J., and Wanner, H., 2007: Doubled length of western European summer heat waves since 1880. *J. Geophys. Res.*, *112*, D15103  
<https://doi.org/10.1029/2007JD008510>
- Djordjević, V., Vuković, A., and Vujadinović-Mandić, M., 2015: Climate change scenarios – impacts and adaptation. Proceedings: Planska i normativna zaštita prostora i životne sredine, 16-18 April 2015, Subotica, Serbia, 29–35.
- Easterling, D.R., Meehl, G.A., Parmesan, C., Chagnon, S.A., Karl, T., and Mearns, L.O., 2000: Climate extremes: Observation, modelling and impacts. *Science* *289*, 2068–2074.  
<https://doi.org/10.1126/science.289.5487.2068>
- Finkel, J.M. and Katz, J.I., 2018: Changing world extreme temperature statistics. *Int. J. Climatol.* *38*, 2613–2617. <https://doi.org/10.1002/joc.5342>
- Gavrilov, M.B., Tošić, I., Unkašević, M., Marković, S.B., and Petrović, P., 2016: The analysis of annual and seasonal temperature trends using the Mann-Kendall test in Vojvodina, Serbia. *Időjárás* *120*, 183–198.
- Hrnjak, I., Lukić, T., Gavrilov, M.B., Marković, S.B., Unkašević, M. and Tošić, I., 2014: Aridity in Vojvodina, Serbia. *Theor. Appl. Climatol.* *115*, 323-332.  
<https://doi.org/10.1007/s00704-013-0893-1>
- IPCC, 2007: Climate change 2007. Impacts, adaptation and vulnerability. Cambridge University press. New York, USA.
- Kadović, R. and Medarević, M., 2007: Forests and climate change. Proceedings of papers, Ministry of agriculture, forestry and water management of Republic of Serbia, Faculty of Forestry, Belgrade, 1–206.
- Keeley, J.E., 2004: Impact of antecedent climate on fire regimes in coastal California. *Inter. J. Wildland Fire* *13*, 173–182. <https://doi.org/10.1071/WF03037>
- Klein Tank, A.M.G., and Können, G.P., 2003: Trends indices of daily temperature and precipitation extremes in Europe, 1946–99. *J. Climatol.*, *16*: 3665–3680.  
[https://doi.org/10.1175/1520-0442\(2003\)016<3665:THODT>2.0.CO;2](https://doi.org/10.1175/1520-0442(2003)016<3665:THODT>2.0.CO;2)
- Lukić, T., Marić, P., Hrnjak, I., Gavrilov, M.B., Mladan, D., Zorn, M., Komac, B., Milošević, Z., Marković, S.B., Sakulski, D., Jordaan, A., Đorđević, J., Pavić, D. and Stojšavljević, R., 2017: Forest fire analysis and classification based on a Serbian case study. *Acta Geogr. Slov.* *57*, 1–13.  
<https://doi.org/10.3986/AGS.918>
- Manojlović, P., 1986: Severoistočna Srbija-fizičko-geografske karakteristike. Istorijski arhiv Krajine, Ključa i Poreča, Negotin (in Serbian).
- McKenzie, D., Gedalof, Z., Peterson, D.L., and Mote, P., 2004: Climatic change, wildfire, and conservation. *Conserv. Biol.* *18*, 890–902. <https://doi.org/10.1111/j.1523-1739.2004.00492.x>
- Moral, F.J., Paniagua, L.L., Rebollo, F.J., and García-Martín, A., 2017: Spatial analysis of the annual and seasonal aridity trends in Extremadura, southwestern Spain. *Theor. Appl. Climatol.* *130*, 917–932. <https://doi.org/10.1111/j.1523-1739.2004.00492.x>
- Moritz, M.A., 2003: Spatio-temporal analysis of controls on shrubland fire regimes: age dependency and fire hazard. *Ecology* *84*, 351–361.  
[https://doi.org/10.1890/0012-9658\(2003\)084\[0351:SAOCOS\]2.0.CO;2](https://doi.org/10.1890/0012-9658(2003)084[0351:SAOCOS]2.0.CO;2)
- Popović, T., Radulović, E., and Jovanović, M.M., 2005: How much is changing climate, what will be our future climate? EnE05 – Conference Environment towards Europe, Belgrade, 212–218.
- Popović, T., Živković, M., and Radulović, E., 2008: Serbia and global warming. Sustainable development and climate change, Niš, June 2008, 47–54.
- RZS, 2008: Statistical office of the Republic of Serbia, Statistical Yearbook, Belgrade, 2002–2008.
- Radaković, M., Tošić, I., Bačević, N., Mladjan, D., Gavrilov, M.B. and Marković, S., 2018: The analysis of aridity in Central Serbia from 1949 to 2015. *Theor. Appl. Climatol.* *133*, 887–898.  
<https://doi.org/10.1007/s00704-017-2220-8>
- Rakićević, T., 1976: Climate characteristics of Eastern Serbia. *Journal of the Geographical Institute "Jovan Cvijić" SASA* *28*, 41–67.
- Santos, C.A.C., Neale, C.M.U., Roca, T.V.R. and da Silva, B.B., 2011: Trends in indices for extremes in daily temperature and precipitation over Utah, USA. *Int. J. Climatol.* *31*, 1813–1822.  
<https://doi.org/10.1002/joc.2205>

- Schunk C., Wastl C., Leuchner M., Schuster C., and Menzel A., 2013: Forest fire danger rating in complex topography – results from a case study in the Bavarian Alps in autumn 2011. *Nat. Hazards Earth Syst. Sci.* 13, 2157–2167. <https://doi.org/10.5194/nhess-13-2157-2013>
- Seidling, W., 2007: Signals of summer drought in crown condition data from the German Level I network. *Eur. J. For. Res.* 126, 529–544. <https://doi.org/10.1007/s10342-007-0174-6>
- Skvarenina, J., Mindas, J., Holec, J., and Tucek, J., 2003: Analysis of the natural and meteorological conditions during two largest forest fire events in the Slovak Paradise National Park. In: *Forest Fire in the Wildland-Urban Interface and Rural Areas in Europe: An Integral Planning and Management Challenge*, Institute of Mediterranean Forest Ecosystems and Forest Products Technology, Athens, Greece, 15–16 May 2003, 29–36.
- Shevchenko, O., Lee, H., Snizhko, S., and Mayer, H., 2014: Long-term analysis of heat waves in Ukraine. *Int. J. Climatol.* 34, 1642–1650. <https://doi.org/10.1002/joc.3792>
- Stevanović, V., 1999: *Red Book of Flora of Serbia*. Institute for Nature Conservation of Serbia, Belgrade.
- Šorak, R. and Rvović, I., 2016: A damage analysis of wildfires in the Republic of Serbia for the 2010–2014 period. *Res. Rev. Dep. Geogr. Tourism Hotel Manage.* 45, 1–10.
- Tabaković-Tošić, M., Marković, M., Rajković, S. and Veselinović, M., 2009: Wildfires in Serbia – chance or frequent phenomenon. *Sustainable forestry*, Proceedings 59–60, Institute for Forestry, Belgrade, 97–125.
- Tomczyk, A.M., Kendzierski, S., Kugiejko, M., and Pilguy, N., 2019: Thermal conditions in the summer season on the Polish coast of the Baltic Sea in 1966–2015. *Időjárás* 123, 57–72. <https://doi.org/10.28974/idojaras.2019.1.4>
- Tošić, I., Unkašević, M., and Putniković, S., 2017: Extreme daily precipitation: the case of Serbia in 2014. *Theor. Appl. Climatol.* 128, 785–794. <https://doi.org/10.1007/s00704-016-1749-2>
- Unkašević, M. and Tošić, I., 2013: Trends in temperature indices over Serbia: relationships to large-scale circulation patterns. *Int. J. Climatol.* 33, 3152–3161. <https://doi.org/10.1002/joc.3652>
- Unkašević, M. and Tošić, I., 2015: Seasonal analysis of cold and heat waves in Serbia during the period 1949–2012. *Theor. Appl. Climatol.* 120, 29–40. <https://doi.org/10.1007/s00704-014-1154-7>
- Vasić M., 1992: *Wildfires*. University of Belgrade, Faculty of Forestry, Belgrade, p.105.
- Vuković, A., Vujadinović, M., Rendulić, S., Djurdjević, V., Ruml, M., Babić, V., and Popović, D., 2018: Global Warming Impact on Climate Change in Serbia for the period 1961–2100. *Therm. Sci.* 22, (6A), 2267–2280. <https://doi.org/10.2298/TSCI180411168V>
- Yan, Z., Jones, P.D., Davies, T.D. et al. (2002) Trends of extreme temperatures in Europe and China based on daily observations. *Clim. Chang* 53, 355–392. [https://doi.org/10.1007/978-94-010-0371-1\\_13](https://doi.org/10.1007/978-94-010-0371-1_13)
- Živanović, S., 2012: Analysis of climate change elements to prediction of forest fires. *Topola* 189/190, 163–170.
- Živanović, S., 2015: Evaluating the impact of climate vulnerability of forest fire. *Acta Agriculturae Serbica*, Vol. XX, 39, 17–28. <https://doi.org/10.5937/AASer1539017Z>
- Živanović, S., Gocić, M., Ivanović, R. and Martić-Buršač, N., 2015: The effect of air temperature on forest fire risk in the municipality of Negotin. *Bull. Serbian Geograph. Soc.* 95, 67–76. <https://doi.org/10.2298/GSGD1504067Z>
- Živanović, S., 2017: Impact of drought in Serbia on fire vulnerability of forests. *Int. J. Bioautomation* 21, 217–226.
- Živanović, S., Gocić, J.M., Vukin, M. and Babić, V., 2018: The importance of the knowledge of the effects of moisture conditions on the frequency and intensity of forest fires. *Forestry*, University of Belgrade-Faculty of Forestry, LXX (3-4), 127–136.
- Živanović, S., Ivanović, R., Gocić, M., Đokić, M. and Tošić, I., 2020: Influence of air temperature and precipitation on the risk of forest fires in Serbia. *Meteorol. Atmos. Phys.* In Press. <https://doi.org/10.1007/s00703-020-00725-6>



# IDŐJÁRÁS

*Quarterly Journal of the Hungarian Meteorological Service  
Vol. 124, No. 3, July – September, 2020, pp. 349–361*

## Dependent weighted bootstrap for European temperature data: is global warming speeding up?

Csilla Hajas<sup>1</sup> and András Zempléni<sup>2,\*</sup>

<sup>1</sup> *Eötvös Loránd University  
Faculty of Informatics  
Department of Information Systems  
Pázmány Péter sétány 1/C, H-1117 Budapest, Hungary*

<sup>2</sup> *Eötvös Loránd University  
Faculty of Science, Department of Probability Theory and Statistics  
Pázmány Péter sétány 1/C, H-1117 Budapest, Hungary*

*\*Corresponding author E-mail: zempleni@caesar.elte.hu*

*(Manuscript received in final form October 23, 2019)*

**Abstract**—Temperature changes are in the focus of climate research. There are many analyses available, but they rarely apply rigorous mathematics for assessing the results.

The main approach of this paper is the dependent weighted bootstrap. It is a simulation method, where both the fitted regression and the dependency among the data are taken into account. We present a simulation study showing that for serially dependent data it is the most accurate in case of estimating the coefficient in a linear regression.

This paper shows an analysis of the gridded European temperature data. We have used the  $0.5^\circ \times 0.5^\circ$  grid of daily temperatures for 68 years (from 1950 to 2017), created by the European Climate Assessment. We investigated the speed of the global warming by changing the starting point of the linear regression. The significance of the differences between the coefficients was tested by the dependent weighted bootstrap. We have shown that the acceleration was significant for large regions of Europe, especially the central, northern and western parts.

The vast amount of results is summarized by a Gaussian model-based clustering, which is the suitable approach if we intend to have clusters that are spatially compact. The number of clusters was chosen as 13, by a suitably modified "elbow rule". This approach allows to compare the speed and acceleration of warming for different regions. The quickest warming in the last 40 years was observed in Central and Southwestern Europe, but the acceleration is more pronounced in Central Europe.

*Key-words:* dependent weighted bootstrap, global warming, linear models, model-based clustering

## 1. Introduction

Determining the speed of global warming is a very important and actual question, especially if significance of estimators is also tested. As mathematicians, we cannot give exact explanations for the changes, but we may try to reveal them and to estimate the statistical error of the estimates. This estimation is not easy at all, as in the data set there are various types of dependencies, which make the use of standard statistical techniques difficult.

Our main aim is to find those mathematical methods, which are most suitable for checking the significance of our results. There are numerous works in the area (see, e.g., *Lu et al.*, 2005), where possible changepoints are introduced to capture the nonlinearity of monthly U.S. temperature data. We are convinced that using daily observations is worth for the efforts, as they convey much more information than, e.g., monthly or annual data.

Our approach is to capture the temporal changes by regression models, and then the spatial aspects can be taken into account by clustering. There are, of course, other approaches in the literature, where the spatial aspects are taken into consideration first (see, e.g., *Jun et al.*, 2008), but our focus of attention is in the significance investigations for the univariate time series with complex and unknown dependence structure. For similar but monthly time series, *Lund et al.* (1995) investigated the so-called periodic correlation structure. Their approach results in general  $3p$  parameters, where  $p$  is the period. In our case  $p = 365$ , thus the number of parameters would be uncontrollable - considering that all are to be estimated for every grid point. Our model has about 60 parameters for the observation sites, which seems to be a good compromise.

The mathematical model in our case is the linear regression - not only for the whole, standardized data set, but for altogether 30 shorter data sets, which were got by omitting the first years sequentially, i.e., the  $k$ th set consists of the years  $(1950+k, \dots, 2017)$ . The main motivation behind this approach is that the actual changes are not easily captured by the commonly used functions (e.g., quadratic models cannot cope well with the complex structure of this data). Using this method we can detect if there is a change in the speed of the warming. For assessing the reliability of the results, we investigate different bootstrap approaches. We have to take care on the dependence in the data - the traditional solution to this phenomenon is the block bootstrap, covered in the book of *Lahiri* (2003). However, for the case of regression models, a new weighted bootstrap method has been developed by *Wu* (1986). A more recent approach by *Shao* (2010) is suitable for the case of dependent residuals - this is the one we used for assessing the reliability of the results and the significance of the change in speed of the temperature increase.

We are also interested in the spatial patterns of the processes. Thus, in Subsection 2.2 we apply a Gaussian model-based clustering (see, e.g., *Fraley and Raftery*, 2007) to the sequence of estimated coefficients.

We give details of the used models in Section 2. Section 3 is devoted to a simulation study on the bootstrap methods. Section 4 is about our results for the modeling of the temperature data. In Section 5 we formulate the conclusions.

## 2. Methods

In this section we briefly introduce the used methods. There is no need to introduce the linear models, as they are well-known to everyone. However, in order to assess the accuracy of the results we got by them, we needed special tools, as the data are both serially and spatially dependent. These will be explained in detail below.

### 2.1. Bootstrap

Bootstrap is a resampling method that can be used for assessing the properties of the estimators. There are many variants of the original idea of *Efron* (1979). One approach, designed especially for assessing the reliability of regression models is the weighted bootstrap of *Wu* (1986). However, all these standard methods are suitable only for the case of independent and identically distributed errors. In case of heteroscedasticity and/or dependency among the random error terms, the standard methods fail, as it is seen by our simulation study as well as in the classical paper of *Singh* (1981).

The dependent weighted bootstrap is suitable for these cases by choosing a resampling method that is capable of reproducing the dependence of the original observations. This is a relatively new concept, first introduced by *Shao* (2010). The traditional tool for such cases was the block bootstrap, which itself has several variants. There are available algorithms for choosing the block size, which minimize the standard error of the bootstrap estimators (*Politis and White*, 2004). However, it is reported in *Shao* (2010), that the new dependent weighted bootstrap has more favorable properties. We also check the methods in case of the linear regression, when we assume dependency among subsequent residuals. It turns out – as shown by our simulations – that the confidence intervals, based on the proposed weighted dependent bootstrap, have better coverage properties in the investigated cases.

In its original form (*Wu*, 1986), the weighted bootstrap sample was constructed from the estimated residuals of the regression model  $r_i$  ( $i = 1, \dots, n$ , where  $n$  denotes the number of observations), by multiplying them with the weights  $w_i$ , which were supposed to be i.i.d. (identically distributed), with  $E(w_i) = 0$  and  $Var(w_i) = 1$ . These properties ensure that for the bootstrapped residuals  $w_i r_i$ , we have  $E(w_i r_i) = 0$  and  $Var(w_i r_i) = Var(r_i)$ . A natural choice may be the  $w_i$ , for which  $P(w_i = 1) = P(w_i = -1) = 0.5$ , thus practically choosing the same residuals as observed, but with random signs. There are of course other possible choices for the distribution of  $w$  (for details see *Wu*, 1986).

However, when the error terms are dependent, the simple method seen above does not work. The bootstrap data generating process must correspond to that of the observations. This can be achieved by the dependent weighted bootstrap, where the conditions  $E(w_i) = 0$  and  $Var(w_i) = 1$  still hold, but a dependence structure is assumed for the weights  $w_i$ . In the original paper, Shao proposed a multivariate normal distribution, with covariance matrix

$$cov(w_i, w_j) = K\left(\frac{i-j}{l}\right), \quad (1)$$

where  $K$  is a kernel function and  $l$  is a suitable norming factor (bandwidth). The generation of many dependent normal variates having such a covariance structure can be realized using the circular embedding algorithm of *Dietrich et al.* (1997), which is implemented in the R package `RandomFields`.

The theoretical properties (consistency) of the dependent weighted bootstrap were proved originally by Shao under somewhat strong conditions ( $m$ -dependency of the weights), applicable, e.g., to the triangular kernel function. However, it has also been proved recently (*Doukhan et al.*, 2015), that the method works for a simpler data generating process as well. Namely, the weights may come from an AR(1) series:  $w_{i+1} = rw_i + \sqrt{(1 - r^2)}\varepsilon_i$ , where  $\varepsilon_i$  is an i.i.d. sequence of normal distributions. The role of  $r$  is similar to that of  $l$ , they both determine the length of the memory in the sequence: a large  $r$  as well as a large  $l$  implies longer range dependence. Thus, the cases we investigate here have also favorable asymptotic properties.

One important problem is yet to be solved: how should we choose the parameter  $l$ ? We have faced a similar question in the paper of *Rakonczai et al.* (2014), where the block size of the bootstrap resampling had to be found. We determined it by the best fitting AR model (VAR in the bivariate case). The fit was measured by the variance of the estimator  $\bar{X}$  (or the trace of its covariance matrix in the bivariate case). To be more exact, in *Rakonczai et al.* (2014), the block size was determined as the  $\hat{b}$ , for which the estimated trace of the bootstrap covariance matrix was the nearest to the one derived from the fitted VAR model

$$\hat{b} = \operatorname{argmin}_{1 \leq b \in Z} \left| \operatorname{tr} \left( \operatorname{Cov}(\bar{X}_{VAR}) \right) - \operatorname{tr} \left( \operatorname{Cov}_*(\bar{X}_b^*) \right) \right|, \quad (2)$$

where  $\operatorname{Cov}_*(\bar{X}_b^*) = \operatorname{Cov}_*(\bar{X}_b^* | x_n)$  (\* refers to the bootstrap sample, i.e., the left hand side gives the covariance of the bootstrap sample based on block size  $b$ , under the observed sample  $x_n$ ). In this paper we have modified (2) on a way that the parameter was  $l$  from the kernel and to be able to estimate the variance of the mean, we fitted an AR(1) model to the data

$$\hat{l} = \operatorname{argmin}_{1 < l < 1} \left| \left( \operatorname{Var}(\bar{X}_{AR}) \right) - \left( \operatorname{Var}_*(\bar{X}_l^*) \right) \right|. \quad (3)$$

## 2.2. Clustering

Our data are spatio-temporal. Spatio-temporal data mining has been developed in the last few years (see for example *Shekhar et al.*, 2011) or Chapter 10 in the book *Giannotti and Pedreschi* (2008). However, we prefer to use a simple, yet suitable and classical data mining tool, the clustering. The first idea for spatial clustering is to apply the density-based methods. However, it turned out that we have not got any valuable results by these methods. Thus, we rather applied the  $k$ -means clustering. This is a traditional, simple, and quick method even in our case of over 20000 data points in the 30 dimensional space. The method turned out to be suitable for detecting areas sharing similar properties, thus, also the spatial aspects were included in the analysis, especially when we used the model-based clustering. Here it is assumed, that the observations come from a multivariate normal distribution, with different parameters. The main question is if the covariances of the clusters are equal or different, and if different, what is the difference. Volume, shape, and orientation are the three aspects considered.

When applying the  $k$ -means clustering, it is a non-trivial question, how to determine the number of clusters. One may use the traditional elbow rule, based on the portion of the explained variance. The model-based clustering suggests a solution to this problem, as here an adapted version of the Bayesian information criterion (BIC) may be applied (see *Fraley and Raftery*, 2007). The method is implemented in the `mclust` package of R. BIC is traditionally defined here as the expression

$$B = 2 \log(L) - m \log(n),$$

where  $L$  denotes the value of the likelihood function at the optimum,  $n$  is the number of observations, and  $m$  the number of parameters in the model ( $B$  is  $-1$  times the "usual" BIC for regression model). So, in this approach the model with the largest BIC value is suggested to be chosen. However, in our case – most likely due to the vast amount of data – the BIC proposes a large number of clusters (around 100), so we came back to the old "elbow rule" and chose a clustering, after which the increase in the BIC is slowed down.

In our case, the results clearly proved that the model-based approach resulted in identifiable areas as clusters, which is very much preferred.

### 3. Simulations

First we checked the classical case, where the errors in the linear model are indeed independent and identically distributed. An independent sample with  $n = 100$  from the model  $y = x + \varepsilon$  was simulated, with  $\varepsilon \sim N(0; 1)$ . The investigated methods were chosen so that the parameters are near to the ones used for the real data analysis:

1. the simple Efron-type bootstrap;
2. the weighted bootstrap for the residuals;
3. the dependent weighted bootstrap with AR(1) structure for the weights and normal innovations, as  $w_n = 0.9w_{n-1} + \sqrt{0.19}\eta_n$ , where  $\eta_n$  is an i.i.d. standard normal;
4. the dependent weighted bootstrap with multivariate normal weights, the covariance was given by  $\sigma_{i,j} = 1 - |i - j|/l$  for  $l = 25$ .

It can be seen from *Table 1*, that both the Efron-type and the independent weighted bootstrap give accurate results, while the intervals based on the two dependent weighted bootstrap methods are too narrow, which underlines that their application is unnecessary, if independence can be accepted. However, the difference is not too large.

*Table 1.* The effect of bootstrap type on the estimated confidence interval for the trend coefficient (now 1) in case of i.i.d. normally distributed error structure. For the dependent weighted bootstrap, the AR(1) coefficient was 0.9. The dependence for the multivariate normal weighted case was given by Eq.(1) with the triangular kernel. The number of repetitions was  $n = 500$

Method conf.bound	Theoretical value	Efron	indep. weighted	AR(1) weighted	Mvnorm weighted
lower	0.931	0.933	0.934	0.947	0.952
upper	1.066	1.065	1.065	1.051	1.045

Next we have simulated sequences of length  $n = 23360$  (the number of observations in our data set) with AR(1) structure for the residuals with  $r = 0.812$  (the average of our estimators) and a trend coefficient of  $8.6 * 10^{-5}$  (again a typical value for our data set). The repetition size was 500, and we compared the performance of the three bootstrap methods, including the block-bootstrap with

the optimal block size, based on the algorithm of *Politis and White* (2004). The results are shown in *Table 2*, containing  $10^5$ -times the estimated values. Here we can observe the superiority of the weighted bootstrap, as it reproduces the theoretical quantiles the best – and the differences here are much more substantial than those of *Table 1*.

*Table 2.*  $10^5$  times the theoretical and estimated quantiles for the trend coefficient in case of normally distributed AR(1) error structure with  $r = 0.812$  and a trend coefficient of  $8.6 * 10^{-5}$ . The block bootstrap is too conservative with extreme quantiles; the independent weighted bootstrap on the other hand is too optimistic. The dependent weighted bootstrap (with the AR(1) dependence, determined by Eq. (3) turned out to be the best. The number of repetitions was 500.

<b>method quantile</b>	<b>0.025</b>	<b>0.05</b>	<b>0.25</b>	<b>0.5</b>	<b>0.75</b>	<b>0.95</b>	<b>0.975</b>
<b>AR(1) process</b>	6.64	6.95	8.05	8.53	9.12	10.11	10.43
block bootstrap	5.34	5.64	7.72	8.86	10.39	12.19	12.62
indep. weighted boot	7.62	7.75	8.30	8.61	8.94	9.41	9.50
dep. weighted boot	6.74	7.14	8.13	8.77	9.40	10.22	10.47

#### ***4. Applications***

Temperature changes are in the focus of attention since global warming became a major threat to the ecosystem on Earth. There is a tremendous amount of information available on the subject (see, e.g., *Weart*, 2017 and the references therein), showing that the temperature sequences have started to rise from as early as 1960s. There are opinions about the link between NAO (North Atlantic Oscillation) index and low frequency variability of the climate (see, e.g., *Cohen and Barlow*, 2005). In our previous manuscript (*Hajas and Zempléni*, 2018) as a comparison, we have also investigated the residuals, after having removed the effect of the daily NAO index on the temperature time series. This effect was not substantial, but the use of these data allowed for checking the robustness of the results.

The used observations are 68 years of daily temperature data of the European Climate Assessment from 1950 to 2017 (E-OBS, <http://www.ecad.eu>). We have used the  $0.5^\circ \times 0.5^\circ$  grid data, available for Europe and parts of Northern Africa. This gridded database can be considered as a standard for climate analysis (see

Haylock et al., 2008). Its quality has been evaluated in Hofstra et al. (2009), and the results show that it may be considered reliable for most of Europe. However, especially in the African and Near Eastern region, there are missing periods of various length, which have to be taken into account. An earlier version of the same temperature data set was used in Varga and Zempléni, (2017), where the changes in the bivariate dependence structure were analyzed.

We have not investigated the time series in detail, but it is obvious that seasonality is its most important feature. So first we have standardized the data for every day of the year by simple nonparametric polynomial (Loess) smoothing, using both first- and second-order standardization for each grid point separately:  $x_{aT+t} = (y_{aT+t} - m_t)/s_t$ , where  $T = 365$  and  $1 \leq t \leq 365$  represents the day of the year.  $m_t$  and  $s_t$  is the smoothed mean and standard deviation for day  $t$ , respectively.

These standardized daily data were used as a basis for the simple linear regression:  $x_{aT+t} = \alpha(aT + t) + \beta$ . We are interested in the steepness of the regression line (measured by the estimated coefficient  $\hat{\alpha}$ ), as well as in the strength of the model (as shown by the coefficient  $R^2$ ). These parameters were calculated for the data we have got by omitting the first  $k$  years ( $k = 1, \dots, 30$ ): i.e., in the  $k$ th equation we consider data from year  $k + 1$  till 68, so the last model corresponds to approximately the last 40 years. This approach is motivated by the fact that the time series exhibit many features like abrupt changes or temporal decrease (especially in the first half of the data set), that are not possible to be captured by a seemingly simple quadratic regression.

The maximum value of the estimated regression coefficients together with the time of their occurrence is shown for each grid point in Fig. 1. We see that these maximal values occur for most of the cases at the very end of the investigated period. We have checked the reliability of the results for a grid of  $10^\circ \times 10^\circ$  (the black rectangle on the right hand panel of Fig. 1) (using the weighted dependent bootstrap), and it turned out that for over 66% the grid points, at least 95% of the simulations gave at least  $k = 27$  as the time point of the maximum, showing that the high values of the right hand side of Fig. 1 have not just been resulted by chance.

A similar plot for the strength of the model is Fig. 2. Not surprisingly, we see the larger values mostly in the regions with higher coefficients. The low values of  $R^2$  are quite natural, as there are many more nonlinear disturbances in the weather, compared to the relatively slow but steady global warming. It is interesting that for large areas of Western Europe we see an early occurrence, while the typical time points for Central and Northern Europe are again the late ones.

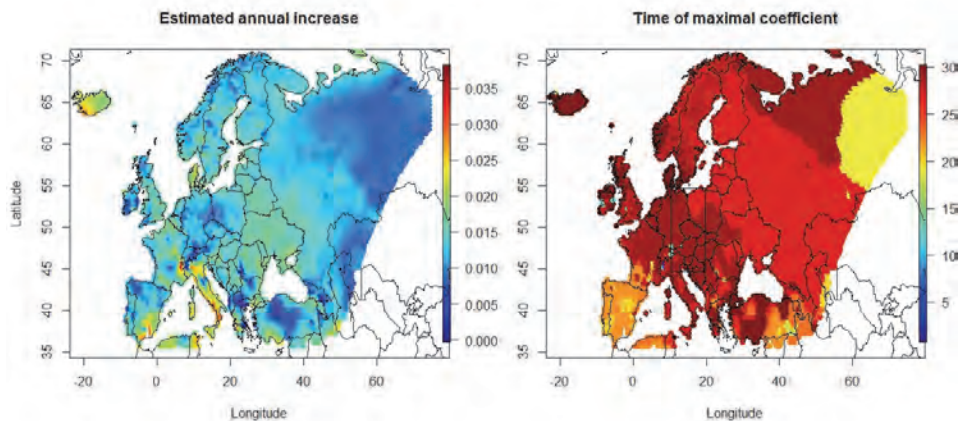


Fig. 1. Maximum of the regression coefficients for the grid points (left) and the time point of their occurrence (30 is the latest, right). On the right panel, a black rectangle shows the region, where the reliability of the results was checked.

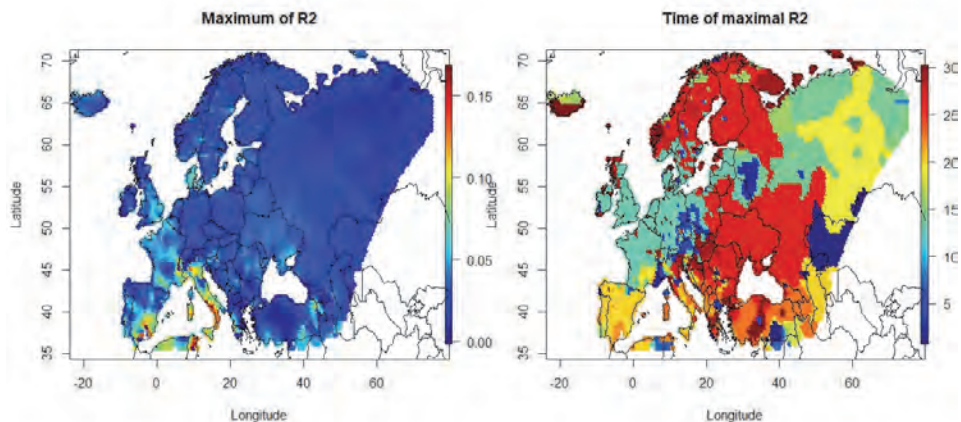


Fig. 2. The maximal  $R^2$  value of the linear regression for the grid points (left) and the time point of their occurrence (30 is the latest, right).

One interesting question is the significance of the results for the climate data we have analyzed. We performed a small study, where the linear coefficient was defined as  $10^{-4}$  and a simple AR(1) structure for the residuals was assumed

$$\varepsilon_n = 0.9\varepsilon_{n-1} + \sqrt{0.19}\eta_n,$$

where the sequence  $\eta_n$  was i.i.d. standard normal. Here we have also used the dependent weighted bootstrap method introduced in Subsection 2.1, and we focused on the steepness coefficient of the linear model. It turned out that the estimators like this are not significant for much shorter series, but  $n \geq 30 \cdot 365$  is sufficient for  $\alpha = 0.05\%$ . We have pursued this idea further by applying the dependent weighted bootstrap method to our data with  $r = 0.9$ , which was chosen as an average solution of Eq. (3). Having repeated the simulations 100 times for each data point for  $k = 10$ ,  $k = 20$ , and  $k = 30$ , we have got 3 times 100 coefficients for the grid points (let us denote them by  $x_{10}$ ,  $x_{20}$ , and  $x_{30}$ ), respectively. We may estimate the significance of the increase of the coefficients by calculating the percentage of the pairs where  $x_{30}$  is larger than, e.g.,  $x_{10}$ . Such values are plotted on Fig. 3. We can see that the speeding up is highly significant for Scandinavia and large parts of Central Europe.

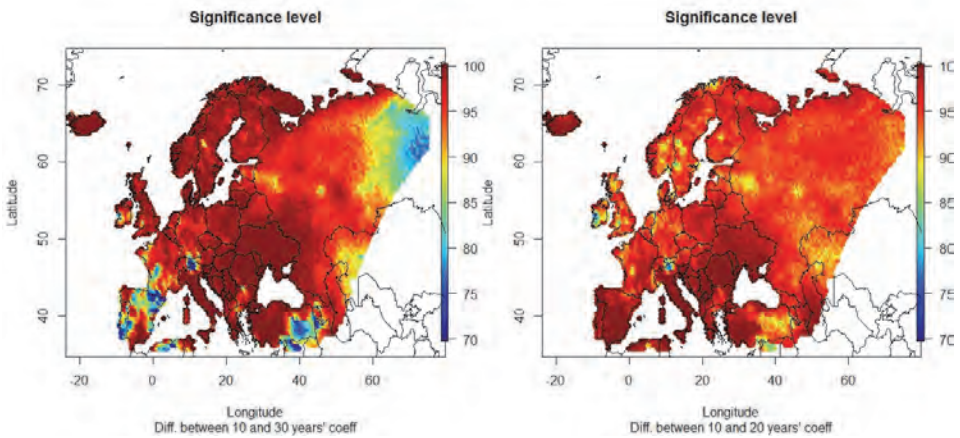


Fig. 3. Significance of the increase of warming, when the last 37 years ( $k = 30$ ) are compared to the last 57 years ( $k = 10$ , left panel) and when the last 47 years ( $k = 20$ ) are compared to the last 57 years ( $k = 10$ , right panel).

We have performed a model-based  $k$ -means clustering of the grid points for the regression coefficients. Similar approach was used for a completely different data in *Hajas and Zempléni (2017)*. The clearly preferred model was the so-called VVV (ellipsoidal covariance structure with variable volume, shape, and orientation).

Fig. 4 shows the time-development of the 13 cluster centers as well as the clustering itself. Every single value is positive, in accordance with the widely accepted phenomenon of the global warming. This phenomenon was investigated at European level (e.g., in *van der Schrier et al., 2013*), proving the existence of the warming, at least from about 1980. But we can show much more: the most affected areas can also be identified. Almost all of the curves show a clear upward trend, i.e., in almost all cases the coefficient increases as the number of omitted years from the beginning of the investigated period increases. This means an acceleration of the temperature increase in the last part of the investigated period. However, the changes in the coefficients (i.e., the speeding up of the temperature increase) are different in the clusters.

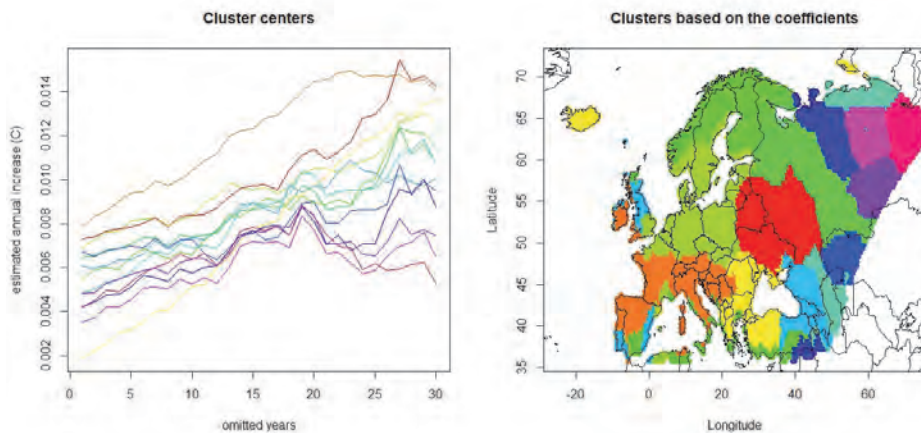


Fig. 4. Cluster centers (left) and the clustering (right), based on the regression coefficients for the grid points (13 clusters, based on the Gaussian mixture method).

The clusters differ mainly in their baseline level, the lines were otherwise quite parallel, at least up to  $k = 20$ , where an interesting change can be observed: in some regions the annual increase remains nearly constant, while for others the speeding up continues. It is of definite meteorological interest to investigate which areas belong to the individual clusters. We may state that Central Europe belongs to the clusters with the highest acceleration of the temperature increase. Also a quick estimated increase is observed in the western part of the Mediterranean region and on Iceland, while the European part of Russia showed the slowest increase. It is, however, interesting that for the Iberian Peninsula the temperature increase is quick, but it has not increased further in the last period – in accordance

to *Fig. 1*, which shows that in this region the maximal coefficient occurs earlier than for most part of Europe (see the orange curve on the left panel of *Fig. 4*). Similar pattern is observable for the northeast, where the increase is the slowest (see *Figs. 1* and *3*).

The quick, further temperature increase in the already warm regions might be interesting from a medical point of view as well, since the further warming of this region might result in quicker than expected outbreaks of tropical epidemics like malaria.

## 5. Conclusions

As a conclusion, we can claim that to analyze the temperature data by focusing on the last decades was a sound idea, as we found interesting patterns in the gridded temperature data. The Gaussian model-based clustering has resulted in a clear pattern of different regions, which might be a useful start for further climatic research.

The bootstrap is indeed an important tool in evaluating the significance of our results. However, one has to be aware of its properties. In case of dependent data, we have to take this dependence into account, when planning the bootstrap data generating process. We have compared the available methods and it turned out that the dependent weighted bootstrap is the most accurate in our case, where the dependency is simply modeled by an AR(1) process. The reason, that it outperforms the well-known block-bootstrap methods, might be the fact that here regression models were investigated.

**Acknowledgement:** We acknowledge the E-OBS dataset from the EU-FP6 project ENSEMBLES (<http://ensembles-eu.metoffice.com>) and the data providers in the ECA&D project (<http://www.ecad.eu>).

The research of A. Zempléni was supported by the Hungarian National Science Foundation (OTKA, K-81403).

## References

- Cohen, J. and Barlow, M., 2005: The NAO, the AO and Global Warming: How Closely Related? *J. Climate* 18, 4498–4513. <https://doi.org/10.1175/JCLI3530.1>
- Dietrich, C. R., Garry N. and Newsam, G.N., 1997: Fast and Exact Simulation of Stationary Gaussian Processes through Circulant Embedding of the Covariance Matrix, *SIAM J. Scientific Comput.* 18, 1088–1107. <https://doi.org/10.1137/S1064827592240555>
- Doukhan, P., Lang, G., Leucht, A., and Neumann, M.H., 2015: Dependent wild bootstrap for the empirical process. *J. Time Series Anal.* 36, 290–314. <https://doi.org/10.1111/jtsa.12106>
- Efron, B., 1979: Bootstrap methods: another look at the jackknife. *Ann. Statistics* 7, 1–26. <https://doi.org/10.1214/aos/1176344552>
- Fraley, C. and Raftery, E.A., 2007: Bayesian regularization for normal mixture estimation and model-based clustering. *J. Classific.* 24, 155–181. <https://doi.org/10.1007/s00357-007-0004-5>
- Giannotti, F. and Pedreschi, D. (eds), 2008: *Mobility, Data Mining and Privacy*, Springer Verlag. <https://doi.org/10.1007/978-3-540-75177-9>

- Haylock, M., Hofstra, N., Klein T., Albert M. G., Klok, E.J., Jones, P.D., and New, M., 2008: A European daily high-resolution gridded data set of surface temperature and precipitation for 1950-2006. *J. Geophys. Res.: Atmospheres* 113. <https://doi.org/10.1029/2008JD010201>
- Hajas, C. and Zempléni, A., 2017: Chess and bridge: clustering the countries, *Annales Univ. Sci. Budapest., Sect. Comp.* 46, 67–79.
- Hajas, C. and Zempléni, A., 2018: Mathematical modelling European temperature data: spatial differences in global warming [Cited 2018 Oct 30]. Available from: <https://arxiv.org/abs/1810.13014>
- Hofstra, N., Haylock, M., New, M., and Jones, P.D., 2012: Testing E-OBS European high-resolution gridded data set of daily precipitation and surface temperature, *J. Geophys. Res. Atmospheres* 114. <https://doi.org/10.1029/2009JD011799>
- Jun, M., Knutti, R., and Nychka, D. W., 2008: Spatial analysis to quantify numerical model bias and dependence: how many climate models are there? *J. Amer. Stat. Assoc.* 103, 934–947. <https://doi.org/10.1198/016214507000001265>
- Lahiri, S.N., 2003: Resampling Methods for Dependent Data. Springer Verlag. <https://doi.org/10.1007/978-1-4757-3803-2>
- Lu, Q., Lund, R.B., and Seymour, P.L., 2005: An Update of United States Temperature Trends, *J. Climate*, 18, 4906–4914. <https://doi.org/10.1175/JCLI3557.1>
- Lund, R.B., Hurd, H., Bloomfield, P., and Smith, R.L., 1995: Climatological Time Series with Periodic Correlation. *J. Climate* 11, 2787–2809. [https://doi.org/10.1175/1520-0442\(1995\)008<2787:CTSWPC>2.0.CO;2](https://doi.org/10.1175/1520-0442(1995)008<2787:CTSWPC>2.0.CO;2)
- Politis, D.N. and White, H., 2004: Automatic block-length selection for the dependent bootstrap, *Econometric Rev.* 23, 53–70. <https://doi.org/10.1081/ETC-120028836>
- Rakonczai, P., Varga, L. and Zempléni, A., 2014: Copula fitting to autocorrelated data with applications to wind speed modelling, *Annales Univ. Sci. R. Eötvös, Sect. Comp.*, 43, 3–19.
- van der Schrier, G., van den Besselaar, E.J.M., Klein Tank, A.M.G. and Verver, G., 2013: Monitoring European average temperature based on the E-OBS gridded data set, *J. Geophys. Res.: Atmospheres* 118, 5120–5135. <https://doi.org/10.1002/jgrd.50444>
- Shao, X., 2010: The dependent wild bootstrap, *JASA*, 105, 218–235. <https://doi.org/10.1198/jasa.2009.tm08744>
- Shekhar, S., Evans, M.R., Kang, J.M., and Mohan, P., 2011: Identifying patterns in spatial information: a survey of methods. *Wiley Interdisc. Rev.: Data Mining Know. Disc.* 1, 193–214. <https://doi.org/10.1002/widm.25>
- Singh, K., 1981: On the asymptotic accuracy of Efron's bootstrap, *Ann. Stat.* 9, 1187–1194. <https://doi.org/10.1214/aos/1176345636>
- Varga, L. and Zempléni, A., 2017: Generalised block bootstrap and its use in meteorology, *Adv. Stat. lim. Meteorol. Oceanogr.* 3, 55–66. <https://doi.org/10.5194/ascmo-3-55-2017>
- Weart, S., 2017: The Discovery of Global Warming, [Cited 2019 Feb]. Available from [https://history.aip.org/climate/20ctrend.htm#L\\_M066](https://history.aip.org/climate/20ctrend.htm#L_M066)
- Wu, C. F. J., 1986: Jackknife, Bootstrap and Other Resampling Methods in Regression Analysis (with discussion). *Ann. Stat.* 14, 1261–1350. <https://doi.org/10.1214/aos/1176350142>



# IDŐJÁRÁS

*Quarterly Journal of the Hungarian Meteorological Service  
Vol. 124, No. 3, July – September, 2020, pp. 363–380*

## **Valorisation of climate conditions in tourist centers of South Serbia**

**Mila Pavlović, Filip Krstić\*, Vedran Živanović, and Aleksandar Kovjanić**

*Department for Regional Geography  
Faculty of Geography  
University of Belgrade  
Belgrade, Serbia;*

*\*Corresponding author E-mail: filipkrstic88@gmail.com*

*(Manuscript received in final form September 16, 2019)*

**Abstract**— Climate is one of the most important factors of tourism development. Tourism trends and activities are largely determined by climatic conditions, as well as potential tourist investments. South Serbia is characterized by climate diversity on a relatively small territory. This region is characterized by heterogeneity and richness in geomorphological, hydrological, and cultural tourism resources. However, more intensive tourism development is limited by a weak financial tourism base. The aims of the work are to evaluate climatic conditions in the main tourism centers of South Serbia and to determine the impact of climate change on the development of tourism in the region. Bioclimatic indicators, primarily the tourism climatic index, were used as a statistical and qualitative method for the evaluation of climatological data for the needs of tourism. The results of the research will point to the advantages, but also to the deficiencies of the climate as a tourism resource of South Serbia.

*Key-words:* climate, tourism, South Serbia, regional development, tourism climatic index

### ***1. Introduction***

Climate has a significant impact on the development of the tourism and recreation sector. In some regions, it represents the resource, which is the development basis for this sector of economy. However, climatic characteristics of a certain region can be both push and pull factors regarding the development of tourism. The adverse climatic characteristics of a particular region (low mean temperatures, increased air humidity, high precipitation, reduced insolation, increased wind

frequency and speed, etc.) represent the push factors, which increase the tourist movement of the local population towards regions with more favorable climatic features. *Smith* (1993) defines climate-dependent tourism as tourism where the climate itself attracts visitors who expect favorable weather conditions in their holiday destination (typical example is the Mediterranean region). Climate changes are recognized by the governing structures and the scientific community as an important problem of social development and the environment. Although estimates vary widely depending on the modeling procedures used, climate change scenarios suggest that the global average surface temperature will increase by 1.4–5.8 °C between 1990 and 2100. Projections regarding global mean sea level indicate a rise of between 0.09 and 0.88 meters throughout the same period (*Gao et al.*, 2017). An increase in the frequency and intensity of extreme weather events (floods, droughts, heat waves, intensive storms, etc.) is also expected (*Amelung et al.*, 2007).

Climate change represents a major threat to sustainable development of all economic sectors. Tourism sector is particularly vulnerable, considering its high dependence on climate as a tourism resource. There are several key risks resulting from climate change, that impact on economic sectors including tourism: risk of disrupted livelihoods resulting from sea level rise and coastal flooding; inland flooding in urban areas and periods of extreme heat; influence on infrastructure network and services; and risks of loss of ecosystems and biodiversity. Surface temperature is projected to rise over the 21st century under all assessed emission scenarios. Heat waves will also occur more often, and they will last longer. Extreme precipitation events will become more intense. These climatic patterns will have negative impact on global tourism industry (*IPCC*, 2014).

Climate change affects the climatic tourism resource of certain regions, as well as the competitiveness of tourism travel and tourism expenditure between different tourism regions. Due to climate changes, some regions are likely to experience substantial increase in attractiveness due to improvements in their weather conditions. Others may become significantly less appealing to tourists, leading to shifts in the temporal visit patterns and/or actual declines in the number of tourists (*Amelung et al.*, 2007). Climate change is considered to be a catalyst for structural changes in tourism. Due to climate change, snow cover in many tourist winter centers in Europe (especially in the Alps) will diminish. This will have a lasting negative impact on tourism industry (*Elsasser and Bürki*, 2002).

Climatic characteristics, as well as their variability, affect the length and quality of the tourism season, and therefore, the profitability of the tourism economic sector. Hence, the vulnerability of the tourism sector due to climate variability, as well as long-term climate change, have been the subject of research of many scientific papers (*Scott and MacBoyle*, 2001; *Belén Gómez*, 2005; *Amelung and Viner*, 2006; *Tzu-Ping and Matzarakis*, 2008; *Perch-Nielsen et al.*, 2010; *Joksimović et al.*, 2013; *Jahic and Mezetovic*, 2014; *Basarin et al.*, 2014; *Agarin, Jetzkowitz and Matzarakis*, 2010; *Anđelković et al.*, 2016; *Roshan*,

*Yousefi et al.*, 2016; *Weir*, 2017; *Kovacs et al.*, 2017; *Valjarević et al.*, 2017; *Gavrilov et al.*, 2018; *Roshan et al.*, 2018; *Vukoičić, et al.*, 2018; *Yan et al.*, 2018; *Fitchett and Hoogendoorn*, 2018). The results of climate changes research in tourism regions are used when planning tourism activities, tourism season, location of tourism centers and infrastructure. This research has an important applicative purpose. The first multidisciplinary studies of climate for the needs of tourism appear in works by *Houghten and Yaglou* (1923), *Bedford* (1948), and *Fanger* (1970). They pointed to the ratio of radiation, insolation, air temperature, humidity, and wind to temperature, humidity, and metabolic processes in the human body (bio-climatological parameters). Early climate indices included simple climatic indicators, while in *Besancenot et al.* (1978), *Mieczkowski* (1985), *de Freitas* (1990), *Becker* (1998), *Belén Gómez* (2004), *Matzarakis et al.* (2008), *Matzarakis* (2009), *Roshan et al.*, (2016) and *Sabzevari et al.* (2018) more complex indicators and equations have been used regarding the energy balance of the human body - indexes of comfort.

From the perspective of tourism, South Serbia is an underdeveloped and unutilized region. Its abundance of natural and anthropogenic tourism resources provides a real potential for affirmation of various types of tourism. Pan-European Corridor X, which is essential for the development of transit tourism in Serbia, passes through central parts of South Serbia (the South Morava valley). However, in order to improve the level of tourism development, it is necessary to provide a quality infrastructure network, a quality receptive superstructure, especially in terms of the quality and quantity of accommodation facilities. There are favorable conditions for the development of several types of tourism in the region: spa and wellness tourism, mountain/ski tourism, city and cultural tourism, rural tourism, and ecotourism.

Within the studied territory, several tourism regions can be distinguished, of which only Kopaonik has used its potential for tourism development. The Kopaonik tourism region is the most developed mountain tourism center of Serbia. It is recognized as a winter tourism center with modern accommodation facilities. Although mountain Kopaonik occupies a central position in Serbia, the Kopaonik meteorological station is taken as a representative of the mountain climate of South Serbia, because it borders this region from the west. Kopaonik is the center of winter sport tourism, and to a lesser extent of recreational, congress, and event tourism (*Bojović*, 2012). Niš is taken as an example of city break and cultural tourism, but in the city and its immediate surroundings there is potential for more intensive development of spa, recreational, adventurous, and transit tourism. The South Morava tourism region is distinguished by the quantity and quality of geomorphological, hydrographic and cultural tourism values. However, as in the rest of the studied region, excluding Kopaonik, the tourism infrastructure is underdeveloped, which has a negative impact. This tourism region has a favorable transport geographical position (Pan-European Corridor X). Vranjska Spa was taken as the spa tourism center in the far south of the region. Kuršumljia is a typical representative of spa tourism taking into account the three

spa resorts in its vicinity, located on the slopes of Kopaonik (Lukovska Spa and Kuršumlijska Spa<sup>1</sup>) and Radan mountain (Prolom Spa). Lukovska Spa is located at the elevation of 681 m, and therefore, it complements its balneological and sports-recreational tourism offer with elements of winter mountain tourism. The mountain zone east and west of the South Morava valley provides opportunities for the development of mountain, recreational, and cultural tourism as well. *Fig. 1* presents the location of studied meteorological stations and tourism destinations.

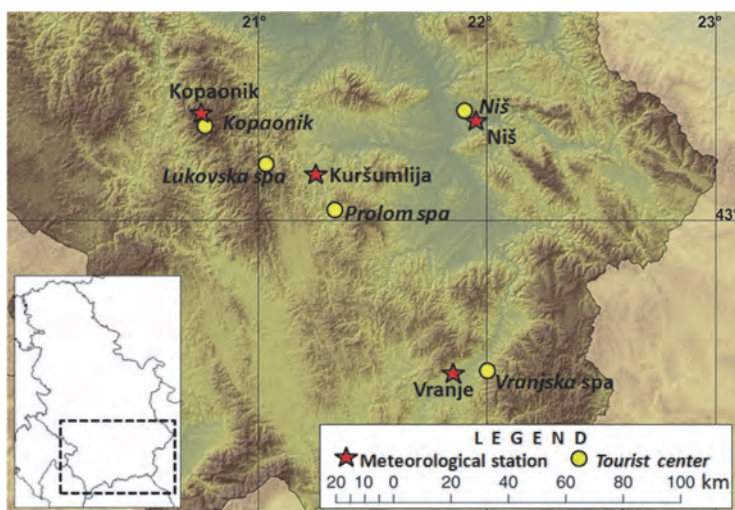


*Fig. 1.* Geographical positions of meteorological stations and studied tourism destinations

The aim of this paper is to point out the tourism potential of South Serbia, taking into account the different types of climate of this region. Also, the aim is to analyze tourism trends and the utilization of tourist capacities in relation to climatic conditions. In order to better understand the climate change and its actuality, the paper analyses the climatic period from 1990 to 2016. We should also point out certain methodological limitations that the authors of the paper have encountered. These constraints primarily relate to the lack of specific time series for individual climatic parameters, which resulted in a smaller number of meteorological stations involved in the research. Also, the network of stations itself is not sufficiently branched out through the region and does not cover all the climatic altitude zones, nor all tourism regions within the studied territory.

<sup>1</sup> Despite its long tradition (over a century long) and the medicinal features of its thermal mineral waters, the Kuršumlijska Spa has had no tourism function since 2006, therefore, it will not be the subject of research in this paper.

## ***2. Materials and methods***

For the purpose of climate valorization in the tourism centers of South Serbia, we selected four tourism centers: Kopaonik, City of Niš, City of Vranje, and Kuršumlija's spas (Lukovska, Prolom, and Kuršumlijska Spa). The primary approach to this choice is regional. The mentioned locations are situated in different parts of South Serbia. Each one is distinguished by different natural conditions, geographical, transport, and tourist positions. The second reason for this choice is the different forms of tourism attractions, conditioned by specific natural and anthropogenic tourism values. One of the main reasons was the availability of the necessary data for calculating the tourism climatic index from nearby meteorological stations.

## ***3. Tourism climatic index (TCI)***

Tourism climatic index (TCI) is a synthetic statistical and qualitative method which aims to determine the impact of the climate (the most relevant climate elements) on the quality of tourism experience (Mieczkowski, 1985). This index is based on bioclimatic indicators, in fact on the degree of physical comfort of people in different climatic conditions. Based on the average monthly values of seven climatic parameters (average daily maximum air temperature, average daily air temperature, average daily minimum air humidity, average daily air humidity, total precipitation, total insolation, and average wind speed), Mieczkowski presented a model which can be used for calculating the tourism climate valorization potential.

The tourism climatic index values are obtained on the basis of the following formula:

$$TCI = 2(4Tc + Tc_{24} + 2R + 2S + W). \quad (1)$$

Since tourism activities mostly occur during the day, temperature and relative air humidity have the greatest importance for calculating *TCI*. *Tc* signifies thermal comfort, which is obtained by combining the maximum daily temperature and the minimum daily relative air humidity. The values of both variables usually occur between 12 and 16 hours p.m., when tourists tend to be most active in the open. Thermal comfort for 24 hours (*Tc<sub>24</sub>*) is obtained by combining the average daily temperature and the average daily relative air humidity. The values of both indicators are derived from the diagram presented in *Fig. 2*. Thermal comfort is defined as condition of thermal neutrality (thermal benefits) in which the heat conditions of the environment and the human body are balanced. *R* signifies the average precipitation (mm), *S* is the average daily insolation (hours per day), and *W* is the average wind speed (m/s). The values of each parameter range from -3 points (extremely unfavorable) to 5 points (optimal). The sum of these

components is multiplied by 2, so that the maximum possible *TCI* score can reach 100. Although these indices are designed based on the available biometric literature and climate data of the time, the system for valuing these subindices as well as the final *TCI* values are descriptive and subjective. *TCI* is a method of systematic evaluation of tourism climate in different regions of the world, using a scale that is easily comparable. The *TCI* values are descriptively evaluated in the following way: the ideal time (index 90 – 100), excellent (80 – 89), very good (70 – 79), good (60 – 69), acceptable (50 – 59), possible (40 – 49), undesirable (30 – 39), very undesirable (20 – 29), extremely undesirable (10 – 19), and impossible (-30 – 9) (Mieczkowski, 1985).

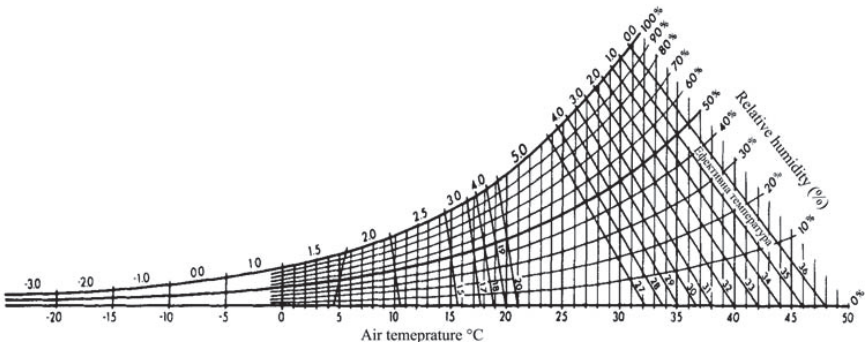


Fig 2. Diagram of thermal comfort evaluation (*T<sub>c</sub>*) (Mieczkowski, 1985).

Despite combining several different components, the obtained results of *TCI* are not compatible with all tourist activities and types of tourism. Certain tourist activities (in accordance with the types of tourism) take place during different climatic conditions compared to those with a diminishing, or even negative impact (according to *TCI*). In particular, *TCI* is not relevant for winter mountain tourism. For tourism centers of this type, the length of snow cover, insolation, air temperature, wind speed, and albedo are of crucial importance (Matzarakis, 2006).

Table 1. Matrix for evaluating precipitation, insolation, and wind

Points	R (mm)	S (h)	W (m/s)
5.0	≤ 14.9	>10	< 0.8
4.5	15.0 – 29.9	9 – 10	0.8 – 1.5
4.0	30.0 – 44.9	8 – 9	1.6 – 2.5
3.5	50.0 – 59.9	7 – 8	2.6 – 3.3
3.0	60.0 – 74.9	6 – 7	3.4 – 5.4
2.5	75.0 – 89.9	5 – 6	5.5 – 6.7
2.0	90.0 – 104.9	4 – 5	6.8 – 7.9
1.5	105.9 – 119.9	3 – 4	-
1.0	120.0 – 134.9	2 – 3	8.0 – 10.7
0.5	135.0 – 149.9	1 – 2	-
0	150.0 – 209.0	0 – 1	>10.7
-0.5	-	-	-
-1.0	210.0 – 269.9	-	-
-1.5	-	-	-
-2.0	270.0 – 329.9	-	-

Source: *Mieczkowski*, 1985

According to Köppen climate classification, in the region of South Serbia the C (moderately warm) and D climate types (moderately cold) are predominant (including several types and subtypes). Therefore, the predominant climate throughout South Serbia, including the research areas of Niš, Vranje, and Kuršumljija, belongs to the Cfb subtype (a moderately warm and humid climate with moderate summer temperatures). The highest parts of Kopaonik mountain, including the meteorological station on this mountain, are located in the Dfc climate zone (a moderately cold and humid climate with moderate summer temperatures). This climate is typical of mountain areas over 1200 m above sea level. We can also identify the transitional subtype between these two climates – the Dfb climate, which is characterized by a moderately cold and humid climate with warm summer temperatures (*Milovanović et al.*, 2017).

#### 4. Results

The continuous development of the four selected tourist centers resulted in an increase in the number of tourist visits. The number of tourists, during the observed ten-year period 2007–2016, increased from 177,193 to 232,555, which resulted in an increase of 31.2%. Positive changes were also reflected in the increase of overnight stays by 28.8%. Looking at these tourism centers collectively, accommodation capacities are occupied by tourists more evenly throughout the year. The most visited month was December (10.1%), while the smallest number of tourists was recorded in November (6.1%).

From 2007 to 2016, the highest average number of tourists was recorded in Kopaonik (81,993 or 46.4%), as indicated by the data in *Table 2*. In accordance with the largest number of tourists, Kopaonik also has a leading position in the number of overnight stays (357,182 or 56.7%). The second largest tourist center is the city of Niš with an average number of about 66,000 tourists. It is followed by Kuršumlija's spas and Vranjska Spa with the smallest average number of tourists. Regarding the place of origin, domestic tourists are predominant (70.5%). During the observed period, there was a constant increase in the number and relative share of international tourists (from 21.8% to 29.5%). Niš is an important tourist center for this part of Serbia and a transit city, in 2016 it had a higher share of foreign tourists in the total number of tourists (52.5%). That same year, the share of international tourists was practically negligible only in Vranjska Spa (6.2%).

*Table 2.* Basic indicators of selected tourist centers

<b>Tourist center</b>	<b>Kopaonik</b>	<b>Lukovska and Prolom Spa</b>	<b>Niš</b>	<b>Vranjska Spa</b>
Average number of tourists 2007-2016	81,993	23,337	66,009	5,737
Average number of overnight stays 2007-2016	357,182	129,856	106,708	35,785
Average number of overnight stays per tourist	4.4	5.6	1.6	6.8

Source: Statistical Office of the Republic of Serbia (2017)

According to the length of the average stay of tourists expressed through the average number of overnight stays of one tourist, the mentioned tourist centers can be classified into two types. Vranjska Spa is an example of a stationary form of tourism. In spite of the smallest number of tourist visits, the longest average stay is recorded in this spa (6.8). Vranjska Spa has a special rehabilitation hospital, which is why this tourist center has a primary healthcare function. The average

number of overnight stays recorded in Kopaonik and in Kuršumljija's spas is smaller than in Vranjska Spa. These tourist centers also have healthcare, sports, and recreational functions. With the shortest average stay of tourists (1.6), Niš is a typical example of a city break and transit tourism destination.

Fig. 3 shows the average number of tourists by months in tourism centers of South Serbia. According to this data, the tourism centers of South Serbia are not characterized by seasonality in tourism travel. However, during the summer months, the largest share of tourist visits (30–36%) and overnight stays (30–42%) is recorded in Niš and in the spa tourism centers of South Serbia. The winter minimum in tourism travel is only noticeable in the spas of Kuršumljija (13.4% of tourist visits and 9.7% of overnight stays). Kopaonik, as the most important center of winter tourism in Serbia, has a somewhat more pronounced seasonality. During the winter months (December-March), an average of 60% of visits and 69% of overnight stays are recorded in Kopaonik. Here, tourism travel is minimal during the summer months (around 14% of tourist arrivals and overnight stays).

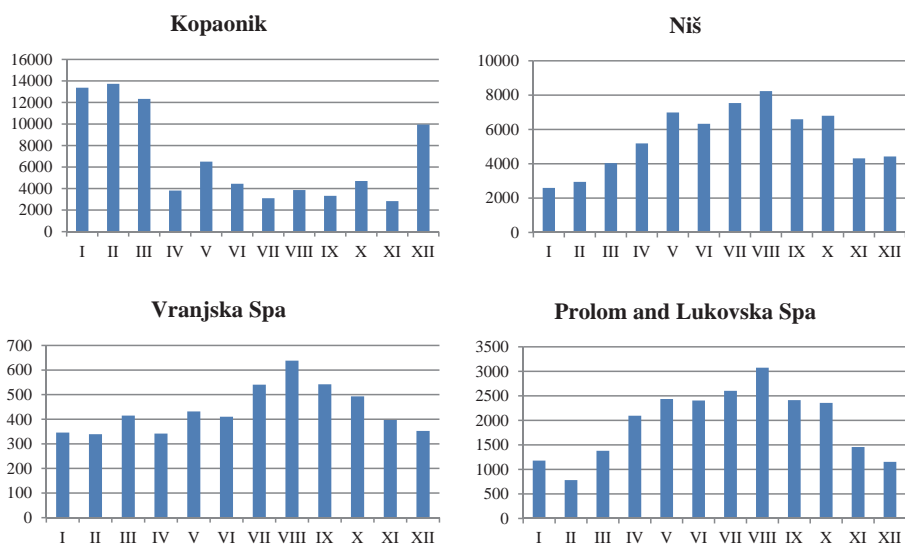


Fig. 3. Average number of tourists by months in Kopaonik, Niš, Prolom, Lukovska, and Vranjska Spa. Source: Statistical Office of the Republic of Serbia (2017).

The climate indicators which are used to determine the *TCI* for selected tourism centers are shown in Table 3. The analysis included the data from the following meteorological stations: Kopaonik (1.710 m), Kuršumljija (382 m), Niš

(210 m), and Vranje (432 m). The data of each indicator refers to the mean monthly values for the 27-year period from 1990 to 2016.

Table 3. Average monthly values of climatic parameters for Kopaonik, Kuršumljija, Niš, and Vranje

<b>Kopaonik</b>	<b>I</b>	<b>II</b>	<b>III</b>	<b>IV</b>	<b>V</b>	<b>VI</b>	<b>VII</b>	<b>VIII</b>	<b>IX</b>	<b>X</b>	<b>XI</b>	<b>XII</b>
$T_{max}$	-0.7	-0.7	1.9	6.1	11.5	15.3	17.6	18	12.7	9.4	4.6	0.2
$T_{avg}$	-4.3	-4.4	-2	2.3	7.3	11.1	13.1	13.3	8.8	5.1	1.6	-3.4
$r_{min}$	26	28	29	30	32	38	31	34	34	24	23	27
$r_{avg}$	82	82	82	81	80	78	75	74	78	81	81	84
$R$	63	64.2	84.4	94.5	119	102.3	90.1	71.2	92.2	79.6	76.9	74.5
$S$	3.1	3.5	4.3	5	8.9	7.7	8.7	8.4	6	5.1	4.9	2.9
$W$	3.6	3.9	4	3.9	3.5	3.1	3	2.9	3.2	3.6	4	3.8
<b>Kuršumljija</b>	<b>I</b>	<b>II</b>	<b>III</b>	<b>IV</b>	<b>V</b>	<b>VI</b>	<b>VII</b>	<b>VIII</b>	<b>IX</b>	<b>X</b>	<b>XI</b>	<b>XII</b>
$T_{max}$	5.3	7.4	12.1	17.4	22.3	26	28.6	29.4	23.5	18	12.1	5.8
$T_{avg}$	0.4	1.8	5.7	10.7	15.1	18.8	20.7	20.5	15.8	10.7	6.5	1.3
$r_{min}$	44	36	31	27	32	34	31	29	33	35	41	45
$r_{avg}$	83	79	74	72	75	74	68	71	78	81	82	84
$R$	44	44.1	53.8	57.5	71.1	55.6	66.3	42.4	58.8	59.1	53.4	56
$S$	2.6	3	4.4	5.9	6.5	8.2	9.3	8.8	6.2	4.3	3.3	2.2
$W$	1	1.2	1.4	1.3	1.2	1.1	1.2	1.2	1.1	0.9	1	1
<b>Niš</b>	<b>I</b>	<b>II</b>	<b>III</b>	<b>IV</b>	<b>V</b>	<b>VI</b>	<b>VII</b>	<b>VIII</b>	<b>IX</b>	<b>X</b>	<b>XI</b>	<b>XII</b>
$T_{max}$	5.2	8.1	13.5	18.7	23.8	27.8	30.5	30.7	25.1	19.2	12.9	6
$T_{avg}$	1	2.9	7.4	12.4	17.2	21	23.1	22.9	17.7	12.5	7.3	2
$r_{min}$	40.3	32.2	24.6	23.9	25.9	26.8	22.9	23.4	26.3	31.3	36.1	43.4
$r_{avg}$	79.3	73.4	65.2	63.8	65.7	64	60	60.3	67.6	73.6	76.2	80.1
$R$	41.4	38.8	43.3	58	67.4	53.4	46.4	44.2	52.8	54.8	50.4	50.9
$S$	2.1	3.4	5.1	5.8	6.9	8.5	8.9	8.9	6.6	4.7	2.9	1.7
$W$	1.1	1.4	1.7	1.4	1.2	1.1	1.1	1	1	1	1.1	1.2
<b>Vranje</b>	<b>I</b>	<b>II</b>	<b>III</b>	<b>IV</b>	<b>V</b>	<b>VI</b>	<b>VII</b>	<b>VIII</b>	<b>IX</b>	<b>X</b>	<b>XI</b>	<b>XII</b>
$T_{max}$	4.6	7.6	12.6	17.5	22.6	26.7	29.4	29.8	24.3	18.5	11.8	5.2
$T_{avg}$	0.3	2.4	6.6	11.3	16.1	20	22.2	22.2	17	11.9	6.6	1.2
$r_{min}$	45	33	24	23	24	26	23	22	24	31	38	46
$r_{avg}$	82	74	67	65	66	64	59	59	67	74	79	83
$R$	38.8	39.1	39.7	54.5	61.1	55.4	46	40.5	52.1	62.7	54.9	51.1
$S$	2.4	3.8	5	5.8	7.4	9.4	10.5	9.8	6.8	4.9	3	1.9
$W$	2.3	3.2	4.1	2.5	2.2	2.7	2.8	2.7	3.1	2	2.1	2.2

Explanation:  $T_{max}$  – maximum daily air temperature ( $^{\circ}$  C),  $T_{avg}$  – average daily air temperature ( $^{\circ}$  C),  $r_{min}$  – minimum daily relative humidity (%),  $r_{avg}$  – average daily relative humidity (%),  $R$  – total precipitation (mm),  $S$  – total daily insolation (h),  $W$ – average wind speed (m/s).

Source: Meteorological yearbook (2017)

## 5. Discussion

According to the data, the average monthly values of the tourism climatic index (*TCI*) are calculated for the period from 1990 to 2016 (*Table 4*). The obtained results indicate a twofold impact of the climate conditions on the development of tourism in South Serbia (there are considerably more favorable climatic conditions in Kuršumljija, Vranje, and Niš, compared to Kopaonik). The natural factor is emphasized as the main determinant that affects the quality and duration of the favorable climatic conditions for the development of tourism.

*Table 4.* Total values of *TCI* by months

Station	Jan	Feb	March	Apr	May	Jun	Jul	Aug	Sep	Oct	Nov	Dec
Kopaonik	34	34	36	38	49	56	65	71	47	47	39	33
Kuršumljija	44	49	54	66	74	85	82	83	80	67	52	43
Niš	45	50	59	65	78	84	83	85	80	67	51	42
Vranje	44	48	55	68	78	87	88	84	80	63	51	40

The average monthly *TCI* values in South Serbia range from 33 (undesirable) to 88 (excellent) index points. The contrast between the summer (July, August, and September) maximum and the winter (December, January and February) minimum of *TCI* values is obvious. It sets summer apart as the most suitable season for the development of tourism in South Serbia. Between Kopaonik and the other three reference meteorological stations, there is a significant difference of *TCI* values. Altitude is the main climatic factor that lowers *TCI* values in Kopaonik. The average monthly temperatures from December to March do not exceed 0° C (from -2 °C to -4.5 °C), while the mean November temperature is 1.6 °C, and in April it is only 2.2 °C. According to the *TCI* and because of extremely low values of air temperature and insolation, the period from November to April is undesirable in terms of climatic conditions for the development of tourism. Due to the fact that Kopaonik is the leading center of ski tourism in Serbia, the significance of *TCI* should be taken with reservations. In the months (December, January, February, and March) with the lowest *TCI* values (from 33 to 36 index points), 60% of the annual tourist traffic is achieved. Because of this fact, it is noticed that *TCI* ignores the qualitative characteristics of some climatic elements that are crucial for the development of winter tourism (length of snow cover and its depth). The same conclusion was drawn on the case of *TCI* assessment for mountain tourist places of Montenegro (*Joksimović et al.*, 2013).

With higher temperature and insolation from May to August, there is a continuous increase in *TCI* values. Unlike the other three observed meteorological stations in South Serbia, the maximum *TCI* values in Kopaonik occur in two months (July – good, August – very good). July and August are the hottest (with a mean monthly temperature above 13°C) and the sunniest (with an insolation value of more than 8h per day) months in Kopaonik. In September, the weather conditions deteriorate, which is followed by an evident drop in the values of all climatic elements, as well as *TCI* (from 71 to 41 index points).

In accordance with different climate factors that shape the climate of lower altitudes in South Serbia, there are significantly different *TCI* values in this part of the region. Although the observed cities are located at the opposite ends of the studied area, Kuršumlija, Niš and Vranje have a very similar monthly regime of *TCI* changes. In all of the three cities, during the winter period, *TCI* ranges between 40 and 49 index points. Compared to Vranje and Kuršumlija, the first spring month (March) in Niš is warmer by 1.5 °C to 2 °C. This is why the value of *TCI* is higher in Niš. The biggest differences in *TCI* values between these three cities are in July (Vranje 88, Niš 83, Kuršumlija 82). Although Niš is the hottest city in the region (the mean temperature in July is 23.1 °C), the length of direct sunshine (insolation) results in increasing the July *TCI* value in Vranje. The surroundings of the Kuršumlija basin, i.e., Kopaonik, Radan and Vidojevica mountains, lead to a reduction of average summer temperatures by one to two degrees. With lower temperatures, slightly higher air humidity (up to 10% higher than in Vranje and Niš), lower wind speeds and a higher insolation value (during July and August Kuršumlija is sunnier than Niš). There are very favorable bioclimatological conditions for the development of tourism in this part of South Serbia. With the rapid decline of air temperatures and insolation in autumn months, the *TCI* decreases, and climatic conditions vary, from good to acceptable.

*Fig. 4* and *Table 5* show the regression and correlation analysis. The aim of this analysis is to determine the connection between the annual *TCI* regime and the number of tourists in the selected tourism centers.

The lowest coefficient of correlation (-0.65) and regression (0.41) is recorded in Kopaonik. *Fig. 4* indicates a negative link between the *TCI* and the number of tourists, which was confirmed by the correlation coefficient value of -0.65 (*Table 5*). Negative values of correlation and regression occur, because *TCI* reaches the highest values in July and August, and the number of tourists in January, February, and March (in these months, *TCI* is on a minimum level). Kopaonik is an example that shows the irrelevance of *TCI* in assessing climate conditions for the development of tourism in winter tourism centers. Exceptionally low temperatures in the winter months and a low insolation value cause the occurrence of minimum *TCI* values in Kopaonik at the peak of the tourist season. In order to increase the relevance of this index, when assessing the climate conditions for the development of winter tourism centers, it is necessary to add new climatic elements such as the height and length of snow cover. Also,

low air temperatures during the winter months should be included to increase the *TCI* values. We can conclude that Kopaonik has insufficiently used its potentials for development of tourist activities during the summer months.

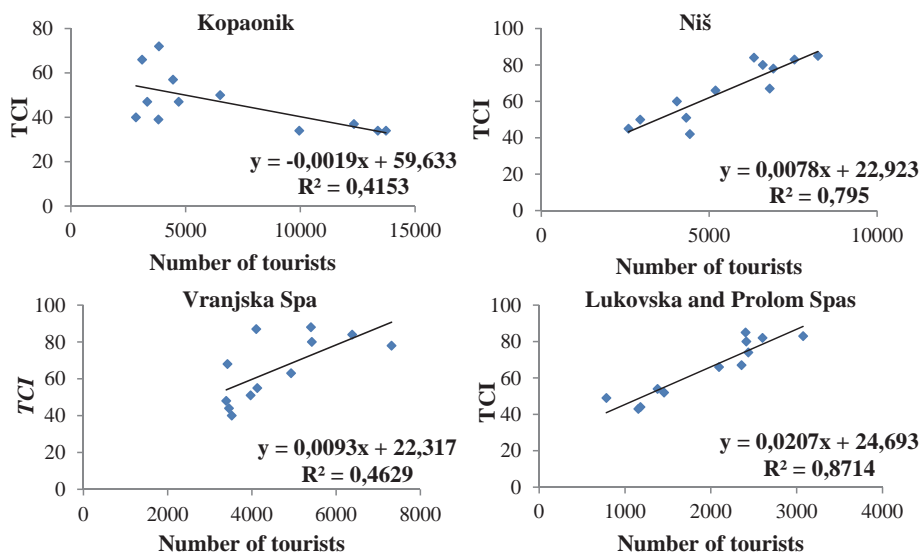


Fig. 4. Regression analysis between the *TCI* values and the number of tourists.

Table 5. Coefficient of correlation

Tourism centres	Coefficient of correlation
Kopaonik	-0.65
Lukovska and Prolom Spa	0.93
Niš	0.89
Vranjska Spa	0.68

Coefficients of regression and correlation show very high values in Niš. The end of summer and the beginning of autumn are the periods with the largest number of tourists in this city. Also, *TCI* still records high values in these months, which leads to a high coefficient of correlation (0.89). In many larger urban centers, autumn is the period of the year with the highest number of tourists. Niš is characterized by a rich touristic offer during the summer months. This is why

the season of increased tourist numbers starts in July. Because of the favorable geographical position, at the point of contact of two major highways of the Balkan Peninsula (E75 and E80), during the summer season Niš is visited by an increasing number of tourists who are in transit towards the Aegean Sea resorts.

Compared to Niš, correlation (0.68) and regression (0.46) coefficients in Vranje show significantly lower values. From November to June, there is on average 3,400 to 4,200 tourists staying in the spa resort. July, August, and September are the months with a slightly larger number of tourists (between 5,400 and 6,300). The reason for low correlation and regression values is a relatively even number of tourists in Vranjska Spa throughout the year on the one hand, and the large seasonal variations of the *TCI* on the other (the number of tourists does not decrease with a decrease of *TCI* values).

The highest correlation (0.93) and regression (0.87) coefficient values are obtained in Kuršumljija (Lukovska and Prolom Spas). The monthly regime of the number of tourists and *TCI* are fully harmonized in this area. The peak of the tourist season coincides with the maximum *TCI* values. Also, during the autumn and winter months, both indicators fall equally. 60% of the annual turnover of tourists is realized from June to September – the months during the year when the climatic conditions for the development of tourism are very good (from 70 to 80 *TCI* index) and excellent (from 80 to 90 *TCI*). The extremely high correlation coefficient indicates a very high valorization of bioclimatic potentials for the development of tourism in Lukovska and Prolom Spas.

## ***6. Conclusion***

Based on the *TCI* value, the territory of South Serbia has very favorable conditions for the development of tourism. However, the climate is not sufficiently valorized as a tourism resource, in comparison to the tourism potential that the region has as a whole. We should take into account the relatively small number of tourists, inadequate tourism infrastructure, and the insignificant role of tourism in the economic structure of this underdeveloped region of Serbia. In addition, the *TCI* shows that the climate, mainly in spa resorts, does not play a decisive role in tourist visits and the utilization of tourism centers in this region.

The tourism climate index used in this paper has certain limitations. The limitations refer to its application in mountain touristic centers. Mountain tourism centers are predominantly focused on the development of winter tourism, which means that certain climatic elements, that are excluded by Mieczkowski (such as snowfall, snow cover and length), have a major impact on the development of tourism. These climatic elements should be used in the process of measuring the *TCI*. Also, it is necessary to modify the influence of low temperatures on the *TCI* values, because they contribute to a better utilization of natural conditions for the development of winter tourism. This opens up the possibility of *TCI*

diversification, i.e., the use of different input data for summer and winter tourism centers. The spatial expansion of tourist movements, the development of tourism in new and formerly underdeveloped areas, the emergence of new types of tourism, as well as climate changes, further encourage the need for diversification of input data in the *TCI* calculation process.

One of the further lines of research in this scientific field could include the whole territory of Serbia. Regionalization of Serbia according to *TCI* would be of great importance in the planning and development of tourism regions. By analyzing the correlation between the *TCI* values and the number of tourists on a monthly basis in certain tourism centers, we become aware of an insufficient utilization of natural potentials for tourism development in certain parts of the year. This type of analysis can influence decisions on the possible extension of the tourism season in tourism centers specialized for only one type of tourism (i.e. Kopaonik and ski tourism).

Climate conditions for the development of tourism are significantly more favorable in Niš, Kuršumlija's spas, and Vranje, than in tourism centers located at higher altitudes. In these centers, favorable bioclimatic conditions in the form of high temperatures during the summer months, high insolation (especially in the summer months), and absence of strong winds year-round are particularly important for tourism. This index does not take into account the key climatic parameters for the development of ski and mountain tourism (negative temperatures in the winter season, snow depth and snow cover duration, absence of strong winds, or occurrence of blizzards). Therefore, there is a discrepancy between the *TCI* value and the number of tourists in the Kopaonik mountain tourism center. Because of these shortcomings, there is a real and practical need for future research with the aim of eliminating them. It is necessary to improve *TCI*, or to make a modified version that would have a larger and more functional application in determining the favorable climatic conditions for the winter tourism.

The development of tourism in continental conditions has had a positive influence on the development of spa tourism in South Serbia in the last years. However, due to the traditional understanding of the concept of spas as rehabilitation centers in Serbia, their tourism function is of secondary importance. In all the selected spa centers, climate conditions are favorable for the development of tourism, especially during the summer season. Climatic characteristics provide an opportunity for the development of different and complementary aspects of tourism. However, tourism centers in South Serbia lack supplementary tourist contents, which would make better use of their tourism resources (Valjarević *et al.*, 2017). The tourism development of Kopaonik should move towards the affirmation of tourism centers on the mountain sides at lower altitudes (in particular from the eastern side), as well as the promotion of alternative forms of tourism in the offseason period, especially bearing in mind the favorable climatic conditions present in this period. The Niš tourism region is

not sufficiently exploited, taking into account the abundance of tourism resources and its favorable transport location.

“According to the size of Serbian territory, further studies might involve a considerably larger and wider area taking into consideration the actual scenarios of climate changes with respect to regional variations. The results of climate indices and their marketing contribute to choosing the most appropriate destinations for a certain type of climate treatment or recreation” (Anđelković *et al.*, 2016). The tourist centers of South Serbia are not sufficiently represented on the international tourism market (Vesić and Živanović, 2018). Due to the insufficient development of tourism in South Serbia, *TCI* as an indicator has greater significance. The values of this indicator can be used when planning future tourism development, a better utilization of accommodation facilities and the development of complementary types of tourism that are dependent on climatic conditions.

**Acknowledgements:** The paper is the result of research within project no. 176008 funded by the Ministry of Education, Science and Technological Development of the Republic of Serbia.

## References

- Agarin, T., Jetzkowitz, J., and Matzarakis, A., 2010: Chapter 15 Climate change and tourism in the eastern Baltic Sea region. In (ed. Christian S.) *Tourism and the Implications of Climate Change: Issues and Actions (Bridging Tourism Theory and Practice, Volume 3.* Emerald Group Publishing Limited, 261–281. [https://doi.org/10.1108/S2042-1443\(2010\)0000003018](https://doi.org/10.1108/S2042-1443(2010)0000003018)
- Amelung, B., Nicholls, S., and Viner, D., 2007: Implications of Global Climate Change for Tourism Flows and Seasonality. *J. Travel Res.* 45, 285–296. <https://doi.org/10.1177/0047287506295937>
- Amelung, B. and Viner, D., 2006: Mediterranean tourism: exploring the future with the Tourism Climatic Index. *J. Sustain. Tourism* 14, 349–366. <https://doi.org/10.2167/jost549.0>
- Anđelković, G., Pavlović, S., Đurđić, S., Belij, M., and Stojković, S., 2016: Tourism Climate Comfort Index (TCCI) – An attempt to evaluate the climate comfort for tourism purposes: the example of Serbia. *Global NEST Journal* 18, 482–493. <https://doi.org/10.30955/gnj.001798>
- Basarin, B., Kržić, A., Lazić, L., Lukić, T., Đorđević, J., Janičijević Petrović, B., Čopić S., Matić, D., Hrnjak, I., and Matzarakis, A. 2014: Evaluation of bioclimate conditions in two special nature reserves in Vojvodina (Northern Serbia). *Carpathian Journal of Earth and Environmental Sciences* 9(4), 93–108.
- Becker, S., 1998: Beach Comfort Index – A New Approach to Evaluate the Thermal Conditions of Beach Holiday Resorts Using a South African Example. *GeoJournal* 44, 297–307. <https://doi.org/10.1023/A:1006871805262>
- Bedford, T., 1948: *Basic Principles of Ventilation and Heating.* Lewis Co, London
- Belén Gómez M., 2004: An Evaluation of Tourist Potential of the Climate in Catalonia (Spain): A Regional Study. *Geografiska Annaler. Series A Physical Geography* 86, 249–264. <https://doi.org/10.1111/j.0435-3676.2004.00229.x>
- Belén Gómez M., 2005: Weather, Climate and Tourism: A Geographical Perspective. *Ann. Tourism Res.* 32, 571–591. <https://doi.org/10.1016/j.annals.2004.08.004>
- Besancenot, J.P., Mouiner, J., and De Lavenne, F., 1978: Les conditions climatiques du tourisme littoral: un methode de recherche comprehensive. *Norois* 99, 357–382. <https://doi.org/10.3406/noroi.1978.3717>

- Bojović, G., 2012: Kopaonik and its spas. Serbian Geographical Society, Belgrade
- de Freitas C.R., 1990: Recreation Climate Assessment. *International J. Climatol.* 10, 89–103. <https://doi.org/10.1002/joc.3370100110>
- Elsasser, H. and Bürki, R., 2002: Climate change as a threat to tourism in the Alps. *Climate Res.* 20, 253–257. <https://doi.org/10.3354/cr020253>
- Fanger, P.O., 1970: *Thermal Comfort: Analysis and Applications in Environmental Engineering*. Copenhagen: Danish Technical Press.
- Fitchett, J. and Hoogendoorn, G., 2018: An analysis of factors affecting tourists' accounts of weather in South Africa. *Int. J. Biometeorol.* 62, 2161–2172. <https://doi.org/10.1007/s00484-018-1617-0>
- Gao Y., Gao, X., and Zhang, X., 2017: The 2 °C Global Temperature Target and the Evolution of the Long-Term Goal of Addressing Climate Change—From the United Nations Framework Convention on Climate Change to the Paris Agreement. *Engineering* 3, 272–278. <https://doi.org/10.1016/J.ENG.2017.01.022>
- Gavrilov, M., Marković, S., Janc, N., Nikolić, M., Valjarević, A., Komac, B., Zorn, M., Punišić, M. and Bačević, N., 2018: Assessing average annual air temperature trends using the Mann-Kendall test in Kosovo. *Acta Geographica Slovenica* 58, 7–25. <https://doi.org/10.3986/AGS.1309>
- Houghten, F.C. and Yaglou, C.P., 1923: Determining equal comfort lines. *J. Amer. Soc. Heating Ventilating Engin.* 29, 165–176.
- IPCC, 2014: *Climate Change 2014: Synthesis Report. Contribution of Working Groups I, II and III to the Fifth Assessment Report of the Intergovernmental Panel on Climate Change* [Core Writing Team, R.K. Pachauri and L.A., Meyer (eds.)]. IPCC Geneva Switzerland.
- Jahić, H. and Mezetović, A., 2014: Qualitative Valorisation of Climate Tourism Potential by Application of the Tourism Climate Index - TCI on the example of Herzegovina-Neretva Canton/County. *Acta geographica Bosniae et Herzegovinae* 2, 91–106.
- Joksimović, M., Gajić, M., and Golić, R., 2013: Tourism climatic index in the valorisation of climate in tourist centers of Montenegro. *Bull. Serbian Geograph. Soc.* 93, 15–34. <https://doi.org/10.2298/GSGD1301015J>
- Kovacs, A., Nemeth, A., Unger J. and Kantor, N., 2017: Tourism climatic conditions of Hungary – present situation and assessment of future changes. *Időjárás* 121, 79–99.
- Matzarakis, A., 2006: Weather and Climate – Related Information for Tourism. *Tourism and Hospitality Planning & Development* 3, 99–115. <https://doi.org/10.1080/14790530600938279>
- Matzarakis, A., 2009: Additional Features of the RayMan Model. In: *The 7th International Conference on Urban Climate (P2-32: 1-4)*. International Association for Urban Climate, Yokohama.
- Matzarakis, A., Andrade, H., and Alcoforado, M.J., 2008: Thermal Bioclimatic Maps for Portugal. In: (eds Alcoforado, M.J., Andrade, H., Lopes, A. and Oliviera, S.): *Estudos sobre Cidades e Alterações Climáticas*. Centro de Estudos Geográficos da Universidade de Lisboa, Área de Investigação em Geo-Ecologia, Lisboa. 37–45.
- Meteorological yearbook, 2017: *Meteorological yearbook 1 – Climate data*. Belgrade (1990–2016) Republic Hydrometeorological Service of Serbia.
- Mieczkowski, Z., 1985: The Tourism Climatic Index: A Method of Evaluating World Climates for Tourism. *The Canadian Geographer/Le Géographe canadien* 29, 220–233. <https://doi.org/10.1111/j.1541-0064.1985.tb00365.x>
- Milovanović, B., Ducić, V., Radovanović, M. and Milivojević, M., 2017: Climate regionalisation of Serbia according to Köppen climate classification. *Journal of the Geographical institute „Jovan Cvijić“ SASA* 67, 103–114. <https://doi.org/10.2298/IJG1702103M>
- Perch-Nielsen, S., Amelung, B., and Knutti, R., 2010: Future climate resources for tourism in Europe based on the daily Tourism Climatic Index. *Climatic change* 103, 363–381. <https://doi.org/10.1007/s10584-009-9772-2>
- Roshan, G., Yousefi, R. and Błażejczyk, K., 2018: Assessment of the climatic potential for tourism in Iran through biometeorology clustering. *Int. J. Biometeorol.* 62, 525–542. <https://doi.org/10.1007/s00484-017-1462-6>
- Roshan, G., Yousefi, R. and Fitchett, M.J., 2016: Long-term trends in tourism climate index scores for 40 stations across Iran: the role of climate change and influence on tourism sustainability. *Int. J. Biometeorol.* 60, 33–52. <https://doi.org/10.1007/s00484-015-1003-0>

- Sabzevari, A.A., Miri, M., Razić, T., Oroji, H., and Rahimi, M., 2018: Evaluating the climate capabilities of the coastal areas of southeastern Iran for tourism: a case study on port of Chabahar. *Int. J. Biometeorol.* 62, 1135–1145. <https://doi.org/10.1007/s00484-018-1516-4>
- Scott, D. and McBoyle, G., 2001: Using a ‘tourism climate index’ to examine the implications of climate change for climate as a tourism resource. In (eds. Matzarakis A. and Freitas, de C.): Proceedings of the First International Workshop on Climate, Tourism and Recreation, International Society of Biometeorology, Greece. 69–86
- Smith, K., 1993: The Influence of Weather and Climate on Recreation and Tourism. *Weather* 48, 398–403. <https://doi.org/10.1002/j.1477-8696.1993.tb05828.x>
- Statistical Office of the Republic of Serbia, 2017: Catering and tourism statistics – Tourist turnover in the Republic of Serbia. Belgrade (2007–2016).
- Tzu-Ping, L. and Matzarakis, A., 2008: Tourism climate and thermal comfort in Sun Moon Lake, Taiwan. *Int. J. Biometeorol.* 52, 281–290. <https://doi.org/10.1007/s00484-007-0122-7>
- Valjarević, A., Vukoičić, D. and Valjarević, D., 2017: Evaluation of the tourist potential and natural attractiveness of the Lukovska Spa. *Tourism Manage. Perspectives* 22, 7–16. <https://doi.org/10.1016/j.tmp.2016.12.004>
- Vesić, M. and Živanović, V., 2018: The current state and strategies for development of tourism in the Area of exceptional features „Vlasina“. 3rd International Thematic Monograph: „Modern Management Tools and Economy of Tourism Sector in Present Era“, pp. 449-461, Association of Economists and Managers of the Balkans in cooperation with the Faculty of Tourism and Hospitality, Belgrade. <https://doi.org/10.31410/tmt.2018.449>
- Vukoičić, D., Milosavljević, S., Penjišević, I., Bačević, N., Nikolić, M., Ivković, R. and Jandžiković B., 2018: Spatial analysis of air temperature and its impact on the sustainable development of mountain tourism in Central and Western Serbia. *Időjárás* 122, 259–283. <https://doi.org/10.28974/idojaras.2018.3.3>
- Weir, B., 2017: Climate change and tourism – Are we forgetting lessons from the past?. *J. Hospital. Tourism Manage.* 32, 108–114. <https://doi.org/10.1016/j.jhtm.2017.05.002>
- Yan, F., Yin, J. and Wu, B., 2018: Climate change and tourism: a scientometric analysis using CiteSpace. *J. Sustain. Tourism* 26, 108–126. <https://doi.org/10.1080/09669582.2017.1329310>

# IDŐJÁRÁS

*Quarterly Journal of the Hungarian Meteorological Service*  
Vol. 124, No. 3, July – September, 2020, pp. 381–399

## Assessment of air temperature trend in South and Southeast Bosnia and Herzegovina from 1961 to 2017

**Dragan Papić<sup>\*1</sup>, Nikola R. Bačević<sup>2</sup>, Aleksandar Valjarević<sup>2</sup>,  
Nikola Milentijević<sup>2</sup>, Milivoj B. Gavrilov<sup>3</sup>, Milenko Živković<sup>1</sup>,  
and Slobodan B. Marković<sup>3</sup>**

<sup>1</sup>*University of Banja Luka  
Faculty of Natural Sciences and Mathematics  
Department of Geography  
78000 Banja Luka, Republic of Srpska, Bosnia and Herzegovina*

<sup>2</sup>*University of Priština  
Faculty of Natural Sciences and Mathematics  
38220 Kosovska Mitrovica, Serbia*

<sup>3</sup>*University of Novi Sad, Faculty of Sciences  
Department of Geography  
Tourism and Hotel Management  
21000 Novi Sad, Serbia*

*\*Corresponding author E-mail: dragan.papic@pmf.unibl.org*

*(Manuscript received in final form September 3, 2019)*

**Abstract**— Recent climate change has been caused by interaction of natural processes and the anthropogenic factor. In turn, it incites the pronounced natural and socio-economic changes. It is the air temperature that plays a pertinent role in understanding the climate change problem. Southeast Europe, including Bosnia and Herzegovina (B&H), is highly relevant for the observations of regional differences in changes of air temperature regime. From the regional-geographical point of view, South and Southeast B&H cover 26.5% (13.568 km<sup>2</sup>) of B&H territory (51.209 km<sup>2</sup>). It is from south and southeast that the Mediterranean impacts from the Adriatic Sea penetrate into the defined region, which further affects the variability of climate conditions in B&H. The paper presents trends in three parameter categories: mean annual, mean maximum, and mean minimum air temperatures in the territory of South and Southeast B&H. The aim of the paper is to demonstrate the likely climate change based on air temperature trends. Methodologically, temperature trends were processed by using the Mann-Kendall trend test. For the purpose of the analysis, available data from four meteorological stations in South and Southeast B&H for a 56-year period were used. Based on the obtained results, a statistically relevant positive trend was observed in all twelve time series. According to the analyzed

trends, the increase of air temperature was dominant in the target area. The application of Geographical Information System (GIS) tools indicated the presence of regional differences in air temperature distribution. An evident phenomenon is the combined impact of the orography of the region and the maritime influence. The occurring climate change affects specific social sectors, so the problem must be addressed properly. Another pertinent fact is that the climate change problem has not been adequately analyzed in the strategic documents in B&H.

*Key-words:* climate change, air temperature trends, Mann-Kendall trend test, GIS tools, South and Southeast Bosnia and Herzegovina

## 1. Introduction

According to highly reliable data from IPCC, the period from 1983 to 2012 was the warmest thirty-year period in Northern Hemisphere over the last 800 years (IPCC, 2014). The mean global surface temperature on Earth determined by the linear trend indicated the 0.85 °C increase during the period from 1880 to 2012. Regional differences referring to the increase of mean global temperature range from 0.65 °C to 1.06 °C (Blunden, *et al.*, 2018). Interactions between natural processes and human activities have caused the global air temperature values for the 2005–2015 decade to increase (0.87 °C) in comparison with the preindustrial values. If the current trend remains unchanged, projections of the global air temperature indicate a 1.5 °C increase for the period from 2030 to 2052 (Papalexiou, 2018; IPCC, 2018). There have been multiple attempts to reduce the anthropogenic impact on global climate. It was in 1989 that the Montreal Protocol was ratified by 197 countries in order to preserve the ozone layer (Downie, 2012). The 1997 Kyoto Protocol projected the reduction of gas emissions affecting the global warming (Breidenich, 1998). The current Paris Agreement on Climate Change ratified in 2015 has resulted in many controversies, as the signatory countries lack the uniformity in its implementation (Teske, 2019). The mean annual air temperature in Europe was 1.6–1.7 °C higher over the last decade (2008–2017), which made this decade the warmest ever documented (EEA, 2018). Apart from reports, many authors have analyzed temperature trends. Klein Tank and Können (2003) used data from 168 European meteorological stations for the period 1946–1999 and specified the tendency of growth of mean European air temperature. From 1977 to 2000, the trends grew in Central and Northeast Europe. Mediterranean air temperature trends were lower and the temperature increase was more evident in winter than in summer (Alcamo *et al.*, 2007). Therefore, the 20th century witnessed the air temperature increase in most Europe, and the changes were most evident in the 1990s (Kovats, *et al.*, 2014). A similar trend continued in the years to follow as it was in the 21st century, that the four warmest years were registered ever since the first measurements started - 2015, 2016, 2017, and 2018 (WMO, 2019). Time-space interruptions and different methods of interpolation have been the main

shortcomings of all measurement results so they should be used carefully (Blunden and Arndt, 2015). Generally, there have been both annual and seasonal increases of mean air temperature in Europe (Brázdil et al., 1996; Brunetti et al., 2004; Feidas, et al., 2004; Brunet et al., 2007; Chen et al., 2015; Werz and Hoffman, 2016).

Earlier studies in Southeast Europe addressed the air temperature trends on regional levels (Jovanović et al., 2002; Dorđević, 2008; Unkašević and Tošić, 2013; Burić et al., 2014; Bajat et al., 2015; Tošić et al., 2016; Gavrilov et al., 2015, 2016, 2018; Trbić, et al., 2017; Bačević et al., 2018; Popov et al., 2018b, Vukoičić et al., 2018) and dealt with aridity as an indicator of climate change in higher regions (Bačević et al., 2017; Radaković et al., 2017; Milentijević et al., 2018).

This paper analyzes recent air temperature trends. Earlier studies in Bosnia and Herzegovina (Trbić et al., 2017; Popov et al., 2017, 2018a, 2018b) also established an increasing trend of mean annual air temperature.

Speaking of the impact of climate change onto specific economic areas in Bosnia and Herzegovina, there is a high risk of extreme climate events such as drought (Sheffield and Wood, 2007; Orłowsky and Senewiratne, 2013; Stagge et al., 2015; Spinoni et al., 2015, 2017). Future projections anticipate a growing frequency of this natural disaster in Europe, so it is crucial to undertake adequate measures. These measures are actually adaptation to the drought phenomenon, which is the cause of many socio-economic changes connected with nature, agriculture, and available water resources (Bressers et al., 2016).

This scientific paper comprises the following sections: 1) introduction; 2) description of research area; 3) used data and methodology; 4) obtained results; 5) discussion; 6) concluding remarks.

## 2. Study area

South and Southeast B&H share the borderline with Republic of Croatia in southwest and south and Republic of Montenegro in southeast, whereas the northern line of delineation follows the municipalities of Livno, Tomislavgrad, Prozor, Konjic, Kalinovik, Foch, and Čajniče (Republic of B&H) (Fig. 1). The research area is located between the 44°23' (the municipality of Livno) and 42°55' (the municipality of Trebinje) northern latitudes and 16°52' (the municipality of Livno) and 19°25' (the municipality of Čajniče) eastern longitudes. The following meteorological stations were used for the purpose of the research: Livno (43°49'22" N, 17°00'04" E, and 739 m altitude), Mostar (43°20'53" N, 17°47' 38" E, and 48 m altitude), Ivan Sedlo (43° 45'04" N, 18°02'10" E, and 955 m altitude), and Bileća (42°52'04" N, 18°25'29" E, and 480 m altitude) (Fig. 1, Table 1).



Fig. 1. Geographical position of South and Southeast B&H with landmarks of analyzed meteorological stations.

Table 1. Meteorological stations in South and Southeast Bosnia and Herzegovina

Station No.	Station location	Altitude	Latitude	Longitude
1	Livno	739 m	43° 49' 22" N	17° 00' 04" E
2	Bileća	480 m	42° 52' 04" N	18° 25' 29" E
3	Mostar	48 m	43° 20' 53" N	17° 47' 38" E
4	Ivan Sedlo	955 m	43° 45' 04" N	18° 02' 10" E

From physical-geographical aspects, the area is characterized by extreme holokarst located in the Outer Dinarides. The region covers watersheds of the Neretva and Trebišnjica rivers and their tributaries, as well as the upper Drina River. Holokarst largely affects the air temperature, particularly in summer, due to bare rocky ground which heats quickly (e.g., Mostar area). The climate is

diverse ranging from the pronounced Mediterranean climate on the Adriatic coast (Neum), the altered Mediterranean climate in the lower Neretva River (Mostar at 48 m altitude) suitable for early vegetable and Mediterranean fruit (this type of climate also occurs in Trebinje and Popovo Polje at around 280 m altitude), the continental climate in most of the region, and, finally, typical mountain climate at high mountain ranges (*Marković, 1972; Rodić, 1975*).

### **3. Data and methods**

#### **3.1. Data**

The paper analyzed air temperature trends in the target area for the period from 1961 to 2017. Data from four meteorological stations published at Meteorological almanacs of the Hidrometeorological Institute of the Republic of Srpska (<https://rhmzrs.com/?script=lat>) and the Hidrometeorological Institute of the B&H Federation (<https://www.fhmzbih.gov.ba>) were used. There were interruptions in measurement at most meteorological stations, especially during the 1991–1995 war. The percentage of the missing data is 8.9% for Livno and Ivan Sedlo and 7.1% for Bileća. An exception is the Mostar meteorological station, at which there were intermittent measurements during the target time frame. Due to reasonable grounds, the missing data were compiled by using an interpolation method (*Kilibarda et al., 2015*). The paper uses linear interpolation which represents the simplest method for interpolation of a data set. It is defined as the arithmetic mean of linear interpolants between two neighboring data pairs (*Hazewinkel, 1990*). MICROSOFT OFFICE EXCEL was the program used for the interpolation of the missing data.

Geographical coordinates and altitudes of meteorological stations are given in *Table 1*. The hypsometry of selected stations differs. For instance, relative altitude difference between Mostar meteorological station (48 m) and the highest meteorological station at Ivan Sedlo (955 m) reaches 907 m, which indicates the diversity of climate conditions. The pronounced hypsometric differences among the stations generate a vertical thermal gradient – the average decline in air temperature is 0.65 °C/100 m altitude (*Oliver, 2005*). The terrain orography and the vicinity of the Adriatic Sea contribute to the climate diversity, so the analyzed data are presented for each meteorological station independently.

The paper displays results obtained through analysis of air temperature as a climate variable. The air temperatures are categorized in three classes: mean (*YT*), mean maximum (*YT $\alpha$* ), and mean minimum air temperatures (*YT $n$* ). The mean air temperature values are available from meteorological yearbooks. The extreme temperature values are presented by using mean maximum and mean minimum air temperature values. These were calculated as a ratio of the sum of mean monthly air temperatures and interval duration, i.e., the number of months in a year (*Milosavljević, 1990*).

The total of twelve time series was determined through the analysis of the aforementioned parameters. Each of the series was assigned an adequate acronym combining the abbreviation of the meteorological station, the year, and the temperature type (*Table 2*).

*Table 2.* List of 12 time series to calculate surface air temperature trends in South and Southeast Bosnia and Herzegovina

Station	Year (Y)
Livno (L)	$L - YT$
	$L - YT_x$
	$L - YT_n$
Bileća (B)	$B - YT$
	$B - YT_x$
	$B - YT_n$
Mostar (M)	$M - YT$
	$M - YT_x$
	$M - YT_n$
Ivan Sedlo (I)	$I - YT$
	$I - YT_x$
	$I - YT_n$

### 3.2. Methods

Three statistical approaches were used in the air temperature trend analysis. The first approach refers to the linear trend equation (*Draper and Smith, 1966*), which was designed for each time series separately. Independent of the initial step, all trends were tested by using the non-parametric MK trend test (*Mann, 1945; Kendall, 1938*). The third step referred to the definition of trend magnitude determined through the trend equation (*Gavrilov et al., 2016*). The MICROSOFT OFFICE EXCEL program was used to determine air temperature trends. XLSTAT software (<https://www.xlstat.com/en>) was used to calculate the  $p$  reliability level and test our hypotheses. GIS is used as a potent tool for the analysis and numerical modeling of a whole range of climate data (*Collins and Bolstad, 1996*).

### 3.2.1. Trend equation

The linear trend method is an extremely relevant technique used in order to analyze, evaluate, and distribute both long-term and short-term changes in air temperature (Herrmann *et al.*, 2005; Heim, 2015; Ghebregabher *et al.*, 2016). Its general form is:

$$y = ax + b, \quad (1)$$

in which  $y$  is the air temperature expressed in °C,  $a$  is the gradient,  $x$  is the time series, and  $b$  is the initial temperature. The air temperature trend value correlates with the gradient. There are three possible scenarios: a) the gradient is higher than zero – the trend is positive (growing); b) the gradient is smaller than zero – the trend is negative (declining), or c) the gradient is equal to zero – there is no trend (without alterations).

### 3.2.2. Trend magnitude

The trend magnitude is determined by using the linear trend equation (Gavrilov *et al.*, 2016) as follows:

$$\Delta y = y(1961) - y(2017), \quad (2)$$

in which  $\Delta y$  is the trend magnitude expressed in °C,  $y(1961)$  is the air temperature at the beginning of the period, and  $y(2017)$  is the air temperature at the end of the period. There are three possible scenarios with the trend magnitude: a)  $\Delta y$  is higher than zero – the trend is negative (declining); b)  $\Delta y$  is smaller than zero – the trend is positive (growing), and c)  $\Delta y$  is equal to zero – there is no trend (without alterations).

### 3.2.3. Mann-Kendall (MK) test

Apart from the regression analysis, the non-parametric Mann-Kendall test was used to additionally assess the presence or absence of the trend (Mann, 1945; Kendall, 1938). The following two hypotheses were tested by using the MK test: the zero hypothesis ( $H_0$ ), which indicates the absence of the trend in the time series and the alternative hypothesis  $H_a$ , in which there is a statistically relevant trend in the time series for the given relevance level ( $\alpha$ ). The  $p$  value has a central role in the MK test (Karmeshu, 2012; Razavi *et al.*, 2016). The  $p$  value determines the hypothesis reliability level. If the  $p$  value is smaller than the selected  $\alpha$  relevance level (commonly  $\alpha=0.05$  or 5%), the hypothesis  $H_0$  should be rejected and the hypothesis  $H_a$  should be adopted. As opposed, if  $p$  is larger than the  $\alpha$  relevance level, then the hypothesis  $H_0$  is adopted (Mudelsee, 2010; Hennemuth *et al.*, 2013).

### 3.2.4. Geographical Information Sistem (GIS) numerical analysis

Geographical Information System (GIS) is a powerful tool for modeling climate data. The greatest advantage of the GIS numerical analysis is the analysis of the region itself with all its integrated climate data. Geostatistical methods of interpolation and semi-variogram are of primary pertinence in the numerical GIS analysis. These classical statistical methods combined with kriging methods provided outstanding results (Valjarević *et al.*, 2018a; Petterson and Hoalst-Pullen, 2011). Other geostatistical methods used for the purpose of this research enabled a better distribution of climate data within a specific territory. The advantage of the Open Source software is the possibility of coding and decoding within the software itself, and the best-known instances of the software were used such as QGIS, SAGA, and GRASS GIS. The greatest benefit of the climate data processing in this software is a specific numerical methodology which adjusts to the target geospace. In this manner, each geospace is processed through a specific numerical analysis, and the errors are minimal as characteristics of both the geospace and the data are taken into account (Valjarević *et al.*, 2018b; Pew and Larsen, 2001).

## 4. Results

### 4.1. Trend parameters

The paper provides results of mean annual air temperature values ( $Y$ ). The data are categorized in line with temperature types. The analysis covers the total of four meteorological stations in Livno, Bileća, Mostar, and Ivan Sedlo, i.e., twelve time series. *Figs. 2–5* display mean annual air temperatures ( $YT$ ), mean annual maximum air temperatures ( $YT_x$ ), and mean annual minimum air temperatures ( $YT_n$ ), as well as trend test equations and linear equations for each meteorological station in South and Southeast B&H for the observed period from 1961 to 2017. Trend magnitudes  $\Delta y(^{\circ}\text{C})$  and trend probability  $p$  for each time series and each meteorological station within the observed territory are provided in *Tables 1* and *2*. The results are displayed in *Table 3* presenting both parameters and trend equations for all twelve time series.

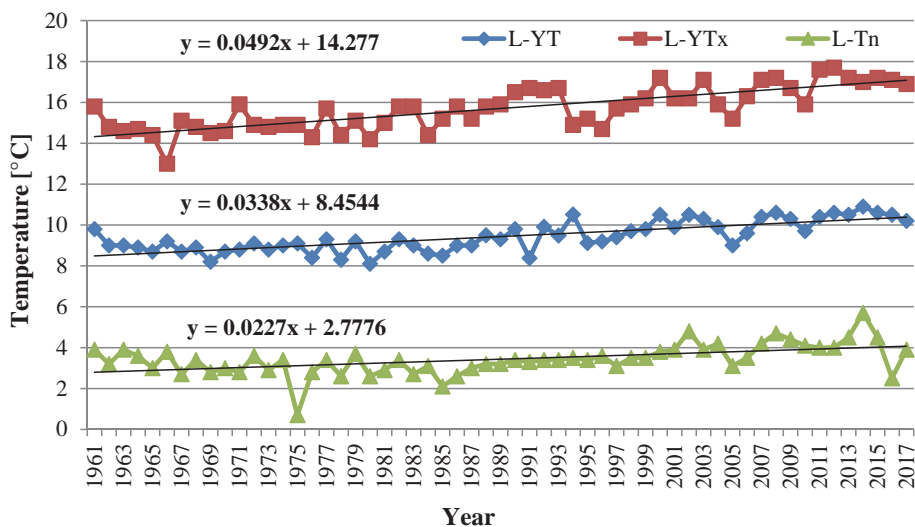


Fig. 2. Average annual mean, maximum, and minimum air temperatures, trend equations, and linear trend in Livno for the observed period 1961–2017.

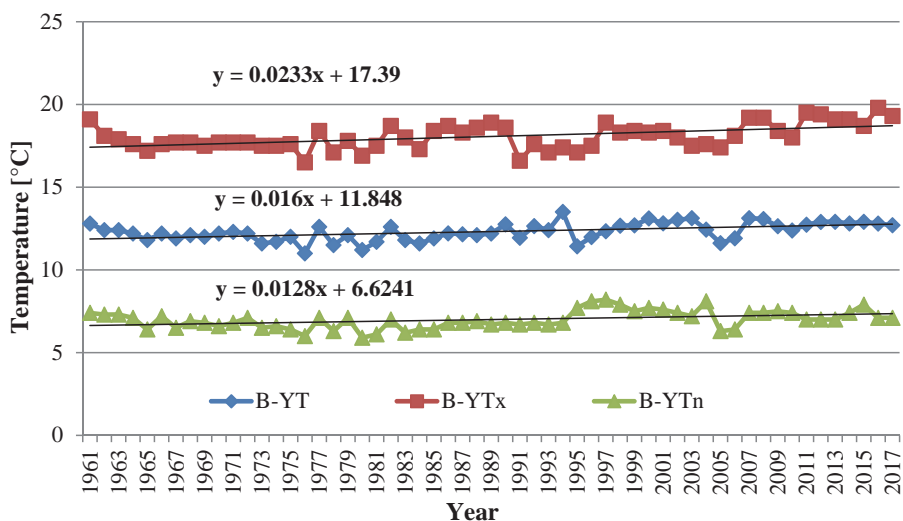


Fig. 3. Average annual mean, maximum, and minimum air temperatures, trend equations, and linear trend in Bileća for the observed period 1961–2017.

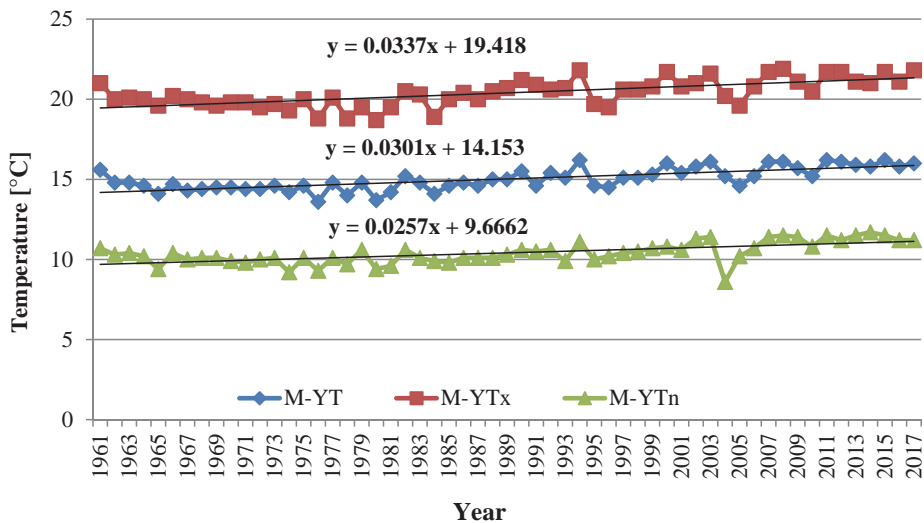


Fig. 4. Average annual mean, maximum, and minimum air temperatures, trend equations, and linear trend in Mostar for the observed period 1961–2017.

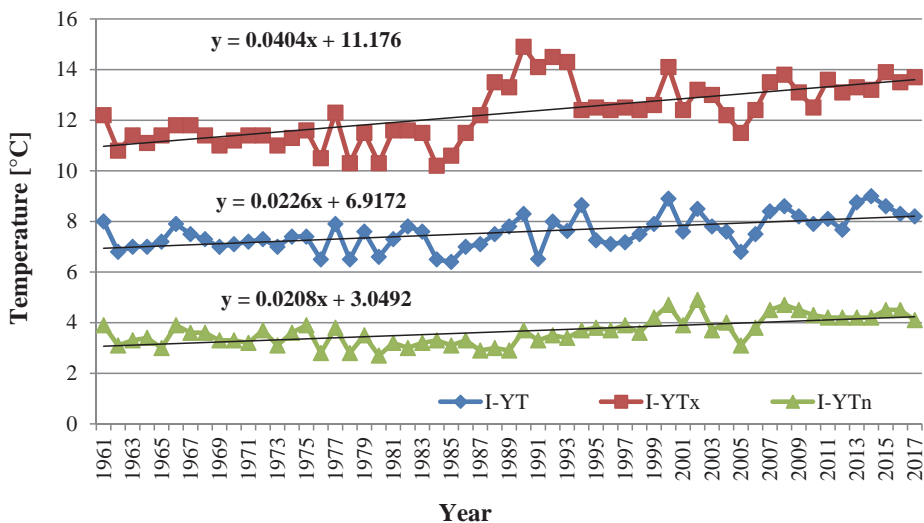


Fig. 5. Average annual mean, maximum, and minimum air temperatures, trend equations, and linear trend in Ivan Sedlo for the observed period 1961–2017.

Table 3. Trend equation  $y$ , trend magnitude  $\Delta y$ , and probability  $p$  of the reliability for 12 time series

Time series	Trend equation	$\Delta y$ (°C)	$p$ (%)
$L - YT$	$y=0.492x+14.277$	1.9	< 0.0001
$L - YTx$	$y=0.0338x+8.4544$	2.8	< 0.0001
$L - YTn$	$y=0.0227x+2.7776$	1.3	< 0.0001
$B - YT$	$y=0.0233x+17.39$	0.9	< 0.0001
$B - YTx$	$y=0.016x+11.848$	1.3	0.0001
$B - YTn$	$y=0.0128x+6.6241$	0.7	0.0059
$M - YT$	$y=0.0337x+19.418$	1.7	< 0.0001
$M - YTx$	$y=0.0301x+14.153$	1.9	< 0.0001
$M - YTn$	$y=0.0257x+9.6662$	1.4	< 0.0001
$I - YT$	$y=0.0404x+11.176$	1.3	< 0.0001
$I - YTx$	$y=0.0226x+6.9172$	2.6	< 0.0001
$I - YTn$	$y=0.0208x+3.0492$	1.2	< 0.0001

#### 4.2. Trend estimation

Main results of the MK air temperature trend test displayed in Table 3 are supported by Figs. 2–5. Hence, the character and intensity of the analyzed air temperature trends in our target region are corroborated. Figs. 2–5 and Table 3 show that the trends for all twelve time series were positive. It is the MK test that helps us infer whether these claims were true.

If probability  $p$  for the time series  $YT$ ,  $YTx$ , and  $YTn$  in the target territory is smaller than  $\alpha$ , the hypothesis  $H_0$  (the trend does not exist) will be abandoned and the hypothesis  $H_a$  (the trend exists) will be adopted for all these time series. The  $p$  value is < 0.0001 in time series  $YT$ ,  $YTx$ , and  $YTn$  for the meteorological stations in Livno, Mostar, and Ivan Sedlo and in time series  $YTn$  for the meteorological station in Bileća. The prevailing hypothesis is  $H_0$ . The risk of abandoning the hypothesis  $H_0$  is smaller than 0.01%. The  $p$  value is 0.0001 for the time series  $YTx$  for the meteorological station in Bileća. The risk of abandoning the hypothesis  $H_0$  is 0.02%. For the time series  $YTn$  for the meteorological station in Bileća, the  $p$  value is 0.0059. The risk of abandoning the hypothesis  $H_0$  is 0.02%.

#### 4.3. GIS numerical analysis

The mean annual air temperatures ( $YT$ ) within the target territory from 1961 to 2017 are displayed in Fig. 6. The spatial distribution of isotherms indicates the

intraregional temperature differences resulting from the terrain orography. For instance, in Ivan Sedlo located within the mountain notch and Livno located in a typical karst field,  $YT$  varies from 8 °C to 10 °C. Mostar meteorological station is located at low altitude (48 m) and is under a direct maritime impact from the Adriatic Sea along the Neretva River valley; its  $YT$  varies from 11 °C to 14 °C and summer temperature is often higher than in the coastline. The temperature regime in Bileća is determined by different climate modifiers, especially in regards to altitude, continental, and maritime impacts, location within the basin and the Bilećko Lake. These are all factors which resulted in  $YT$  value of 12 °C. The construction of the artificial accumulation of water in Bileća in 1968 caused the change of microclimate elements as the mean air temperature decreased, and the air humidity and mean precipitation sum increased (Marković, 1990).

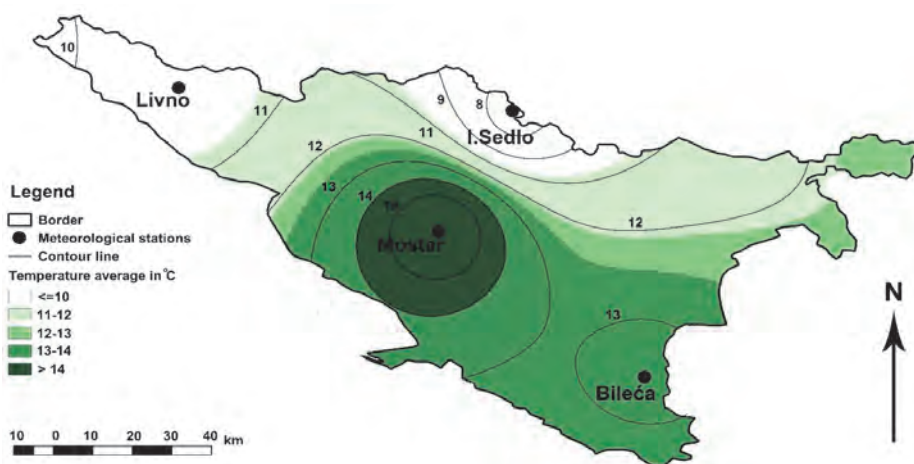


Fig. 6. Distribution of  $YT$  in South and Southeast Bosnia and Herzegovina territory in the period 1961–2017.

Mean maximum annual air temperatures ( $YT_x$ ) in the target territory from 1961 to 2017 are displayed in Fig. 7. For instance, in Ivan Sedlo  $YT_x$  is 13 °C and in Livno it is 16 °C. The lowland positioned station in Mostar has the  $YT_x$  of 20 °C, and in Bileća it is 19 °C.

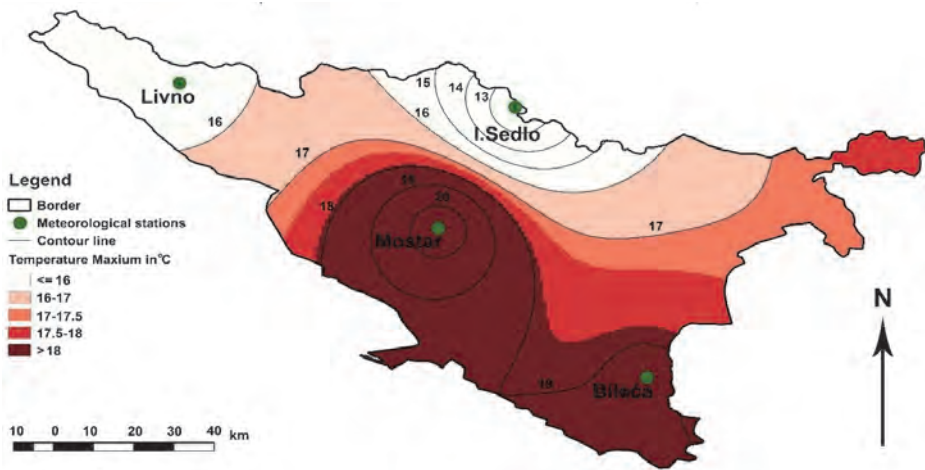


Fig. 7. Distribution of  $YT_x$  in South and Southeast Bosnia and Herzegovina territory in the period 1961–2017.

Mean minimum annual air temperatures ( $YT_n$ ) in the target territory in the period 1961–2017 are displayed in Fig. 8. In line with the map,  $YT_n$  is 4 °C for Ivan Sedlo and Livno, whereas it is 10 °C in Mostar and 6 °C in Bileća.

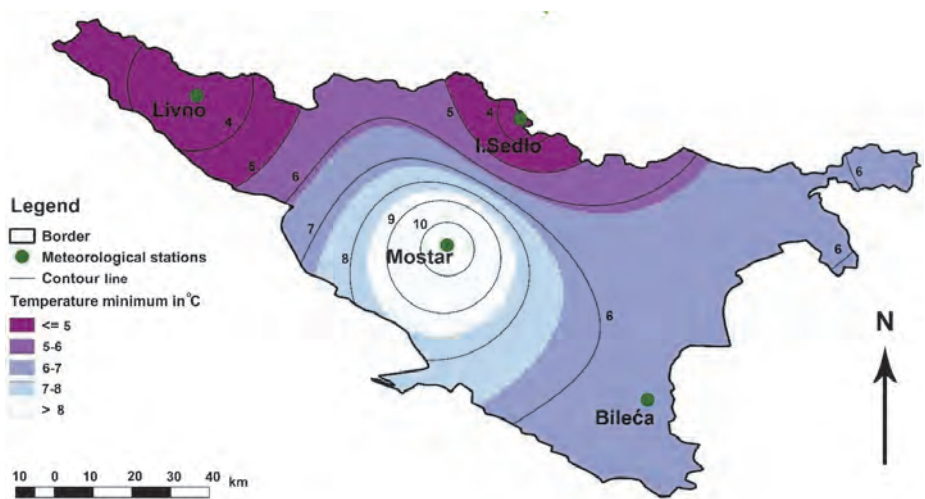


Fig. 8. Distribution of  $YT_n$  in South and Southeast Bosnia and Herzegovina territory in the period 1961–2017.

## 5. Discussion

According to the obtained results, the air temperature increase prevails in South and Southeast Bosnia and Herzegovina. The trend magnitude (*Table 3*) identifies an evident increase of values of mean, mean maximum, and mean minimum air temperatures. When it comes to individual instances, most pronounced changes occur with mean maximum air temperatures. The mean increase is 2.8 °C in Livno, 2.3 °C in Ivan Sedlo, 1.9 °C in Mostar, and 1.3 °C in Bileća. In cases of mean annual air temperatures, the results are as follows: Livno 1.9 °C, Mostar 1.7 °C, Ivan Sedlo 1.3 °C, and Bileća 0.9 °C. The least pronounced changes occur with mean minimum air temperatures and these are registered in Ivan Sedlo (1.2 °C) and Bileća (0.7 °C). Identical results are difficult to find in the large body of works. The trend of increase of mean air temperature in Europe has been growing since 1979 both seasonally and annually (*Klein-Tank and Können, 2003*). Speaking of regional level, there have been similar trends. For instance, *Brázdil et al., (1996)* found that in ten states of Central and South Europe there was an increase in cases of mean maximum and mean minimum air temperatures (from 1951 to 1990). A study performed by *Brunetti et al., (2004)* identified a trend in mean annual air temperatures. The mean annual air temperature trend varies from 0.4 °C/100 years in North Italy to 0.7 °C/100 years in the south of the state. A statistically relevant increase of trends of mean, mean maximum, and mean minimum air temperatures was identified in all of Slovenian territory and it varied from 0.3 °C to 0.5 °C per decade (*Milošević et al., 2013, 2017*). In addition, *Mamara et al., (2016)* processed data from 52 meteorological stations in Greece and found a statistically negative trend between 1960 and 1976. On the other hand, a statistically positive trend was identified between 1977 and 2004. It was in northern parts of Greece that the warming was particularly intensive. Similarly, an air temperature increase was determined in Vojvodina (*Gavrilov et al., 2015*), Kosovo (*Gavrilov et al., 2018*), and Montenegro (*Burić et al., 2014*). A general conclusion is that there is a correspondence between air temperature changes in B&H and in the wider region.

## 6. Conclusions

The annual and seasonal trends of mean, mean maximum, and mean minimum air temperatures in South and Southeast B&H from 1961 to 2017 were analyzed. The air temperature trends were analyzed for twelve time series by using: a) trend equation, b) trend magnitude, and c) MK trend test. There was a positive trend for all twelve time series for mean, mean maximum, and mean minimum air temperatures. The regional positive trends of air temperatures represent a climate change pattern in Northern Hemisphere, which is in line with conclusions of the Intergovernmental Panel on Climate Change (IPCC, 2014).

Climate change does not only affect the nature but the society as well. Agriculture is a particularly sensitive sector as its ratio in total economy is 7% of the B&H Gross Domestic Product (GDP). The population engaged in the sector suffers directly, too. In addition, pronounced climate change threatens food safety, which raises the need for adaptation of agricultural production in affected regions. Nevertheless, the whole process is an interaction among geographical, socio-economic, political, cultural, ecological, and institutional factors. Unfortunately, the problem of climate change has not been paid adequate attention in B&H strategic documents (Trbić *et al.*, 2018). Opportunities to adapt the economy sector to climate change in B&H are defined in the document titled „*Climate change adaptation and low emission development strategy for Bosnia and Herzegovina*“. Its application should reduce negative impacts of climate change and increase adaptation options and usage of development opportunities caused by climate change (Radusin *et al.*, 2013). In line with the set tasks, this document should be implemented into the B&H development strategy. Future studies should focus on climate change projections and analysis of climate change impact on the economy sector.

## *References*

- Alcamo, J., Moreno, J.M., Nováky, B., Bindi, M., Corobov, R., Devoy, R.J.N., Giannakopoulos, C., Martin, E., Olesen, J.E., and Shvidenko, A., 2007: Europe. In (Eds. M.L. Parry, O.F. Canziani, J. Palutikof, P. van der Linden and C. Hanson), *Climate Change 2007: Impacts, Adaptation and Vulnerability. Contribution of Working Group II to the Fourth Assessment Report of the Intergovernmental Panel on Climate Change* (541-580). Cambridge University Press, Cambridge, United Kingdom and New York, NY, USA.
- Bajat, B., Blagojević, D., Kilibarda, M., Luković, J. and Tošić, I., 2015: Spatial Analysis of the Temperature Trends in Serbia during the Period 1961–2010. *Theor. Appl. Climatol.* 121, 289–301. <https://doi.org/10.1007/s00704-014-1243-7>
- Bressers, J.T.A., Bressers, N., and Larrue, C., 2016: *Governance for Drought Resilience: Land and Water Drought Management in Europe*. Springer. <https://doi.org/10.1007/978-3-319-29671-5>
- Breidenich, C., Magraw, D., Rowley, A., and Rubin, J., 1998: The Kyoto Protocol to the United Nations Framework Convention on Climate Change. *Amer. J. Int. Law* 92, 315–331. <https://doi.org/10.2307/2998044>
- Bačević, R.N., Vukoičić, Z.D., Nikolić, M., Janc, N., Milentijević, N., and Gavrilov, B.M., 2017: Aridity in Kosovo and Metohija, Serbia. *Carpathian J. Earth Environ. Sci.* 12, 563–570.
- Bačević, R.N., Pavlović, M., and Rmaltitudejanin, I., 2018: Trend Assessing Using Mann-Kendall's Test for Priština Meteorological Station Temperature and Precipitation Data, Kosovo and Metohija, Serbia, *Publ. Nat. Sci.*, (8)2, 39–43. <https://doi.org/10.5937/univtho8-19513>
- Blunden, J. and Arndt, D.S., 2015: State of the Climate in 2014, *Bull. Amer. Meteorol. Soc.* 96(7), ES1–32. <https://doi.org/10.1175/2015BAMSStateoftheClimate.1>
- Blunden, J., Arndt, D.S., and Hartfield, G., 2018: State of the Climate in 2017, *Bull. Amer. Meteorol. Soc.* 99(8), Si–S332. <https://doi.org/10.1175/2018BAMSStateoftheClimate.1>
- Brázdil, R., Budykov, M., Auer, I., Böhm, R., Cegnar, T., Fasko, P., Lapin, M., Gajic-Capka, M., Zaninovic, K., Koleva, E., Niedzwiedz, T., Szalai, S., Ustrnul, Z. and Weber, R.O., 1996: Trends of maximum and minimum daily temperatures in central and southeastern Europe. *Int. J. Climatol.* 16, 765–782. [https://doi.org/10.1002/\(SICI\)1097-0088\(199607\)16:7<765::AID-JOC46>3.0.CO;2-O](https://doi.org/10.1002/(SICI)1097-0088(199607)16:7<765::AID-JOC46>3.0.CO;2-O)

- Brunetti, M., Buffoni, L., Mangianti, F., Maugeri, M., and Nanni, T., 2004: Temperature, precipitation and extreme events during the last century in Italy. *Glob. Planet. Change*, 40, 141–149. [https://doi.org/10.1016/S0921-8181\(03\)00104-8](https://doi.org/10.1016/S0921-8181(03)00104-8)
- Brunet, M., Jones, P.D., Sigro, J., Saladie, O., Aguilar, E., Moberg, A., Della-Marta, P.M., Lister, D., Walther, A. and López, D., 2007: Temporal and spatial temperature variability and change over Spain during 1850–2005. *J.Geophys. Res.: Atmospheres*, 112, 1984–2012. <https://doi.org/10.1029/2006JD008249>
- Burić, D., Luković, J., Ducić, V., Dragojlović, J., and Doderović, M., 2014: Recent trends in daily temperature extremes over southern Montenegro (1951–2010), *Nat. Haz. Earth Syst. Sci.*, 14, 67–72. <https://doi.org/10.5194/nhess-14-67-2014>
- Chen, D., Walther, A., Moberg, A., Jones, P., Jacobeit, J. and Lister, D., 2015: European Trend Atlas of Extreme Temperature and Precipitation Records. Springer, Netherlands. <https://doi.org/10.1007/978-94-017-9312-4>
- Collins, F.C. and Bolstad, P.V., 1996: A comparison of spatial interpolation techniques in temperature estimation. In Proceedings of the Third International Conference/Workshop on Integrating GIS and Environmental Modeling. National Center for Geographic Information Analysis (NCGIA). Santa Fe, NM, Santa Barbara, CA, January 21–25.
- Downie, D.L., 2012: The Vienna Convention, Montreal Protocol and Global Policy to Protect Stratospheric Ozone. In (Eds. P. Wexler et al.) Chemicals, Environment, Health: A Global Management Perspective. Taylor & Francis, Oxford. <https://doi.org/10.1201/b11064-20>
- Draper, N.R., and Smith, H., 1966: Applied Regression Analysis. John Wiley & Sons, New York, USA.
- Dorđević, S.V., 2008: Temperature and precipitation trends in Belgrade and indicators of changing extremes for Serbia. *Geographica Pannonica*, 12(2), 62–68. <https://doi.org/10.5937/GeoPan0802062D>
- EEA, 2018: National Climate Change Vulnerability and risk assessments in Europe, EEA Report No.1/2018. <https://www.eea.europa.eu/publications/national-climate-change-vulnerability-2018> (accessed 06.02.2019)
- EXCEL, <https://products.office.com/en-us/home> (accessed 09.03.2019)
- Federal Hydrometeorological Service of Bosnia and Herzegovina, <https://www.fhmzbih.gov.ba/> (accessed 09.02.2019)
- Feidas, H., Makrogiannis, T., and Bora-Senta, E., 2004: Trend analysis of air temperature time series in Greece and their relationship with circulation using surface and satellite data: 1955–2001. *Theor. Appl. Climatol.* 79, 185–208. <https://doi.org/10.1007/s00704-004-0064-5>
- Gavrilov, M.B., Marković, S.B., Jarad, A., and Korać, V.M., 2015: The analysis of temperature trends in Vojvodina (Serbia) from 1949 to 2006. *Thermal Sci.* 19, 339–350. <https://doi.org/10.2298/TSCI150207062G>
- Gavrilov, M.B., Tošić, I., Marković, S.B., Unkašević, M. and Petrović, P., 2016: The analysis of annual and seasonal temperature trends using the Mann-Kendall test in Vojvodina, Serbia. *Időjárás* 122, 203–216. <https://doi.org/10.28974/idojaras.2018.2.6>
- Gavrilov, M.B., Marković, S.B., Janc, N., Nikolić, M., Valjarević, A., Komac, B., Zorn, M., Punišić, M. and Bačević, N., 2018: Assessing average annual air temperature trends using the Mann-Kendall test in Kosovo. *Acta geographica Slovenica*, 58, 8–25, <https://doi.org/10.3986/AGS.1309>
- Ghebregabher, M.G., Yang, T. and Yang, X., 2016: Long-Term Trend of Climate Change and Drought Assessment in the Horn of Africa. *Adv. Meteorol.* 2016, Article ID 8057641, 12. <https://doi.org/10.1155/2016/8057641>
- Hazewinkel, M., 1990: Encyclopaedia of Mathematics. Springer, Netherlands. <https://doi.org/10.1007/978-94-009-5991-0>
- Herrmann, S.M., Anyamba, A., and Tucker, C.J., 2005: Recent trends in vegetation dynamics in the African Sahel and their relationship to climate. *Glob. Environ. Change*, 15, 394–404. <https://doi.org/10.1016/j.gloenvcha.2005.08.004>
- Hennemuth, B., Bender, S., Bülow, K., Dreier, N., Keup-Thiel, E., Krüger, O., Mudersbach, C., Radermacher, C., and Schoetter, R., 2013: Statistical methods for the analysis of simulated and

- observed climate data, applied in projects and institutions dealing with climate change impact and adaptation, CSC Report No. 13.  
[https://www.climate-service-center.de/imperia/md/content/csc/projekte/csc-report13\\_englisch\\_final-mit\\_umschlag.pdf](https://www.climate-service-center.de/imperia/md/content/csc/projekte/csc-report13_englisch_final-mit_umschlag.pdf) (accessed 10.03.2019)
- Heim, R.R., 2015: An overview of weather and climate extremes – Products and trends, *Weather Climate Extr.* 10(B), 1–9. <https://doi.org/10.1016/j.wace.2015.11.001>
- IPCC, 2014: Climate Change 2014: Synthesis Report. Contribution of Working Groups I, II and III to the Fifth Assessment Report of the Intergovernmental Panel on Climate Change [Core Writing Team, (eds. R.K. Pachauri and L.A. Meyer). IPCC, Geneva, Switzerland, 151.
- IPCC, 2018: Summary for Policymakers. In: Global warming of 1.5°C. An IPCC Special Report on the impacts of global warming of 1.5°C above pre-industrial levels and related global greenhouse gas emission pathways, in the context of strengthening the global response to the threat of climate change, sustainable development, and efforts to eradicate poverty (eds. V. Masson-Delmotte, P. Zhai, H. O. Pörtner, D. Roberts, J. Skea, P. R. Shukla, A. Pirani, W. Moufouma-Okia, C. Péan, R. Pidcock, S. Connors, J. B. R. Matthews, Y. Chen, X. Zhou, M. I. Gomis, E. Lonnoy, T. Maycock, M. Tignor, T. Waterfield). World Meteorological Organization, Geneva, Switzerland, 32.
- Jovanović, G., Reljin, I., and Savić, T., 2002: NAO Influence on climate variability in FRY. 18th International conference on Carpathian meteorology. Belgrade.
- Karmeshu, N., 2012: Trend detection in annual temperature and precipitation using the Mann Kendall test – a case study to assess climate change on select states in the northeastern United States. Master's thesis, 27, University of Pennsylvania, Philadelphia.
- Kendall, M., 1938: A new measure of rank correlation. *Biometrika*, 30, 81–89.  
<https://doi.org/10.2307/2332226>
- Kilibarda, M., Tadić Perčec, M., Hengl, T., Luković, J. and Bajat, B., 2015: Global geographic and feature space coverage of temperature data in the context of spatio-temporal interpolation, *Spatial Stat.* 14(A), 22–38. <https://doi.org/10.1016/j.spasta.2015.04.005>
- Klein Tank, A.M.G. and Können, G.P., 2003: Trends in Indices of Daily Temperature and Precipitation Extremes in Europe, 1946–99. *J. Climate*, 16, 3665–3680.  
[https://doi.org/10.1175/1520-0442\(2003\)016<3665:TIIODT>2.0.CO;2](https://doi.org/10.1175/1520-0442(2003)016<3665:TIIODT>2.0.CO;2)
- Kovats, R. S., Valentini, R., Bouwer, L. M., Georgopoulou, E., Jacob, D., Martin, E., Rounsevell, M. and Soussana, J. F., 2014: Europe. In: (eds. Barros, V. R., Field, C. B., Dokken, D. J., Mastrandrea, M. D., Mach, K. J., Bilir, T. E., Chatterjee, M., Ebi, K. L., Estrada, Y. O., Genova, R. C., Girma, B., Kissel, E. S., Levy, A.N., MacCracken, S., Mastrandrea, P. R., White, L.L.) Climate Change 2014: Impacts, Adaptation, and Vulnerability. Part B: Regional Aspects. Contribution of Working Group II to the Fifth Assessment Report of the Intergovernmental Panel on Climate Change. Cambridge University Press, Cambridge, United Kingdom and New York, NY, USA.
- Mamara, A., Argiriou, A.A. and Anadranistakis, M., 2016: Recent Trend Analysis of Mean Air Temperature in Greece Based on Homogenized Data. *Theor. Appl. Climatol.* 126, 543–573.  
<https://doi.org/10.1007/s00704-015-1592-x>
- Mann, H. B., 1945: Non-parametric Tests Against Trend. *Econometrica* 13, 245–259.  
<https://doi.org/10.2307/1907187>
- Marković, J. Đ., 1972: Geografske oblasti Socijalističke Federativne Republike Jugoslavije. Zavod za udžbenike i nastavna sredstva Srbije, Beograd (in Serbian).
- Marković, Đ.J. 1990: Enciklopedijski geografski leksikon Jugoslavije. Svjetlost, Sarajevo (in Serbian).
- Milentijević, N., Dragojlović, J., Ristić, D., Cimbaljević, M., Demirović, D. and Valjarević, A., 2018: The assessment of aridity in Leskovac Basin, Serbia (1981-2010), *J. Geograph. Inst. "Jovan Cvijić"*, 68, 249–264. <https://doi.org/10.2298/IJGI1802249M>
- Milosavljević, M., 1990: Klimatologija. Naučna knjiga, Beograd (in Serbian).
- Milošević, D., Savić, S. and Žiberna, I., 2013: Analysis of the Climate Change in Slovenia: Fluctuations of Meteorological Parameters for the Period 1961–2011 (Part I). *Bull. Serbian Geograph. Soc.* 93, 1–14. <https://doi.org/10.2298/GSGD1301001M>

- Milošević, D., Savić, S., Stankov, U., Žiberna, I., Pantelić, M., Dolinaj, D. and Leščešen, I., 2017: Maximum temperatures over Slovenia and their relationship with atmospheric circulation patterns. *Geografije* 122, 1–20. <https://doi.org/10.37040/geografije2017122010001>
- Mudelsee, M., 2010: Climate Time Series Analysis: Classical Statistical and Bootstrap Methods. Springer, Dordrecht, The Netherlands.
- Oliver, E. J., 2005: Temperature Distribution. In (Ed. E. J. Oliver), *Encyclopedia of World Climatology*, 711–716. Springer, Dordrecht, The Netherlands.
- Orlowsky, B., and Seneviratne, S. I., 2013: Elusive drought: uncertainty in observed trends and short- and long-term CMIP5 projections. *Hydrol. Earth Syst. Sci.* 17, 1765–1781. <https://doi.org/10.5194/hess-17-1765-2013>
- Popov, T., Gnjato, S. and Trbić, G., 2017: Trends in extreme temperatures indices in Bosnia and Herzegovina: A case study of Mostar. *Herald*, 21, 107–132. <https://doi.org/10.7251/HER2117107P>
- Popov, T., Gnjato, S., Trbić, G. and Ivanišević, M., 2018a: Recent Trends in Extreme Temperature Indices in Bosnia and Herzegovina. *Carpathian J. Earth. Environ. Sci.* 13, 211–224. <https://doi.org/10.26471/cjees/2018/013/019>
- Popov, T., Gnjato, S. and Trbić, G., 2018b: Changes in temperature extremes in Bosnia and Herzegovina: A fixed thresholds-based index analysis. *J. Geograph. Inst. "Jovan Cvijić" SASA*, 68, 17–33. <https://doi.org/10.2298/IJGI1801017P>
- Papalexioiu, S.M., Agha Kouchak, A., Trenberth, K.E., and Foufoula-Georgiou, E., 2018. Global, Regional, and Megacity Trends in the Highest Temperature of the Year: Diagnostics and Evidence for Accelerating Trends, *Earth's Future*, 6, 71–79. <https://doi.org/10.1002/2017EF000709>
- Patterson, M. W., and Hoalst-Pullen, N., 2011: Dynamic equifinality: The case of southcentral Chile's evolving forest landscape. *Appl. Geography* 31, 641–649. <https://doi.org/10.1016/j.apgeog.2010.12.004>
- Pew, K. L., and Larsen, C. P. S., 2001: GIS analysis of spatial and temporal patterns of human-caused wildfires in the temperate rain forest of Vancouver Island, Canada. *Forest Ecol. Manage.* 140, 1–18. [https://doi.org/10.1016/S0378-1127\(00\)00271-1](https://doi.org/10.1016/S0378-1127(00)00271-1)
- Radaković, G.M., Tošić, A.I., Bačević, R.N., Mađan, D., Marković, S.B., and Gavrilov, M.B., 2017: The analysis of aridity in Central Serbia from 1949-2015. *Theor. Appl. Climatol.* 133, 887–898. <https://doi.org/10.1007/s00704-017-2220-8>
- Razavi, T., Switzman, H., Arain, A., and Coulibaly, P., 2016: Regional climate change trends and uncertainty analysis using extreme indices: A case study of Hamilton, Canada, *Climate Risk Manage.* 13, 43–63. <https://doi.org/10.1016/j.crm.2016.06.002>
- Radusin, S., Oprašić, S., Cero, M., Abdurahmanović, I., Vukmir, G., Avdić, S., Cupać, R., Tais, M., Drešković, N., Trbić, G. and Jakšić, B., 2013: Second national communication of Bosnia and Herzegovina under the United Nations framework convention on climate change. UNDP, Banjaluka.
- Republic Hydrometeorological Service of Republika Srpska, <https://rhmzrs.com/?script=lat> (accessed 09.02.2019)
- Rodić, D. P., 1975: *Geografija Jugoslavije*. Naučna Knjiga, Beograd (in Serbian).
- Sheffield, J., and Wood, E.F., 2007: Projected changes in drought occurrence under future global warming from multi-model, multi-scenario, IPCC AR4 simulations. *Climate Dynamics*, 31, 79–105. <https://doi.org/10.1007/s00382-007-0340-z>
- Spinoni, J., Naumann, G. and Vogt, J., 2015: Spatial patterns of European droughts under a moderate emission scenario. *Adv. Sci. Res.* 12, 179–186. <https://doi.org/10.5194/asr-12-179-2015>
- Spinoni, J., Naumann, G., and Vogt, V. J., 2017: Pan-European seasonal trends and recent changes of drought frequency and severity. *Glob. Planetary Change* 148, 113–130. <https://doi.org/10.1016/j.gloplacha.2016.11.013>
- Stagge, J. H., Rizzi, J., Tallaksen, L. M. and Stahl, K., 2015: Future Meteorological Drought Projections of Regional Climate. *Tech. Rep.*, 25, DROUGHT-R&SPI Project.
- Teske, S., 2019: *Achieving the Paris Climate Agreement Goals*. Springer, Netherlands. <https://doi.org/10.1007/978-3-030-05843-2>
- Trbić, G., Popov, T. and Gnjato, S., 2017: Analysis of air temperature trends in Bosnia and Herzegovina. *Geographica Pannonica* 21, 68–84. <https://doi.org/10.5937/GeoPan1702068T>

- Trbić, G., Bajić, D., Djurdjević, V., Ducić, V., Cupac, R., Markež, Đ., Vukmir, G., Dekić, R. and Popov, T., 2018: Limits to Adaptation on Climate Change in Bosnia and Herzegovina: Insights and Experiences. In: (eds. *Leal Filho W., Nalau J.*) Limits to Climate Change Adaptation. Climate Change Management. Springer, Cham, Switzerland. [https://doi.org/10.1007/978-3-319-64599-5\\_14](https://doi.org/10.1007/978-3-319-64599-5_14)
- Tošić, I., Zorn, M., Ortar, J., Unkašević, M., Gavrilov, M.B. and Marković, S.B., 2016: Annual and seasonal variability of precipitation and temperatures in Slovenia from 1961 to 2011, *Atmos. Res.* 168, 220–233. <https://doi.org/10.1016/j.atmosres.2015.09.014>
- Unkašević, M. and Tošić, I., 2013: Trends in temperature indices over Serbia: relationships to large-scale circulation patterns. *Int. J. Climatol.* 33, 3152–3161. <https://doi.org/10.1002/joc.3652>
- Valjarević, A., Djekić, T., Stevanović, V., Ivanović, R. and Jandžiković, B., 2018a: GIS Numerical and remote sensing analyses of forest changes in the Toplica region for the period of 1953–2013. *Appl. Geography* 92, 131–139. <https://doi.org/10.1016/j.apgeog.2018.01.016>
- Valjarević, A., Srećković-Batočanin, D., Valjarević, D. and Matović V. A., 2018b: GIS-based method for analysis of a better utilization of thermal-mineral springs in the municipality of Kursumlija (Serbia). *Renew. Sust. Energy Rev.* 92, 948–957. <https://doi.org/10.1016/j.rser.2018.05.005>
- Vukočić, D., Milosavljević, S., Penjišević, I., Bačević, N., Nikolić, M., Ivanović, R. and Jandžiković, B., 2018: Spatial analysis of air temperature and its impact on the sustainable development of mountain tourism in Central and Western Serbia. *Időjárás* 122, 259–283. <https://doi.org/10.28974/idojaras.2018.3.3>
- XLSTAT, <http://www.xlstat.com/en/> (accessed 10.03.2019)
- Werz, M. and Hoffman, M., 2016: Europe's twenty-first century challenge: climate change, migration and security, *European View* 15, 145–154. <https://doi.org/10.1007/s12290-016-0385-7>
- WMO, 2019: Statement on the State of the Global Climate in 2018. WMO-No. 1233. World Meteorological Organization. Geneva, Switzerland.



# IDŐJÁRÁS

*Quarterly Journal of the Hungarian Meteorological Service*  
Vol. 124, No. 3, July – September, 2020, pp. 401–418

## Forecast skill of regional ensemble system compared to the higher resolution deterministic model

Simona Tascu<sup>1</sup>, Mirela Pietrisi<sup>3,1</sup>, Christoph Wittmann<sup>2</sup>, Florian Weidle<sup>2</sup>,  
and Yong Wang<sup>2</sup>

<sup>1</sup> *Meteo Romania (National Meteorological Administration)*  
*Bucharest, Romania*

<sup>2</sup> *Zentralanstalt für Meteorologie und Geodynamik (ZAMG)*  
*Vienna, Austria*

<sup>3</sup> *University of Bucharest, Faculty of Physics*  
*P.O.BOX MG 11, Magurele, Bucharest, Romania*

*\*Corresponding author E-mail: mirela.niculae@meteoromania.ro*

*(Manuscript received in final form July 8, 2019)*

**Abstract**—The 11 km regional ensemble ALADIN-LAEF (Aire Limitée Adaption Dynamique Développement InterNational – Limited Area Ensemble Forecasting) is evaluated by comparison with the 5 km deterministic model ALARO (ALADIN and AROME combined model – Application of Research to Operations at Mesoscale), in order to investigate the advantages and disadvantages facing short-range ensemble and high-resolution forecasts. To make rational decisions about the benefits or challenges of both systems, the forecast skill was measured through probabilistic and deterministic approaches over a 2-month period from late spring to summer season of 2013. The verification uses observations from 1219 SYNOP stations and 1 km × 1 km precipitation analysis from INCA (*Integrated Nowcasting through Comprehensive Analysis*) nowcasting system. The evaluation was carried out for three essential meteorological variables: 2 m temperature, 10 m wind speed, and 6-hour cumulated precipitation. From the probabilistic point of view, the results show that ALADIN-LAEF outperforms ALARO-LAGGED ensemble system, being statistically more reliable. From the deterministic point of view, the high-resolution deterministic system simulates better the precipitation forecast structure with respect to the observations. Compared to the ensemble system, the deterministic system cannot provide guidance concerning the forecast uncertainties or probabilities, making the ensemble products a powerful tool for risk assessment and decision making.

**Key-words:** ensemble forecast, numerical models, time-lagged, ALADIN-LAEF, ALARO

## 1. Introduction

An accurate weather forecast is crucial in severe weather conditions that could lead to a large variety of damages including loss of lives. Furthermore, increasingly skilful numerical weather forecasts convey essential information for several domains of public interest, like health, agriculture, energy, tourism.

Despite the significant increase in forecast skill, uncertainties in the initial conditions and the model formulation itself affect the accuracy of the forecast. The inherent errors in the initial conditions could amplify in time, due to the complexity and chaotic character of the atmospheric system, leading sometimes to completely different solutions (Lorenz, 1963). These errors are due to the irregular distribution (relative sparseness) of the observation network, the measurement instruments errors, as well as to data assimilation. The benefit of using data assimilation algorithms is unquestionable in the numerical weather prediction field (Law and Stuart, 2012). Nonetheless, small uncertainties are coming from data assimilation algorithms due to mathematical assumptions (Du, 2007). The forecast uncertainty arisen from the imperfection of the model itself was quantified for the first time through stochastic perturbations of the physical tendencies (SPPT scheme) in the ECMWF model (Buizza *et al.*, 1999; Palmer, 2001). Other approaches to simulate the model uncertainties are based on multi-physics schemes (Murphy *et al.*, 2004) or on the use of Poor Man's Ensemble (Ebert, 2001; Corazza *et al.*, 2018).

To quantify these uncertainties, a widely used technique is the ensemble prediction system (Palmer, 2017): a single deterministic forecast provides one single scenario and a simple decision strategy, while an ensemble system is able to provide probabilistic information and multiple scenarios. Several studies have been done on the comparison of global ensemble and deterministic systems (Buizza, 2008; Palmer *et al.*, 2005/06; Rodwell, 2005/06). The results show that a coarser resolution ensemble with more members can outperform a higher resolution ensemble with less members.

Here we use the regional ensemble system ALADIN-LAEF (Wang *et al.*, 2011) and the ALARO deterministic model (Termonia *et al.*, 2017). The operational ALADIN-LAEF system has been developed at ZAMG (ZentralAnstalt für Meteorologie und Geodynamik, Vienna, Austria) within the framework of Regional Cooperation for Limited-Area modelling in Central Europe (RC-LACE, Wang *et al.*, 2018). ALADIN-LAEF runs in operational mode on European Centre for Medium-Range Weather Forecasts's (ECMWF) supercomputer (Wang *et al.*, 2011). The system is used in different downstream applications such as hydrology, transportation, energy, agriculture, and civil warnings (Vokoun and Hanel, 2018; Wastl *et al.*, 2018). The limited area ALARO model development started in 2003 as a version of ALADIN system. It is able to cover a large variety of horizontal resolution ranges, up to the so-called convection permitting scales (Termonia *et al.*, 2017).

This paper presents the benefit of using regional ensemble over deterministic systems – even if both the horizontal and vertical resolutions of the deterministic model are much higher. This issue is addressed by a verification study, from the probabilistic and deterministic points of view. The paper is structured as follows: Section 2 introduces the ALADIN-LAEF and ALARO models setup and the time-lagged ensemble; Section 3 describes the dataset and verification methodologies; Section 4 encapsulates the results from a 2-month period verification for surface parameters, and a case study is performed; the conclusions are drawn in Section 5.

## ***2. Models setup and time-lagged ensemble method***

### *2.1. ALADIN-LAEF – Limited Area Ensemble Forecasting*

ALADIN-LAEF is a single model limited area ensemble system based on the ALARO model (Wang *et al.*, 2011, 2018) and runs operationally two times per day at 00 and 12 UTC, on a horizontal resolution at approximately 11 km, with 45 levels in the vertical and a forecast range up to 72-hour. The integration domain covers Europe and large parts of the North Atlantic, the Mediterranean Sea, and the Black Sea. ALADIN-LAEF consists of 16 perturbed members, using the first 16 members of 50 from ECMWF’s ensemble prediction system ENS (Buizza *et al.*, 2000) as coupling model (Weidle *et al.*, 2013).

To provide meaningful initial perturbations for the ensemble members, a breeding-blending cycle is applied for atmospheric fields (Wang *et al.*, 2011). This method combines large-scale perturbations from the driving ECMWF ENS members with ALADIN-LAEF breeding vectors that contain perturbations on scales that can be resolved by ALADIN-LAEF (Toth and Kalnay, 1993). To assure a smooth transition between large-scale and small-scale perturbations, a digital filter initialization (DFI) is used (Wang *et al.*, 2014). The DFI is applied on low truncations of both the ALADIN-breeding vectors and the fields from the driving model. The filtered breeding vectors are subtracted on the full resolution from the unfiltered ones, and this difference is then added to the filtered fields from ECMWF ENS. This method assures that the initial perturbations are consistent with both the driving ECMWF ENS member and ALADIN-LAEF itself. Surface perturbations are generated by running a surface assimilation scheme with randomly perturbed observations. An optimal interpolation (OI) assimilation of 2 m temperature and relative humidity observations is applied to perturb the uppermost surface fields in ALADIN-LAEF.

A multi-physics approach is implemented in ALADIN-LAEF to account for model uncertainties. Different model configurations with various parameterizations and tuning settings are applied for each perturbed ensemble member. Different settings are used for shallow and deep convection,

microphysics, radiation, and turbulence parameterizations. In addition, different approaches and tunings for screen-level diagnostics and gust diagnostics are applied in the multi-physics package of ALADIN-LAEF.

## 2.2. ALARO deterministic model

The ALARO model can be described as the further development of the spectral limited area model ALADIN, in order to be able to run the model using grid spacing around 5 km or below. These scales pose a particular challenge to model developers as convection is neither fully resolved nor can be sufficiently described with a classical parameterized convection scheme. Therefore, the main differences between ALARO and ALADIN concern the deep convection scheme in the physics package. For ALARO, a prognostic convection scheme called Modular Multiscale Microphysics and Transport scheme (3MT) was developed by *Gerard and Geleyn (2005)*, *Gerard (2007)*, *Gerard et al. (2009)*. Further, a prognostic microphysics scheme is included together with a statistical scheme describing the sedimentation of precipitating hydrometeors (*Geleyn et al., 2008*). Turbulence is parameterized using a so-called pseudo prognostic TKE (turbulent kinetic energy) scheme, details can be found in *Váňa et al. (2008)*. Surface processes are described using a two-layer version of the ISBA scheme (Interactions between Soil, Biosphere, and Atmosphere, *Noilhan and Planton, 1989*). At ZAMG, the ALARO model is used in operational mode since March 2011. It is run up to 72-hour lead time, four times per day, using approximately 5 km grid spacing and 60 levels in the vertical. While the three-dimensional (3D) initial state for the atmosphere and the lateral boundary conditions are provided by the high resolution analysis and forecast of the Integrated Forecasting System (IFS HRES) from ECMWF, the surface is initialized using an optimal interpolation method.

## 2.3. Time-lagged ensemble using ALARO deterministic model

Since ALARO deterministic model is integrated in operational mode at ZAMG, four times per day up to a lead time of 72-hour, it is possible to generate a time-lagged ensemble (ALARO-LAGGED) with no additional computational costs. The construction of this ensemble is based on a combination of several deterministic integrations (*Hoffmann and Kalnay, 1983*). In our case, the time-lagged ensemble covers a forecast range of 48-hour and consists of forecasts from consecutive ALARO model runs, covering the same target time period. For a given day, the ensemble with initial time at 12 UTC contains 5 members, as shown in *Table 1*.

Table 1. ALARO-AUSTRIA time-lagged ensemble

12 UTC(one day before):													
member 5 -	00	06	12	18	24	30	36	42	48	54	60	66	72
18 UTC(one day before):													
member 4 -	00	06	12	18	24	30	36	42	48	54	60	66	
00 UTC(current day):													
member 3 -		00	06	12	18	24	30	36	42	48	54	60	
06 UTC(current day):													
member 2 -			00	06	12	18	24	30	36	42	48	54	
12 UTC(current day):													
member 1 -				00	06	12	18	24	30	36	42	48	

### 3. Dataset and verification methodologies

#### 3.1. Model dataset

The numerical forecast generated by the deterministic and ensemble systems is provided on regular latitude - longitude grids, having the resolution of  $0.1^\circ \times 0.14^\circ$  for ALADIN-LAEF, while for ALARO the denser grid of  $0.04^\circ \times 0.06^\circ$  is kept. The high-resolution grid for ALARO is used to preserve the mesoscale features of the forecasts. The verification domain covers most of Europe, a region between 2.55 to 31.8° E and 38.6 to 54.95° N (not shown).

#### 3.2. Observation dataset

SYNOP data from 1219 stations are used for verification. Model data were interpolated to the observation sites through a bilinear interpolation.

INCA is an analysis and a nowcasting system (Haiden *et al.*, 2009) developed at ZAMG. The system is run on a 3D grid with a horizontal resolution of 1 km. Depending on the parameter, the analysis and nowcasting are performed on a two-dimensional (2D) grid (e.g., precipitation) or a 3D grid (e.g., temperature, wind). For the 3D grid, a vertical resolution around 100–200 m is used. The system is fed by surface station observations, remote sensing data (radars and satellites), numerical weather prediction model data, and high-resolution topographic data.

### 3.3. Verification methodologies

An important question arises from whether the high-resolution deterministic ALARO model could compete with the lower resolution ALADIN-LAEF ensemble. This question can be answered by assessing the two systems based on deterministic and probabilistic approaches.

Both systems were evaluated by applying the traditional verification scores (like BIAS and RMSE), as well as the following ones:

- spread - skill relationship, based on the scatter diagram of ensemble spread and root mean square error of the ensemble mean;
- continuous ranked probability skill score (CRPSS), a skill score which is based on CRPS value (*Hersbach, 2000*) and verifies the model performance related to a reference;
- percentage of outliers, a measure of reliability quantifying the relative number of observations which lie outside the predicted density function for a given parameter.

The pointwise verification is not suitable for the precipitation field, because these scores do not fully account for the unique characteristics due to its discontinuity in space and time (*Casati et al., 2004*).

The traditional metrics offer little diagnostics about the types of errors (displacement, location, and intensity), therefore an advanced verification technique is applied. One spatial verification approach used in this study is the object-based method SAL (structure-amplitude-location). This method is a spatial three-component feature-based quality measure which quantifies the precipitation forecast performance according to three aspects: structure of the precipitation field (S), amplitude (A), and location (L) of the predicted mass center of the precipitation field (*Wernli et al., 2008*).

## 4. Results

To evaluate the performance of the described ensemble systems, a 2-month verification was performed for the period ranging from April 23 to June 23, 2013. The forecast output frequency is 6-hour and the verification length is up to 48-hour lead time, which is the maximum forecast range of ALARO-LAGGED. Even though both runs (00 and 12 UTC) of ALADIN-LAEF are available, only the 12 UTC runs are considered for this study.

First, the probabilistic approach is applied to evaluate the surface parameters: 2 m temperature (T2m), 10 m wind speed (W10m) and 6-hour cumulated precipitation (PREC) against SYNOP data. The computed scores are CRPSS, percentage of outliers and spread - skill relationship, as well as BIAS and RMSE of ensemble mean and ensemble spread. To reduce the forecast bias

at each SYNOP station, the 2 m temperature forecasts are height corrected using a standard temperature gradient.

Second, the deterministic approach is applied to verify the 6-hour cumulated precipitation against INCA analysis field (which represent a combination of radar and rain gauge data). The gridded analysis data are used for the computation of SAL score. The comparison of ALADIN-LAEF's ensemble mean and median and ALARO's most recent run was carried out.

#### 4.1. Comparison of ALADIN-LAEF with ALARO-LAGGED

This section compares, from the probabilistic point of view, the skill of ALADIN-LAEF and ALARO-LAGGED against SYNOP data. *Fig. 1* shows the metrics (BIAS and RMSE of the ensemble mean and spread) of both systems for the surface parameters.

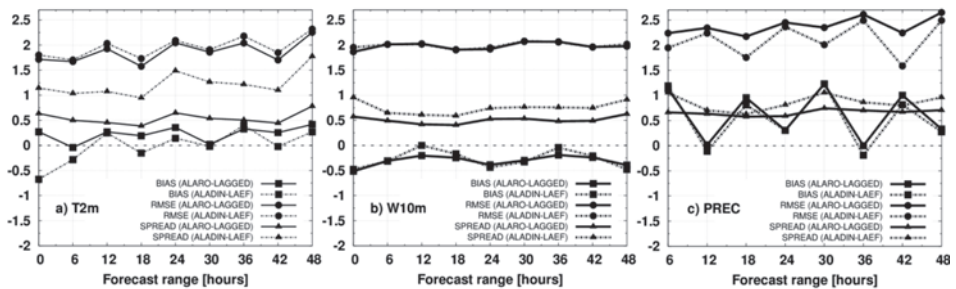


*Fig. 1.* BIAS and RMSE of ensemble mean and ensemble spread for ALARO-LAGGED (solid) and ALADIN-LAEF (dashed): a) T2m (°C); b) W10m (m/s); and c) PREC (mm).

For T2m, ALARO-LAGGED performs better than the limited area ensemble system in the first lead times (00 and 06 forecast ranges), for which ALADIN-LAEF has a strong negative BIAS (*Fig. 1a*). After 12-hour lead time, ALADIN-LAEF shows slightly less or equal BIAS than ALARO-LAGGED, except for 18 and 42 forecast ranges (morning hours) when the BIAS is considerably smaller. *Fig. 1b* shows that the W10m BIAS of both systems have comparable negative values for all lead times. The exception is made for 12- and 36-hour lead time when ALADIN-LAEF has almost no BIAS. For PREC, *Fig. 1c* shows a similar BIAS for both systems. ALARO-LAGGED system presents only positive values, better values for 12 and 36h (BIAS close to 0), while ALADIN-LAEF presents small negative values for these forecast ranges.

Likewise, *Fig. 1* presents RMSE and spread as a function of lead time for surface parameters. In terms of RMSE, the forecast errors are similar for both

systems. The ALADIN-LAEF system has a larger spread, which means that it is more reliable than ALARO-LAGGED, but the discrepancy between the ensemble spread and RMSE leads to the fact, that both systems are not enough statistically reliable (Buizza *et al.*, 2005). It is expected that ALARO-LAGGED will have a small spread, considering the lagged ensemble members are partially correlated. They are obtained using the same model, high-resolution forecasts with different ages.

The spread - skill relationship is presented in Fig. 2. The scatter diagram shows that ALARO-LAGGED simulates too little uncertainty, meaning the spread is underestimated, having only points which are not uniformly distributed. Fig. 2c (PREC) indicates a good correlation between spread and skill, especially for ALADIN-LAEF the relation is slightly better. Thereby, the ALADIN-LAEF system is more reliable than ALARO-LAGGED. Statistical reliability can be underlined by the usage of percentage of outliers, quantifying the number of cases where the analysis is outside of the predicted density function. As it can be seen from Fig. 3, ALARO-LAGGED has more outliers than ALADIN-LAEF.

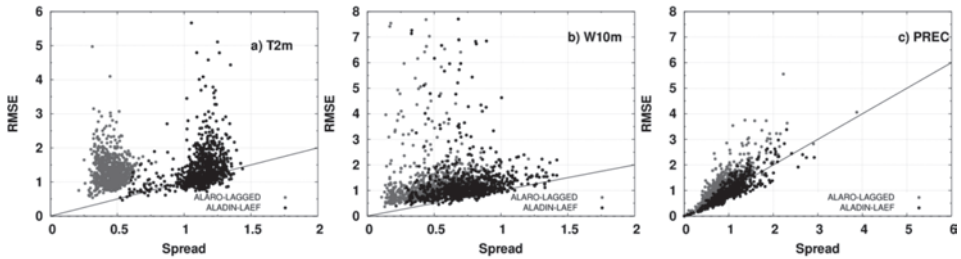


Fig. 2. RMSE-Spread relation for ALARO-LAGGED (grey) and ALADIN-LAEF (black): a) T2m (°C); b) W10m (m/s); and c) PREC (mm).

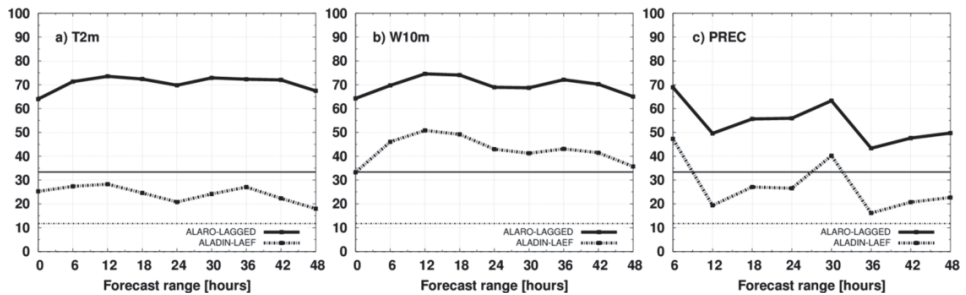


Fig. 3. Percentage of outliers (%) for ALARO-LAGGED (solid) and ALADIN-LAEF (dashed): a) T2m; b) W10m; and c) PREC.

Results revealed that ALARO-LAGGED has a similar RMSE (forecast accuracy), a smaller spread, and more outliers when compared to the ALADIN-LAEF. Therefore, having less dispersion, it is not able to cover many possible atmospheric situations. Considering all these findings, it can be concluded that ALADIN-LAEF is statistically more reliable.

#### 4.2. Skill score of ALADIN-LAEF and ALARO-LAGGED (reference ALARO)

The computation of the skill score CRPSS uses as reference system the ALARO deterministic model. Fig. 4 shows the quantitative skill of both ensembles. For all verified parameters, CRPSS has positive values throughout the forecast ranges. Even though both systems present positive values of the score, for ALADIN-LAEF they are significantly higher than ALARO-LAGGED. Based on the CRPSS results, ALADIN-LAEF ensemble is more skilful than ALARO-LAGGED. It is worth to underline that ALARO-LAGGED has an advantage since the most recent run from ALARO-LAGGED is used as the reference deterministic model.

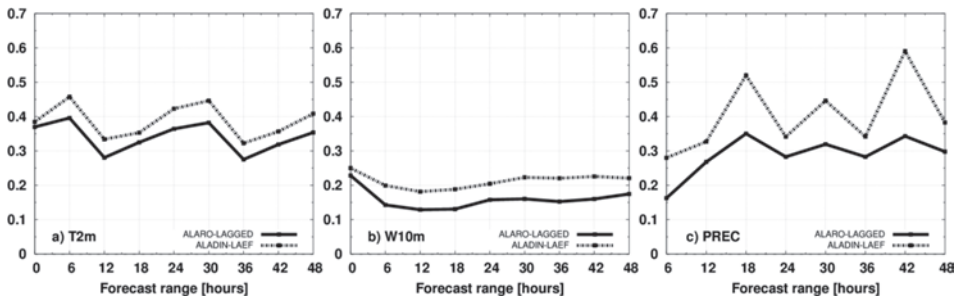


Fig. 4. Comparison of CRPSS for ALARO-LAGGED (solid) and ALADIN-LAEF (dashed): a) T2m; b) W10m; and c) PREC.

#### 4.3. Deterministic comparison of ALADIN-LAEF and ALARO systems

To perform the comparison of both systems in a deterministic sense, a single forecast from each system is needed. The solutions provided by ALARO deterministic model and ALADIN-LAEF (mean and median of the ensemble) are evaluated in this section. The SAL component scores have been computed to evaluate the precipitation forecasts of ALADIN-LAEF (median and mean) and ALARO. Verification was performed using several domains in Austria that are characterized by different topographic conditions (flatlands, alpine region, and hilly region).

In order to get more details, the evaluation was done for different observed precipitation thresholds, i.e., the SAL components are calculated separately for events with observed areal precipitation means greater than 0.1 mm, 1 mm, 2 mm, 3 mm, 5 mm, and 10 mm. Taking into account the chosen size of the domains, area mean values greater than 5 mm or even 10 mm represent rare extreme cases and are therefore not taken into account for computing mean S, A, or L values over the given verification period. *Table 2* shows the mean values for S, A, and L over all verification domains for different lead times.

*Table 2.* The S, A, L values: mean over all domains for ALARO (ALARO), ALADIN-LAEF's ensemble mean (LMEAN), and ALADIN-LAEF's ensemble median (LMEDI)

	06	12	18	24	30	36	42	48
S-ALARO	0.04	-0.22	-0.29	0.23	0.04	-0.23	-0.27	0.31
S-LMEAN	1.10	0.72	0.54	1.24	1.15	0.76	0.74	1.28
S-LMEDI	0.91	0.55	0.29	1.07	0.98	0.42	0.26	1.05
A-ALARO	-0.53	-0.49	-0.30	-0.03	-0.25	-0.55	-0.52	0.05
A-LMEAN	0.17	-0.33	-0.31	0.45	0.20	-0.36	-0.36	0.54
A-LMEDI	-0.47	-0.59	-0.54	0.17	-0.24	-0.49	-0.47	0.31
L-ALARO	0.22	0.21	0.21	0.20	0.23	0.23	0.24	0.24
L-LMEAN	0.22	0.20	0.20	0.27	0.23	0.23	0.23	0.29
L-LMEDI	0.20	0.19	0.22	0.26	0.21	0.24	0.25	0.29

*Fig. 5* shows the mean structure components for the 2-month period as a function of lead time, for a representative region in the southern part of Austria. The number of events used to build the mean values is indicated by the thin black bars in the same figure. It can be seen that:

- ALARO yields the best precipitation forecasts in terms of structure compared to the ensemble mean and median of ALADIN-LAEF, i.e., the size and shape of the precipitation simulated by ALARO corresponds better to the observed object characteristics (S values closer to 0). This result can be expected, as ALARO is run on a significantly higher horizontal resolution than ALADIN-LAEF.
- Comparing the ensemble mean and median of ALADIN-LAEF, the median yields slightly more structured forecasts, i.e., smaller values for S than the mean. This fact also meets expectations as the mean usually yields a smoother field.
- A diurnal cycle is visible for all systems, showing that the difference in terms of the observed objects gets usually bigger during night, leading to even negative S values. This diurnal behavior could be explained on the assumption that the transition from primary convection to more organized

one is not sufficiently simulated. This is mainly caused by a wrong or too early timing of triggering in the models, conducting to an early decrease of convection objects, leading to smaller objects compared to observations during the evening and early night. In reality, convection usually starts later during the day and lasts longer, as it is often more organized than in the models (Wittmann *et al.*, 2010). This behavior is also visible in the A component as described later.

- *Table 2* shows the S values averaged over all regions. The results differ in terms of absolute values of the S component for each domain (not shown), although the differences among the systems (ALARO vs. ALADIN-LAEF) and the characteristic of the diurnal cycle are consistent over all domains.
- A comparison of the results for different area mean thresholds seems to reveal that structure scores tend to get better, i.e., closer to 0, when concentrating on cases with higher precipitation rates (not shown). Also, the diurnal cycle is less pronounced. This could be correlated with the fact that strong precipitation events are often related to some large scale forcing which is less dependent on the general diurnal cycle of convection.

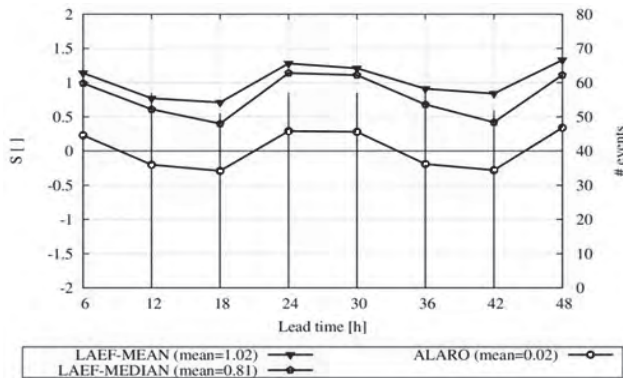


*Fig. 5.* S component of: ALARO (ALARO), ALADIN-LAEF's ensemble mean (LAEF-MEAN) and ALADIN-LAEF's ensemble median (LAEF-MEDIAN) for the southern part of Austria, for area mean precipitation greater than 0 mm.

The interpretation of the A component (evaluating the area mean precipitation for a given domain) is more difficult, as the results are less clear than for the structure component. *Fig. 6* and *7* show the A component for a domain in the central part of Austria.

- The diurnal cycle already mentioned above is also visible in the amplitude component: during (early) day, precipitation activity is overestimated, while there is an underestimation during evening and night. Again, this can possibly be explained by a general shift of the (convective) precipitation diurnal cycle, with the convection starting too early in the model (*Fig. 6*).
- For higher precipitation thresholds, underestimation gets larger (especially for ALADIN-LAEF), and there is a decrease in overestimation, therefore the diurnal cycle is less pronounced (*Fig. 7*).

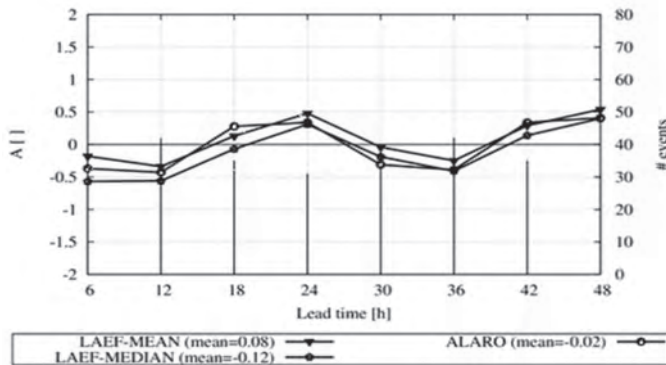


*Fig. 6.* A component of ALARO (ALARO), ALADIN-LAEF's ensemble mean (LAEF-MEAN), and ALADIN-LAEF's ensemble median (LAEF-MEDIAN) for the central part of Austria, for area mean precipitation greater than 0.1 mm.

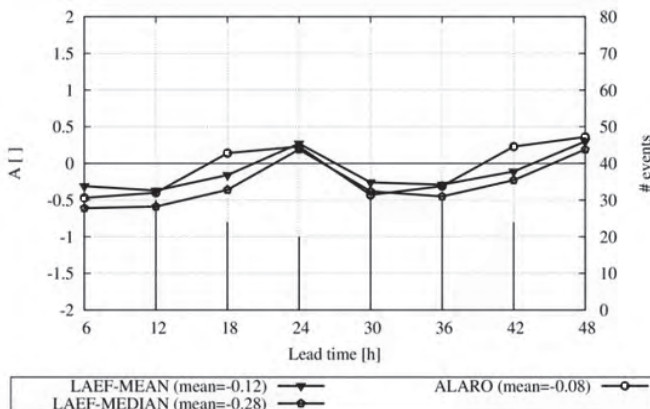


*Fig. 7.* A component of: ALARO (ALARO), ALADIN-LAEF's ensemble mean (LAEF-MEAN) and ALADIN-LAEF's ensemble median (LAEF-MEDIAN) for the central part of Austria, for area mean precipitation greater than 0.5 mm.

The evaluation of the mean L component scores does not reveal a clear view, as the results do not differ significantly among the model systems. As it was already stated in other studies (*Wittmann et al.*, 2010), the L score seems to be more suitable to be used in case studies. Mean values over an extended verification period do not reveal a clear picture.

#### 4.4. Case study

In addition to the statistical scores computed for the 2-month period, a comprehensive case study is carried out for a major flood event that took place in Central Europe from May 31 to June 3, 2013, affecting the Danube, Elbe, and Moldova river catchments.

The large amount of precipitation was linked to the subsequent passage of three cyclones formed over Southeastern Europe, traveling around the quasi-stationary upper-level low. A detailed description of the synoptic situation is given by *Grams et al.* (2014). The effect of this precipitation event on the runoff and level of various rivers in Central Europe was huge, since the soil was already saturated or close to saturation before the start of the event. From climatological point of view, May 2013 was one of the three wettest months of May in the last 150 years in the Upper Danube basin in Austria (*Blöschl et al.*, 2013).

To evaluate the performance of the systems described in the previous sections, the investigation of this case will focus on Austria and the surrounding regions, using several rectangular domains. The domain “RR Zentrum” (11.00 to 14.00 E longitude, 47.10 to 48.40 N latitude) is the most affected one, with peak precipitation values up to 300 mm in 72 hours (*Fig. 8*). The 72-hour cumulated precipitation map (May 31, 2013, 00 UTC – June 3, 2013, 00 UTC) is provided by INCA analysis. The highest precipitation rates are identified in the interval from June 1, 2013, 18 UTC to June 2, 2013, 06 UTC. Thereby, the analysed interval is divided in two periods of 6-hour forecast range, as shown in *Fig. 9* (a: June 1, 2013, 18 UTC – June 2, 2013, 00 UTC and b: June 2, 2013, 00 UTC – June 2, 2013, 06 UTC).

Focus will be on the capabilities of the ALADIN-LAEF and ALARO-LAGGED ensembles to simulate the quantitative precipitation forecasts on the short time range. To assess the uncertainty of the analyzed ensembles, a so-called “spaghetti” plot is represented in *Fig. 10*. It shows the area mean 6-hour cumulated precipitation for forecast ranges up to 48-hour, for both ensembles and the INCA analysis, covering the “RR-Zentrum” domain. The forecasts are initialized at different times: May 31, 2013, 12 UTC (*Fig. 10a*) and June 1, 2013, 12 UTC (*Fig. 10b*).

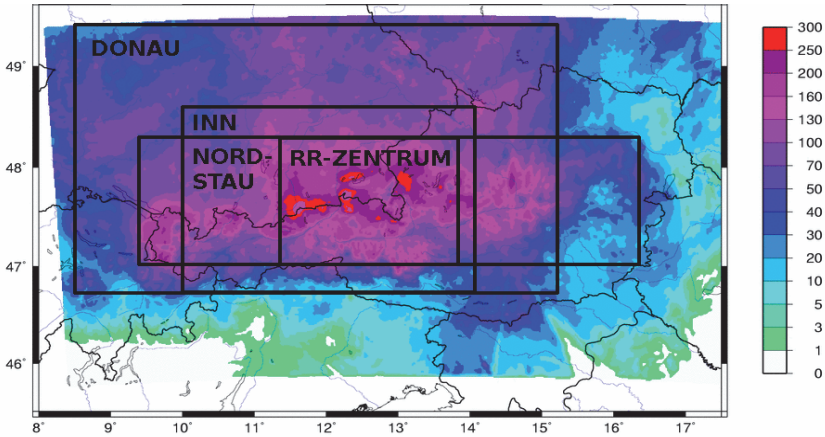


Fig. 8. INCA 72-hour cumulated precipitation [mm] in the period of May 31, 2013, 00 UTC – June 3, 2013, 00 UTC.

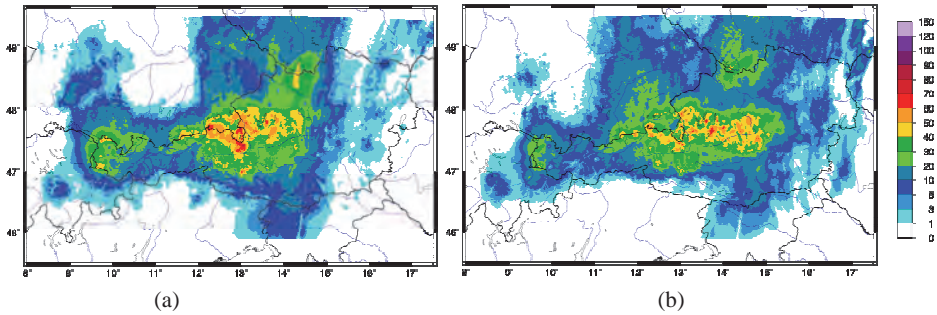


Fig. 9. INCA 6-hour cumulated precipitation [mm] in the periods of June 1, 2013, 18 UTC – 02.06.2013, 00 UTC (a) and 02.06.2013, 00 UTC – 02.06.2013, 06 UTC (b).

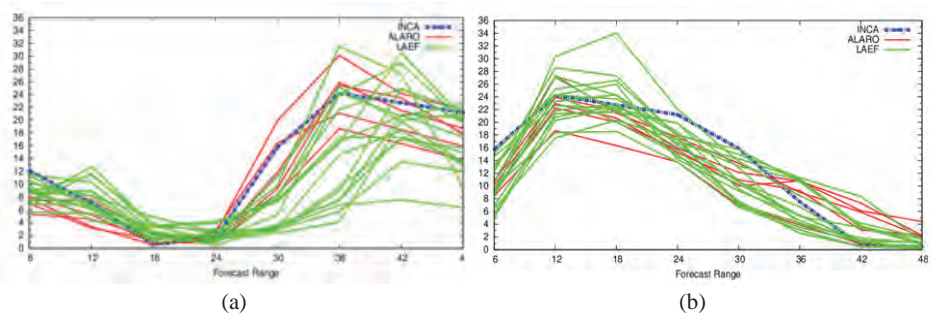


Fig. 10. 6-hour cumulated precipitation [mm] for RR-Zentrum starting from May 31, 2013, 12 UTC (a) and June 1, 2013, 12 UTC (b): INCA (blue), ALADIN-LAEF members (LAEF, green), and ALARO-LAGGED members (ALARO, red).

The members of ALADIN-LAEF and ALARO-LAGGED are rather close to INCA in the first 24 hours, showing only small spread (*Fig. 10a*). After 24-hour lead time, when the precipitation rates start to increase (up to 24 mm in 6-hour at lead time 36-hour), the ALADIN-LAEF shows larger spread than ALARO-LAGGED. Also, the mean precipitation rates are underestimated by many ALADIN-LAEF members with respect to the INCA analysis. These results are underlined by the verification scores obtained for the 2-month verification period, shown in subsection 4.1.

In *Fig. 10b*, it can be noticed that both systems have a smaller spread at the beginning of the interval, the maximum precipitation amount (at 12-hour lead time) is now better captured by more members of ALADIN-LAEF. Yet, ALARO-LAGGED underestimates the precipitation rate occurring from 12 to 30-hour lead time and decreases the precipitation too early. For higher lead times (36–48-hour), ALARO-LAGGED slightly overestimates, while ALADIN-LAEF stays closer to the observed values.

## 5. Conclusions

The forecast skill of the 11 km regional ensemble ALADIN-LAEF, compared to the 5 km deterministic ALARO model, has been investigated, in order to understand the advantages and shortcomings of both systems. ALADIN-LAEF's members are generated by using the first 16 members (from 50) of ECMWF ENS, with different initial conditions perturbations. To quantify the uncertainties in the forecasting system, the breeding-blending and multi-physics approaches are applied. The time-lagged ensemble comprises 5 successive forecasts of ALARO deterministic model from different runs. The forecast quality of the systems was assessed through probabilistic and deterministic measures over a 2-month period, at the beginning and during the convective season of 2013, for the main surface parameters (2 m temperature, 10 m wind speed, and 6-hour cumulated precipitation). A special focus on mesoscale convective systems that generated heavy precipitation over Central Europe was also evaluated.

The main conclusions of this study are:

- (1) In general, the probabilistic verification reveals that ALADIN-LAEF, compared to ALARO-LAGGED, shows more spread, less outliers, and it is more skilful in terms of CRPSS. Hence, the low-resolution ensemble system is able to cover many possible scenarios through the spread, and it is statistically more reliable.
- (2) Regarding the deterministic verification (conducted for 6-hour cumulated precipitation forecasts), in terms of SAL, the results reveal the advantages of the high-resolution deterministic model ALARO compared to the lower-

resolution regional ensemble ALADIN-LAEF. The ALARO precipitation forecast structure is better simulated compared to the observed objects. The structure and amplitude components show similar behavior of the diurnal cycle for both systems. The premature trigger of the convection masks sometimes the difficulty to simulate the diurnal cycle, mainly because the convective precipitation starts too early in the model.

- (3) The high-resolution deterministic model is able to better reproduce the mesoscale convective systems and to solve the complexity of topography. However, the deterministic system is not able to provide information about forecast uncertainties or probabilities.
- (4) The regional ensemble system provides advantages compared to the deterministic one. Thus, the ensemble products represent a powerful tool in risk assessment and decision making.

**Acknowledgments:** The results are obtained in the frame of the RC-LACE project. We would like to thank our colleagues from the INCA department for providing the observation datasets.

## *References*

- Blöschl, G., Nester, T., Komma, J., Parajka J., and Perdigao, R., 2013: The June 2013 flood in the Upper Danube Basin, and comparisons with the 2002, 1954 and 1899 floods. *HESS* 17, 5197–5212. <https://doi.org/10.5194/hess-17-5197-2013>
- Buizza, R., Miller, M., and Palmer, T.N., 1999: Stochastic representation of model uncertainties in the ECMWF ensemble prediction system, *Quart. J. Roy. Meteorol. Soc.* 125, 2887–2908. <https://doi.org/10.1002/qj.49712556006>
- Buizza, R., Barkmeijer, J., Palmer T.N., and Richardson, D.S., 2000: Current status and future developments of the ECMWF Ensemble Prediction System. *Meteorol. Appl.* 7, 163–175. <https://doi.org/10.1017/S1350482700001456>
- Buizza, R., Houtekamer, P.L., Toth, Z., Pellerin, G., Wei, M., and Zhu, Y., 2005: A comparison of the ECMWF, MSC, and NCEP Global Ensemble Prediction Systems, *Mon. Weather Rev.* 133, 1076–1097. <https://doi.org/10.1175/MWR2905.1>
- Buizza, R., 2008: Comparison of a 51-Member Low-Resolution (TL399L62) Ensemble with a 6-Member High-Resolution (TL799L91) Lagged-Forecast Ensemble. *Mon. Weather Rev.* 136, 3343–3362. <https://doi.org/10.1175/2008MWR2430.1>
- Casati, B., Ross, G. and Stephenson, D. B., 2004: A new intensity-scale approach for the verification of spatial precipitation forecasts. *Met. Apps.* 11, 141–154. <https://doi.org/10.1017/S1350482704001239>
- Corazza, M., Sacchetti, D., Antonelli, M., and Drofa, O., 2018: The ARPAL operational high resolution Poor Man’s Ensemble, description and validation. *Atmos. Res.* 203, 1–15. <https://doi.org/10.1016/j.atmosres.2017.11.031>
- Du, J., 2007: Uncertainty and ensemble forecast. *Sci. Technol. Inf. Lecture Ser.* Available online at <https://www.nws.noaa.gov/ost/climate/STIP/uncertainty.htm>
- Ebert, E., 2001: Ability of a Poor Man’s Ensemble to Predict the Probability and Distribution of Precipitation. *Mon. Weather Rev.* 129, 2461–2480. [https://doi.org/10.1175/1520-0493\(2001\)129<2461:AOAPMS>2.0.CO;2](https://doi.org/10.1175/1520-0493(2001)129<2461:AOAPMS>2.0.CO;2)
- Geleyn, J.-F., Catty, B., Bouteloup, Y., and Brožková, R., 2008: A statistical approach for sedimentation inside a microphysical precipitation scheme. *Tellus A* 60, 649–662. <https://doi.org/10.1111/j.1600-0870.2008.00323.x>

- Gerard, L. and Geleyn, J.-F., 2005: Evolution of a subgrid deep convection parametrization in a limited-area model with increasing resolution. *Quart. J. Roy. Meteorol. Soc.* 131, 2293–2312. <https://doi.org/10.1256/qj.04.72>
- Gerard, L., 2007: An integrated package for subgrid convection, clouds and precipitation compatible with the meso-gamma scales. *Quart. J. Roy. Meteorol. Soc.* 133, 711–730. <https://doi.org/10.1002/qj.58>
- Gerard, L., Piriou, J.-M., Brožková, R., Geleyn, J.-F., Banciu, D., 2009: Cloud and precipitation parameterization in a meso-gamma scale operational weather prediction model. *Mon. Weather Rev.* 137, 3960–3977. <https://doi.org/10.1175/2009MWR2750.1>
- Grams, C.M., Binder, H., Pfahl, N.P.S., and Wernli, H., 2014: Atmospheric processes triggering the Central European floods in June 2013. *Nat. Hazards Earth Syst. Sci. Discuss.* 2, 427–458. <https://doi.org/10.5194/nhessd-2-427-2014>
- Haiden, T., Kann, A., Pistorik, G., Stadlbacher, K., Wittmann, C., 2009: Integrated Nowcasting through Comprehensive Analysis (INCA) system description., ZAMG Rep., Vienna, Austria. [http://www.zamg.ac.at/fix/INCA\\_system.pdf](http://www.zamg.ac.at/fix/INCA_system.pdf)
- Hersbach, H., 2000: Decomposition of the continuous ranked probability score for ensemble prediction system, *Weather Forecast.* 15, 559–570. [https://doi.org/10.1175/1520-0434\(2000\)015<0559:DOTCRP>2.0.CO;2](https://doi.org/10.1175/1520-0434(2000)015<0559:DOTCRP>2.0.CO;2)
- Hoffmann, R.N. and Kalnay, E., 1983: Lagged average forecasting, an alternative to Monte Carlo forecasting, *Tellus*, 35A, 100–118. <https://doi.org/10.1111/j.1600-0870.1983.tb00189.x>
- Law, K. J. and Stuart, A. M., 2012: Evaluating Data Assimilation Algorithms. *Mon. Wea. Rev.* 140, 3757–3782. <https://doi.org/10.1175/MWR-D-11-00257.1>
- Lorenz, E., 1963: Deterministic non-periodic flows. *J. Atmos. Sci.* 20, 130–141. [https://doi.org/10.1175/1520-0469\(1963\)020<0130:DNF>2.0.CO;2](https://doi.org/10.1175/1520-0469(1963)020<0130:DNF>2.0.CO;2)
- Murphy, J., Sexton, D.M.H., Barnett, D.N., Jones, G.S., Webb, M.J., Collins, M., Stainforth, D.A., 2004: Quantification of modelling uncertainties in a large ensemble of climate change simulations, *Nature* 430, 768–772. <https://doi.org/10.1038/nature02771>
- Noilhan, J. and Planton, S., 1989: A Simple Parameterization of Land Surface Processes for Meteorological Models. *Mon. Weather Rev.* 117, 536–549. [https://doi.org/10.1175/1520-0493\(1989\)117<0536:ASPOLS>2.0.CO;2](https://doi.org/10.1175/1520-0493(1989)117<0536:ASPOLS>2.0.CO;2)
- Palmer, T., 2001: A nonlinear dynamical perspective on model error: A proposal for nonlocal stochastic-dynamic parametrisation in weather and climate prediction models. *Quart. J. Roy. Meteorol. Soc.* 127, 279–304. <https://doi.org/10.1002/qj.49712757202>
- Palmer, T., Buizza, R., Hagedorn, R., Lawrence, A., Leutbecher, M., and Smith, L., 2005/06: Ensemble prediction: A pedagogical perspective, *ECMWF Newsletter* 106.
- Palmer, T., 2017: The primacy of doubt: Evolution of numerical weather prediction from determinism to probability, *J. Adv. Model. Earth Syst.* 9, 730–734. <https://doi.org/10.1002/2017MS000999>
- Rodwell, M., 2005/06: Comparing and combining deterministic and ensemble forecasts: How to predict rainfall occurrence better. *ECMWF Newsletter* 106.
- Termonia, P., Fischer, C., Bazile, E., Bouyssel, F., Brožková, R., Bénard, P., Bochenek, B., Degrauwe, D., Derková, M., El Khatib, R., Hamdi, R., Mašek, J., Pottier, P., Pristov, N., Seity, Y., Smoliková, P., Španiel, O., Tudor, M., Wang, Y., Wittmann, C., Joly, A2017: The ALADIN system and its canonical model configurations AROME CY41T1 and ALARO CY40T1. *Geosci. Model Dev.* 11, 257–281. <https://doi.org/10.5194/gmd-11-257-2018>
- Toth, Z. and Kalnay, E., 1993: Ensemble forecasting at NMC: the generation of perturbation. *Bull. Amer. Meteor. Soc.* 74, 2317–2330. [https://doi.org/10.1175/1520-0477\(1993\)074<2317:EFANTG>2.0.CO;2](https://doi.org/10.1175/1520-0477(1993)074<2317:EFANTG>2.0.CO;2)
- Váňa, F., Bénard, P., Geleyn, J.-F., Simon, A., and Seity, Y., 2008: Semi-Lagrangian advection scheme with controlled damping: An alternative to nonlinear horizontal diffusion in a numerical weather prediction model. *Quart. J. Roy. Meteor. Soc.* 134, 523–537. <https://doi.org/10.1002/qj.220>
- Vokoun, M. and Hanel, M., 2018: Comparing ALADIN-CZ and ALADIN-LAEF Precipitation Forecasts for Hydrological Modelling in the Czech Republic, *Advances in Meteorology*, 2018, 14 pages. <https://doi.org/10.1155/2018/5368438>

- Wang, Y., Belluš, M., Wittmann, C., Steinheimer, M., Weidle, F., Kann, A., Ivatek-Šahdan, S., Tian, W., Ma, X., Taşcu, S., Bazile, E., 2011: The Central European limited-area ensemble forecasting system: ALADIN-LAEF, *Quart. J. Roy. Meteor. Soc.*, 137, 483–502. <https://doi.org/10.1002/qj.751>
- Wang, Y., Bellus, M., Geleyn, J.-F., Ma, X., Tian, W. and Weidle, F., 2014: A new method for generating initial condition perturbations in a regional ensemble prediction system: blending. *Mon. Weather Rev.* 142, 2043–2059. <https://doi.org/10.1175/MWR-D-12-00354.1>
- Wang, Y., Belluš, M., Ehrlich, A., Mile, M., Pristov, N., Smoliková, P., Španiel, O., Trojáčková, A., Brožková, R., Cedilnik, J., Klarić, D., Kovačić, T., Mašek, J., Meier, F., Szintai, B., Taşcu, S., Vivoda, J., Wastl, C., Wittmann, C2018: 27 years of Regional Cooperation for Limited Area Modelling in Central Europe (RC LACE). *Bull. Amer. Meteorol. Soc.* 99, 1415–1432. <https://doi.org/10.1175/BAMS-D-16-0321.1>
- Wastl C., Simon, A., Wang, Y., Kulmer, M., Baár, P., Bölöni, G., Dantinger, J., Ehrlich, A., Fischer, A., Frank, A., Heizler, Z., Kann, A., Stadlbacher, K., Szintai, B., Szűcs, M., Wittmann, C2018: A seamless probabilistic forecasting system for decision making in Civil Protection, *Meteorol. Zeit.* 27, 417–430. <https://doi.org/10.1127/metz/2018/902>
- Weidle, F., Wang, Y., Tian, W., and Wang, T., 2013: Validation of Strategies using Clustering Analysis of ECMWF EPS for Initial Perturbations in a Limited Area Model Ensemble Prediction System, *Atmosph.-Ocean* 51, 284–295. <https://doi.org/10.1080/07055900.2013.802217>
- Wernli, H., Paulat, M., Hagen, M., and Frei, C., 2008: SAL - a novel quality measure for the verification of quantitative precipitation forecasts. *Mon. Weather Rev.* 136, 4470–4487. <https://doi.org/10.1175/2008MWR2415.1>
- Wittmann, C., Haiden, T., and Kann, A., 2010: Evaluating multi-scale precipitation forecasts using high resolution analysis. *Adv. Sci. Res.* 4, 89–98. <https://doi.org/10.5194/asr-4-89-2010>

# IDŐJÁRÁS

*Quarterly Journal of the Hungarian Meteorological Service*  
Vol. 124, No. 3, July – September, 2020, pp. 419–426

## Short Contribution

### From Geiger to the modern micrometeorology – the textbook of Dénes Berényi<sup>1</sup>

**Thomas Foken**

*University of Bayreuth,  
Bayreuth Center of Ecology and Environmental Research (BayCEER)  
Universitätsstraße 30, D-95447 Bayreuth, Germany*

*Corresponding author E-mail: thomas.foken@uni-bayreuth.de*

*(Manuscript received in final form July 3, 2020)*

**Abstract**—The short historical outline describes the significance of Dénes Berényi's textbook "Mikroklimatologie" (Microclimatology, 1967, in German) for the present day. Despite its limited distribution, it is an important document of the transition from the phenomenological to the physical based description of local climatological processes. In any case, it remains an important reference for climatology before 1960.

*Key-words:* Dénes Berényi, microclimatology, micrometeorology, history, textbook

## 1. Introduction

More than 50 years ago in 1967, Dénes Berényi published his textbook "Microclimatology" in German. The manuscript was written around 1962 (*Fig. 1*). The textbook has been largely forgotten both because of the language and because of the political situations in Europe.

Before the Second World War, German language was a leading language not only in meteorology but also in Central Europe, and not only in Germany, Austria, and Switzerland. This may have prompted the author to choose this language, especially since Geiger's famous book "Das Klima der bodennahen Luftschicht" (The climate near the ground) was still read in German. Due to the

---

<sup>1</sup> Lecture held at Hungarian Meteorological Service, Budapest, November 21, 2017

political division of Europe, however, Berényi's work became hardly known in the western part of Central Europe, while the eastern part was relatively insignificant in the international scientific landscape. Thus, the book was reserved only for a very small circle of readers, however, it would have deserved much more attention.

The author, Professor Dénes Berényi (1900–1971, *Fig. 2*) is the founder of the meteorological station at the University of Debrecen, where he also received his doctorate in 1927. He also lectured there on microclimatology. In 1951, he became the head of the Department of Meteorology and in 1952 he was appointed professor. He is the author of 6 books and about 80 publications. His memory is kept by the Hungarian Meteorological Society's Dénes Berényi Memorial Prize, awarded since 1993 (*Szegedi, 2008; Varga, 2014*).

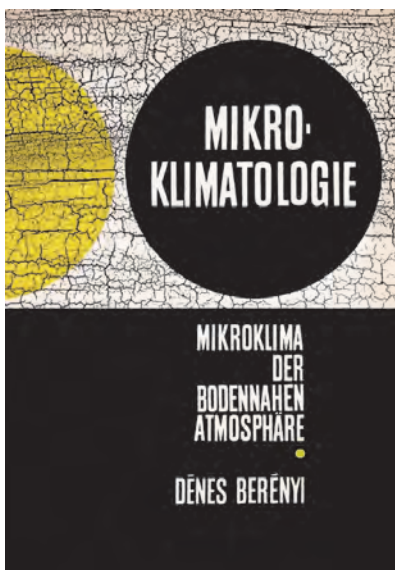


*Fig. 1.* Title of Dénes Berényi's book (*Berényi, 1967*).



*Fig. 2.* Professor Dénes Berényi (*Szegedi 2008; Varga, 2014*)

If one remembers the book today, it is its position in the transition from the classical microclimatic description in the sense of Rudolf Geiger (1894–1981) to modern textbooks of micrometeorology, which are strongly influenced by physics. The following article will show this transition by means of comparisons of contents. However, the book has a special significance in the history of science, as it covers many East European and Russian sources that would otherwise be completely forgotten.

## 2. From Geiger to Berényi

Rudolf Geiger, together with Wladimir Köppen, is not only the developer of the climate classification according to Köppen-Geiger, which is still used today, but he can also be described, without restriction, as the nestor of microclimatology. His book "Das Klima der bodennahen Luftschicht" (Geiger, 1927) has not only been published in many new editions (1941, 1950, 1961, reprint 2013), there is also an extension in English language available (Geiger et al., 1995, 2009). There is probably no one who works in this field and has not yet gained inspiration from this book. It would be too much to say that the book is structured according to ecosystems, but the structure does follow certain forms of vegetation (Table 1). On the way to Berényi, however, some other scientists have to be mentioned: Geiger's book was also based on Wilhelm Schmidt's (1925) fundamental work on the exchange coefficient. There is also a theoretical book on atmospheric turbulence by Heinz Lettau (1939) just before the Second World War. Not to forget the first comprehensive work on the energy balance of the earth by Fritz Albrecht (1940) and the first textbook on micrometeorology by Oliver Graham Sutton (1953). However, Geiger's influence on Berényi's work is unmistakable, at least for the descriptive parts of the microclimate. Berényi, however, had a significant improvement in the physical-mathematical formulations, and the characterized the transition from classical microclimatology to micrometeorology.

Table 1. Comparison of the content of Geiger's book „Das Klima der bodennahen Luftschicht“ and Berényi's book „Mikroklimateologie“

Geiger	Berényi
*new in 4th edition	
Earth's surface energy balance – the basic of microclimatology *	Introduction to microclimate
Air layer over flat surfaces without vegetation	Solar radiation
Influence of the underlying surface	Heat exchange near the surface
Quantitative determination of the energy balance *	Daily and annual cycle of microclimatological elements
Influence of the plant cover	
Forest climatology	
Influence of the topography on the microclimate	
Interrelationship between animals and humans to microclimate	

### 3. Important contributions from Berényi

If one looks at the structure of Berényi's book (*Table 1*), it is immediately noticeable, in contrast to Geiger, that at the beginning of the book, the importance of radiation from the sun is shown, followed by the energy turnover on the earth's surface. The climatology is considered separately for the individual elements like radiation, temperature, wind, etc. In his fourth edition of the book, *Geiger* (1961) also gave more space to the heat balance on the earth's surface in the introductory section, but not with the clarity of Berényi's work. In principle, the structure introduced by Berényi has more or less established itself in the micrometeorological textbooks of the last 50 years, *Monteith* (1975, further editions with *Unsworth* 1990, 2008, and 2013), *Stull* (1988), *Arya* (1998, further editions 2001 and 2012), *Foken* (2008, further edition 2017). The development of micrometeorology in these years has recently been described in detail (*Hicks and Baldocchi*, 2020). While Geiger showed only the principles of energy turnover at the earth's surface, Berényi gives quantitative values (*Fig. 3*), referring to *Baur and Philipps* (1934, 1935) and *Houghton* (1954). Today, such presentations are included in all climatology and meteorology textbooks.

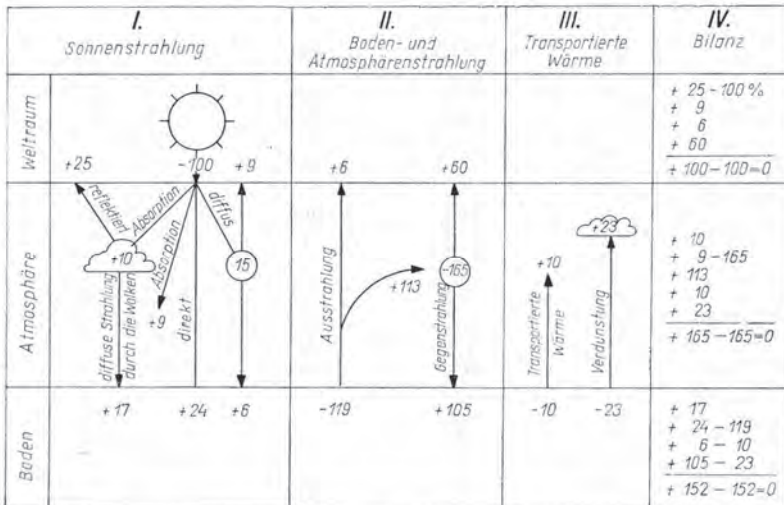
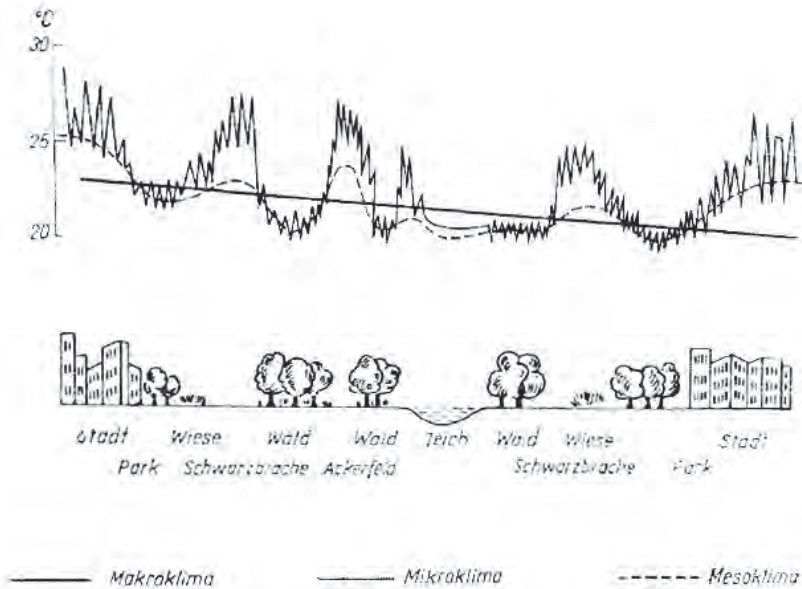


Fig. 3. Heat balance at the earth's surface and in the atmosphere (*Houghton*, 1954; *Berényi*, 1967)

A further detail to be emphasized is the division of the scales into macro, meso, and micro – even before the introduction of *Orlanski's* (1975) scheme – based on a work by *Saposhnikova* (1950) with an interesting spatial averaging of the air temperature (*Fig. 4*). This introduces a principle of order, as is common today, even though *Berényi* does not yet link it to the temporal scales. However, the many and differently defined scale concepts in climatology are overcome (*Hupfer, 1991*).



*Fig. 4.* Classification of the scales of the climate (*Saposhnikova, 1950; Berényi, 1967*)

*Berényi* has a strong hydrodynamic reference in his book, since he begins the theoretical sections with *Prandtl's* (1925) mixing length approach alongside the work of *Schmidt* (1925) and uses essential hydrodynamic works of the 1920s and 1930s, which formed the theoretical foundation of micrometeorology. Also important are the inclusion of turbulence and the description of the vortex structure near the ground. Here he refers to an illustration by *Obukhov* (1951), which is shown in *Fig. 5*. Thus, the book has crossed the border from the phenomenological description of the microclimate to a clearly theoretical underpinning corresponding to the approaches of the 1960s.

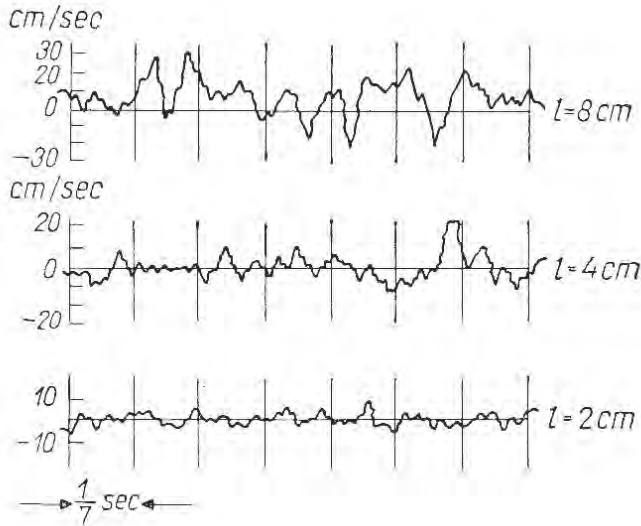


Fig. 5. Difference of the wind velocity between two points (Obukhov, 1951; Berényi, 1967)

Somewhat surprising is the extensive absence of the similarity theory of Monin and Obukhov (1954), although it was already published in German in the 1950s (Monin and Obukhov, 1958). When listing the approaches to turbulent energy exchange, there is only a footnote that the method according to Monin and Obukhov can also be used, and that Kiss-Tóth (1959) has successfully applied it to the region of Lake Balaton. It is possible, however, that a paragraph in the book has been deleted, because the bibliography (consecutive numbering) contains some references to which there is no text in the book.

#### 4. Significance of the book for the present day

The transition to a modern mathematical-physical based micrometeorology and thus also microclimatology was made with the Workshop on Micrometeorology (Haugen, 1973), so the earlier written book of Berényi was a pioneer in some areas, but it is only of historical interest today. In any case, the far-sightedness of the author must be emphasized, as he based Geiger's approach more on physics. Thus, the work stands at the transition from the classical mixture length and exchange coefficient based approach to the similarity and turbulence theory. In the context of changing climate, local climatic changes are also of great interest. Here, examples from the book can be quite helpful because of the strong physical base.

Apart from this scientific-historical aspect, it is above all a source for many forgotten Hungarian local climatological works before 1960, but also from the Russian and East European area, which are completely underrepresented in Geiger's book. In any case, the book remains an important document of the Hungarian meteorological and climatological sciences.

## *References*

- Albrecht, F.*, 1940: Untersuchungen über den Wärmehaushalt der Erdoberfläche in verschiedenen Klimagebieten, Reichsamt f. Wetterdienst. *Wiss. Abh., Bd. VIII, Nr. 2*, 1–82. (In German)  
<https://doi.org/10.1007/978-3-662-42530-5>
- Arya, S.P.*, 1998: Introduction to Micrometeorology. Academic Press, San Diego
- Baur, F. and Philipps, H.*, 1934: Der Wärmehaushalt der Lufthülle der Nordhalbkugel im Januar und Juli. *Gerl. Beitr. Geophys.*, *42*, 160–207. (In German)
- Baur, F. and Philipps, H.*, 1935: Der Wärmehaushalt der Lufthülle der Nordhalbkugel im Januar und Juli. *Gerl. Beitr. Geophys.*, *45*, 82–134. (In German)
- Berényi, D.*, 1967: Mikroklimatologie, Mikroklima der bodennahen Atmosphäre. Akadémiai Kiadó, Budapest. (In German)
- Foken, T.*, 2008: Micrometeorology. Springer, Berlin, Heidelberg.  
<https://doi.org/10.1007/978-3-540-74666-9>
- Geiger, R.*, 1927: Das Klima der bodennahen Luftschicht, 1. Aufl. ed., Friedr. Vieweg & Sohn, Braunschweig. (In German)
- Geiger, R.*, 1961: Das Klima der bodennahen Luftschicht. Ein Lehrbuch der Mikroklimatologie. 4. neubearbeitete und erweiterte Auflage, Verlag Friedrich Vieweg & Sohn, Braunschweig. (In German), reprint 2013 <https://doi.org/10.1007/978-3-658-03519-8>
- Geiger, R., Aron, R.H., and Todhunter, P.*, 1995: The climate near the ground. 5 ed., Friedr. Vieweg & Sohn Verlagsges. mbH, Braunschweig, Wiesbaden. <https://doi.org/10.1007/978-3-322-86582-3>
- Geiger, R., Aron, R.H., and Todhunter, P.*, 2009: The Climate near the Ground. Rowman & Littlefield, Lanham, XVIII.
- Haugen, D.A.*, 1973: Workshop on Micrometeorology, Am. Meteorol. Soc., Boston.
- Hicks, B.B., and Baldocchi, D.D.*, 2020: Measurement of Fluxes Over Land: Capabilities, Origins and Remaining Challenges. *Bound.-Lay. Meteorol.* <https://doi.org/10.1007/s10546-020-00531-y>
- Houghton, H.G.*, 1954: On the annual heat balance of the norther hemisphere *J. Meteorol.*, *11*, 1–9.  
[https://doi.org/10.1175/1520-0469\(1954\)011<0001:OTAHBO>2.0.CO;2](https://doi.org/10.1175/1520-0469(1954)011<0001:OTAHBO>2.0.CO;2)
- Hupfer, P.*, 1991: Das Klimasystem der Erde, Akademie-Verlag, Berlin. (In German)
- Kiss-Tóth, E.*, 1959: Különböző talajok fölötti légrétegek hőfórgalma a Balaton térségében. *Időjárás* *63*, 1–6. (In Hungarian)
- Lettau, H.*, 1939: Atmosphärische Turbulenz. Akad. Verlagsges., Leipzig. (In German)
- Monin, A.S. and Obukhov, A.M.*, 1954: Osnovnye zakonomernosti turbulentnogo peremesivanija v prizemnom sloe atmosfery. *Trudy geofiz. inst. AN SSSR* *24* (151), 163–187. (In Russian)
- Monin, A.S. and Obukhov, A.M.*, 1958: Fundamentale Gesetzmäßigkeiten der turbulenten Vermischung in der bodennahen Schicht der Atmosphäre. In (ed.: *Goering, H.*) Sammelband zur statistischen Theorie der Turbulenz. Akademie-Verlag, Berlin, 199–226. (In German)
- Monteith, J.L.*, 1975: Principles of Environmental Physics, Edward Arnold Publishers Ltd., London.
- Obukhov, A.M.*, 1951: Charakteristiki mikrostrukturny vetra v prizemnom sloje atmosfery. *Izv. AN SSSR, ser. Geofiz.*, *3*, 49–68. (In Russian)
- Orlanski, I.*, 1975: A rational subdivision of scales for atmospheric processes. *Bull. Amer. Meteorol. Soc.*, *56*, 527–530.
- Prandtl, L.*, 1925: Bericht über Untersuchungen zur ausgebildeten Turbulenz. *Z. angew. Math. Mech.* *5*, 136–139. (In German) <https://doi.org/10.1002/zamm.19250050212>
- Saposhnikowa, S.A.*, 1950: Mikroklimat i mestnoj klimat, Leningrad. (In Russian)

- Schmidt, W.*: Der Massenaustausch in freier Luft und verwandte Erscheinungen. Henri Grand Verlag, Hamburg. (In German)
- Stull, R.B.*, 1988: An Introduction to Boundary Layer Meteorology. Kluwer, Dordrecht.  
<https://doi.org/10.1007/978-94-009-3027-8>
- Sutton, O.G.*, 1953: Micrometeorology. McGraw Hill, New York.
- Szegedi, S.*, 2008: History of the meteorological observations in Debrecen. *AGD Landscape and Environment* 2, 1–5.
- Varga, M.*, 2014: Történelmi Arcképek: Berényi Dénes. *Légekör* 59, 139. (In Hungarian)

## INSTRUCTIONS TO AUTHORS OF *IDŐJÁRÁS*

The purpose of the journal is to publish papers in any field of meteorology and atmosphere related scientific areas. These may be

- research papers on new results of scientific investigations,
- critical review articles summarizing the current state of art of a certain topic,
- short contributions dealing with a particular question.

Some issues contain “News” and “Book review”, therefore, such contributions are also welcome. The papers must be in American English and should be checked by a native speaker if necessary.

Authors are requested to send their manuscripts to

*Editor-in Chief of IDŐJÁRÁS*  
P.O. Box 38, H-1525 Budapest, Hungary  
E-mail: [journal.idojaras@met.hu](mailto:journal.idojaras@met.hu)

including all illustrations. MS Word format is preferred in electronic submission. Papers will then be reviewed normally by two independent referees, who remain unidentified for the author(s). The Editor-in-Chief will inform the author(s) whether or not the paper is acceptable for publication, and what modifications, if any, are necessary.

Please, follow the order given below when typing manuscripts.

*Title page* should consist of the title, the name(s) of the author(s), their affiliation(s) including full postal and e-mail address(es). In case of more than one author, the corresponding author must be identified.

*Abstract:* should contain the purpose, the applied data and methods as well as the basic conclusion(s) of the paper.

*Key-words:* must be included (from 5 to 10) to help to classify the topic.

*Text:* has to be typed in single spacing on an A4 size paper using 14 pt Times New Roman font if possible. Use of S.I.

units are expected, and the use of negative exponent is preferred to fractional sign. Mathematical formulae are expected to be as simple as possible and numbered in parentheses at the right margin.

All publications cited in the text should be presented in the *list of references*, arranged in alphabetical order. For an article: name(s) of author(s) in Italics, year, title of article, name of journal, volume, number (the latter two in Italics) and pages. E.g., *Nathan, K.K.*, 1986: A note on the relationship between photo-synthetically active radiation and cloud amount. *Időjárás* 90, 10–13. For a book: name(s) of author(s), year, title of the book (all in Italics except the year), publisher and place of publication. E.g., *Junge, C.E.*, 1963: *Air Chemistry and Radioactivity*. Academic Press, New York and London. Reference in the text should contain the name(s) of the author(s) in Italics and year of publication. E.g., in the case of one author: *Miller* (1989); in the case of two authors: *Gamov* and *Cleveland* (1973); and if there are more than two authors: *Smith et al.* (1990). If the name of the author cannot be fitted into the text: (*Miller*, 1989); etc. When referring papers published in the same year by the same author, letters a, b, c, etc. should follow the year of publication. DOI numbers of references should be provided if applicable.

*Tables* should be marked by Arabic numbers and printed in separate sheets with their numbers and legends given below them. Avoid too lengthy or complicated tables, or tables duplicating results given in other form in the manuscript (e.g., graphs). *Figures* should also be marked with Arabic numbers and printed in black and white or color (under special arrangement) in separate sheets with their numbers and captions given below them. JPG, TIF, GIF, BMP or PNG formats should be used for electronic artwork submission.

*More information* for authors is available: [journal.idojaras@met.hu](mailto:journal.idojaras@met.hu)

Published by the Hungarian Meteorological Service

---

Budapest, Hungary

**ISSN 0324-6329 (Print)**

**ISSN 2677-187X (Online)**